STEFFEN, ROBERTSON AND KIRSTEN CE INC

in association with

METAGO ENVIRONMENTAL ENGINEERS

Report to the

WATER RESEARCH COMMISSION

on

THE PREDICTION OF POLLUTION LOADS
FROM COARSE
SULPHIDE-CONTAINING WASTE MATERIALS

by

A R JAMES

PRETORIA
June 1997

THE PREDICTION OF POLLUTION LOADS FROM COARSE SULPHIDE-CONTAINING WASTE MATERIALS

PREPARED FOR THE WATER RESEARCH COMMISSION

BY

STEFFEN, ROBERTSON AND KIRSTEN CE INC.

IN ASSOCIATION WITH

METAGO ENVIRONMENTAL ENGINEERS

DECEMBER 1996

Executive Summary

THE PREDICTION OF POLLUTION LOADS
FROM COARSE SULPHIDE-CONTAINING WASTES

The aims of the project were as follows:

- To develop a model to predict the pollution load emanating from coarse, sulphide-containing waste materials, such as opencast coal backfill or spoil piles.

- To evaluate kinetic laboratory testing methods which determine the propensity of these materials to develop acid drainage.

- To evaluate the practicality of inundation (water cover) of acid generating materials as a control technology under South African conditions.

The project documentation is contained in three Sections as follows:

Section 1 describes the processes which give rise to contaminated drainage from coarse sulphide-containing wastes and the development of a modelling approach which is considered appropriate and practical for coarse sulphide-containing waste materials. An approach is proposed which utilises a combination of a physical model and a computer based mathematical model. The physical model is used to simulate a range of processes for which the development of a rigorous mathematical model is not an achievable objective, or, for which the requirements of data collection are potentially too onerous to be of practical use to industry.

Section 2 describes the computer based mathematical model, *Salmine version 1.0* which has been developed as the main focus of this project. The model is available on computer diskette. The results of simple field drum tests, carried out at two mines to evaluate kinetic test methods appropriate to coarse wastes, are documented, together with the results of trial laboratory kinetic tests using humidity cells. Some proposed modifications to the humidity cell kinetic test are proposed to enable the determination of several empirical parameters, required as input to the

Salmine model. It is concluded that the prediction of drainage characteristics from coarse wastes is extremely complex, but that the model has the potential to provide a useful tool to evaluate the effect on the drainage characteristics, of alternative control options. The model has not been adequately verified. The verification of the model requires that it be tested against a large scale column, in which all processes simulated in the model will be active. It is recommended that future research focus on the verification of the model and the application and implementation of the proposed kinetic test apparatus and procedure.

Section 3 is concerned exclusively with the third objective of the project, namely the practicality of subaqueous disposal of sulphide-containing materials, as a drainage quality control technology under South African conditions. The mechanisms of oxygen flux to an inundated waste, namely diffusion of dissolved oxygen through the water, and advective transport of dissolved oxygen, are reviewed. The effect of inundation of the waste on the mobility of stored oxidation products is discussed. It is concluded that for sub-aqueous disposal to be effective, the sulphide-containing waste should be inundated as soon after mining as possible, to reduce the build up of stored contaminants, which will be mobilised once the waste is inundated. Several practical methods to inundate sulphide-containing wastes for both opencast and underground mines are proposed. It is recommended that these options be considered in future, at the mine planning and development stage.

CONTENTS

SECTION ONE

PROCESSES WHICH GIVE RISE TO
CONTAMINATED DRAINAGE
FROM COARSE SULPHIDE-CONTAINING WASTES
AND THE DEVELOPMENT OF AN APPROACH
TO PREDICT DRAINAGE CHARACTERISTICS

FOR A REPORT TO THE
WATER RESEARCH COMMISSION
ON THE PROJECT

THE PREDICTION OF POLLUTION LOADS
FROM COARSE SULPHIDE-CONTAINING WASTES

PREPARED BY STEFFEN, ROBERTSON AND KIRSTEN
IN CONJUNCTION WITH
METAGO ENVIRONMENTAL ENGINEERS

DECEMBER 1996

Contents

CHAPTER ONE: A DESCRIPTION OF THE PROJECT

CHAPTER TWO: PROCESSES WHICH GIVE RISE TO CONTAMINATED

DRAINAGE FROM COARSE SULPHIDE-CONTAINING WASTES

CHAPTER ONE : A DESCRIPTION OF THE PROJECT

1   BACKGROUND TO THE PROJECT

This report documents the work which has been carried out to develop a mathematical model and kinetic test procedure to predict pollution loads which would emanate from coarse sulphide-containing mine waste materials. This project was commissioned by the Water Research Commission (WRC) in 1992 and completed in 1996.

Sulphide-containing mine waste materials, once placed in an oxidising environment in the presence of water or water vapour, will oxidise and release sulphates, metals and proton acidity (H^+) into the drainage water. The increased acidity may result in further leaching of secondary metals or other contaminants as the contaminated water migrates downwards through the waste towards the drainage exit points. Partial or complete neutralisation of the acidity, due to the presence of neutralising minerals, may lead to an increase in the pH of the migrating water along the path of flow. In the process of neutralisation, however, further cations and anions may be dissolved thus increasing the total dissolved solids content (TDS) of the leachate or drainage water.

Current acid rock drainage (ARD) prediction methods are reasonably able to predict the formation of ARD and, to a lesser extent, the associated drainage water quality from the more homogenous fine materials such as mine tailings. However these methods are not necessarily suitable for use in the case of coarse materials, where particle sizes typically range from rock or gravel-size materials down to clay fractions. Examples of waste piles which fall into this category include coal discard dumps, opencast mine spoil piles and rock piles. Coarse wastes are not restricted to any particular type of mine.

In the case of coarse sulphide-containing wastes or waste piles, hereafter referred to as coarse wastes or coarse waste piles, the prediction of the drainage quality, pollution load and flow rate (drainage characteristics), is complicated by factors such as the high spatial variability of the material and the influence of additional processes which, in the case of fine wastes, have an insignificant effect on the water quality, but which in the case of coarse wastes, can have a potentially significant or dominant effect.

Current prediction models such as the RATAP model, have focused primarily on fine materials and do not account for the high degree of spatial variability with respect to the values of a number of important parameters including:

- The concentration and reactivity of sulphide minerals.

- The concentration, distribution and availability of neutralising minerals which influences the extent to which acid drainage will be neutralised and the time required for the available neutralising potential to be depleted.

- A range of factors which affect the extent to which the products of oxidation and leaching are flushed from the waste by migrating water. These factors include the permeability, porosity and the presence and distribution of preferential flow paths within the coarse waste.

In addition, physical and chemical processes which are insignificant or absent in fine materials, may predominate in coarse rock materials, for example:

- Convective transport of oxygen or rapid pressure equilibration may predominate over diffusive transport in certain coarse waste piles.

- Temperature and thermal effects which can be important in coarse rock dumps, are generally insignificant in fine tailings materials.

An added complexity of coarse waste piles is that certain material properties may change with time due to weathering processes. Slaking, chemical weathering,

internal erosion of particles and settlement may lead to changes in the specific surface area, permeability and availability of neutralising minerals which may in turn significantly alter the drainage characteristics.

Coarse wastes are common in South Africa, particularly in areas subject to extensive opencast coal mining. The effect of mining and coarse waste piles on surface and groundwater reserves in certain catchments such as the Olifants River and Upper Vaal catchment, is severe (DWA&F white paper F-92). Furthermore the pollution load generated by the presence of spoil piles and other waste materials is expected to continue for many centuries and is likely to increase in future as the natural neutralising potential of the wastes is depleted.

Given the importance and significance of the contaminant load which emanates from coarse wastes in South Africa, the WRC and the mining industry identified the need to review the current status of prediction modelling and develop a method which can be used with a reasonable or useful degree of accuracy, to predict the drainage characteristics from coarse waste piles.

Once the natural neutralising potential of the waste materials is depleted, the pH of mine drainage waters reduces into the acidic range at which stage the solubility of metals increases considerably. In the early stages of acid mine drainage, drainage water is characterised by neutral pH, high sulphate (SO_4), and calcium (Ca) concentrations and relatively low concentrations of metals such as iron and manganese. With the subsequent onset of acidic drainage comes the problem of elevated metal concentrations in the drainage water. For example, in the case of coal mine wastes, iron, manganese and aluminium comprise the metals of major concern. In the case of hard rock mines a range of other metals such as copper, nickel, lead, zinc and uranium may be of concern since they may present a threat to downstream users and the aquatic environment even at relatively low concentrations.

2 PROJECT OBJECTIVES

Arising from the problem described above is the need to be able to control the drainage characteristics so as to reduce the impact on downstream users and the aquatic environment to an acceptable level, both now, and in the decades and centuries to come. In order to achieve this goal it will be necessary to continually improve existing control technologies and continue to develop new technologies to reduce the impact of ARD. Of the controls currently available, it is generally accepted that primary (oxidation inhibiting) and secondary controls (contaminant migration inhibiting) are generally the most cost effective and reliable given the long time spans involved. Tertiary controls which are concerned with treating contaminated drainage, represent a last resort and given the time spans involved are in most cases the least reliable and most expensive option.

Given that the focus of design of a mine waste facility, whether it be a tailings dam, spoil pile, discard dump or other, should firstly be on the development of suitable primary and secondary control measures, the need arises to be able to predict the effect that a particular control will have on the mine drainage characteristics in future. In particular, it is necessary to be able to predict the effect that the control will have on :

- the rate of oxidation of the sulphide minerals

- the extent and rate of depletion of available neutralising minerals

- the extent and rate of removal of oxidation products (flushing) from the waste facility.

- the rate of depletion and leaching (conversion from solid phase to aqueous phase) of secondary metals within the waste facility

The first two objectives of the project are concerned with improving the ability to

predict the mine drainage characteristics. These objectives were stated as follows at the start of the project:

☞   To develop a model to predict the pollution load emanating from coarse, sulphide containing rock materials, such as opencast coal backfill or spoil piles.

☞   To evaluate kinetic laboratory testing methods which determine the propensity of these materials to develop acid drainage.

A final objective of the project which is unrelated to the previous two objectives, was concerned with the evaluation of a control technology which is rapidly gaining acceptance internationally, namely subaqueous disposal of sulphide- containing mine wastes. As discussed earlier, the most important aspect of controlling mine drainage is the development and application of suitable cost effective control measures. Of the control technologies currently available internationally, subaqueous disposal is considered to be an effective control measure. Whereas countries such as Canada have an abundance of Lakes and suitable water bodies, South Africa has none and the only practical options for subaqueous disposal are :

•   placement of wastes below the natural water table (usually in a disused section of an opencast or underground mine, or

•   the construction of artificial facilities which maintain the waste at or very near to saturation.

The third objective of this research project is thus :

☞   To evaluate the practicality of inundation (water cover) of acid generating materials as a control technology under South African conditions.

3   PROJECT DELIVERABLES

The deliverables for this project comprise:

Section 1:   Processes Which Give Rise to Contaminated Drainage From Coarse Sulphide-containing Wastes and the Development of an Approach to Drainage Predictions

This Section provides a description of the processes which influence drainage characteristics from coarse waste piles. The proposed method of approach to the prediction of the drainage characteristics, is briefly outlined. This Section provides essential background information to the model which is described in Section 2. The proposed approach to the prediction of pollution loads incorporates the results of static tests (acid base accounting), a small-scale physical model or kinetic test, and a computer based mathematical model.

Section 2:   A Model to Predict Pollution Loads From Coarse Sulphide-containing Wastes

This Section focuses on the development of the model and describes the mathematical sub-models which have been developed or incorporated into the prediction model, Salmine. Section 2 also describes the field and laboratory test programme which was undertaken as part of this project to evaluate and develop a suitable kinetic test method for coarse wastes. The proposed kinetic test apparatus can be applied to assess a range of parameters required as input to the computer model. The model is obtainable on diskette. A demonstration example of the application of the Salmine model is also presented.

Section 3 :   The Practicality of Subaqueous Disposal of Sulphide-containing Materials as a Control technology under South African Conditions

This Section comprises a report on the conditions required to achieve effective control of the drainage quality by applying subaqueous disposal as a control technology. The aspect of the project is not specific to coarse waste materials.

4 METHODOLOGY

The project was divided into three aspects which proceeded concurrently. These aspects are briefly described below:

Literature Review:

The literature review addressed the following:

- The processes associated with acid rock drainage including sulphide oxidation, neutralisation, migration of water and flushing of contaminants.

- Mathematical models which have been developed to represent the above processes to predict drainage characteristics.

- Static and kinetic testing methods which have been applied to coarse wastes.

- The theory of subaqueous disposal and the requirements for effective subaqueous disposal.

Field and Laboratory Tests

Laboratory and field test trials were set up to evaluate small-scale physical models and kinetic test procedures. During the course of the project, a more sophisticated test apparatus was developed to suit the specific requirements of the Salmine

model. Materials for the tests were taken from two mines one of which was believed to be strongly acid generating and the other, net alkaline. The laboratory tests were run over a period of 18 weeks with alternate wetting and drying cycles. The field tests were run at the Mines over a period of 77 weeks. Field tests were subjected to natural rainfall and evaporation.

Development of the Mathematical Model

A computer-based mathematical model was developed to assist in predicting the mine drainage characteristics. The model was developed in a spreadsheet format for use in the Windows application, Excel version 5.0. The computer model simulates some of the physical and chemical processes which cannot readily be represented (within the constraints of reasonable test times and costs) by the proposed kinetic test procedure. The computer model is, therefore, used to a large extent to extrapolate the results of the kinetic tests, to the large scale waste pile.

The computer model was then evaluated by applying the model to selected situations and assessing the reasonableness of the results. Large-scale tests to fully assess the model were not included as part of this project due to cost constraints.

CHAPTER TWO

PROCESSES WHICH GIVE RISE TO

CONTAMINATED DRAINAGE FROM

COARSE SULPHIDE-CONTAINING WASTES

1   INTRODUCTION

This chapter provides background information to understand the processes associated with the acid rock drainage (ARD) problem. The following aspects are addressed:

*   The key differences between coarse and fine sulphide-containing waste material is described.

*   The effect of mining on the relative rates at which various processes influence drainage water quality, is discussed.

*   The processes active in a coarse sulphide-containing waste which give rise to acid rock drainage, (ARD) are described.

*   An approach to the prediction of drainage characteristics from coarse wastes, which involves a combination of static tests, kinetic tests and mathematical modelling, and which forms the basis of the prediction model developed in this project, is outlined.

2 COARSE VERSUS FINE SULPHIDE-CONTAINING WASTE MATERIALS

The focus of this project is on the prediction of the water quality in *coarse* sulphide waste materials such as spoil piles. Fine wastes, such as tailings, typically fall into the particle size range $2\mu m$ to 2mm, representing the sand and silt size fractions. Coarse waste, typically shows a greater diversity of grading envelopes with particle sizes often varying from the clay size fraction, through to the boulder size fraction, over a relatively short distance. The grading envelope in coarse wastes exhibits considerable spatial variability in both the horizontal and vertical directions. The implication of the differences in the particle size distributions between coarse and fine wastes are as follows:

- Coarse wastes typically exhibit a higher *permeability* resulting in enhanced air and seepage flux.

- Coarse wastes exhibit a high *spatial variability* with respect to geochemical parameters, often resulting in frequent localised hot spots or zones in which the sulphide oxidation reaction proceeds at an elevated rate compared to the that in the immediate surrounding zone.

- Coarse wastes are subject to a greater variety of mechanisms by which *oxygen* is *transported* into the waste. The relative contribution of each oxygen supply mechanism may change from waste to waste and time to time.

- *Preferential flow* paths exist within the coarse waste which result in a large proportion of the flow taking place through a small proportion of the cross sectional area. Preferential flow paths exist due to the presence of zones of coarser or less dense material and fissures. The preferential flow paths give rise to the establishment of concentration gradients which show an increase

in the contaminant concentrations moving outwards from the main flow channels.

Based on the above, it is reasonable to expect the results of water quality monitoring of a coarse waste to exhibit considerably higher variability in space and in time than is the case for a tailings dam which has greater homogeneity. The prediction methodology applied should therefore take into consideration the variability implicit in the parameters, and be capable of predicting the range of likely contaminant concentrations or loads.

3 THE EFFECT OF MINING ON THE RELATIVE RATES OF ARD PROCESSES

The key rates which determine or control the drainage water quality may be summarised as follows:

- The rate of sulphide oxidation or the rate at which contaminants are produced as a direct result of the oxidation process.

- The rate of depletion of sulphide minerals within the waste.

- The rate or proportion of available oxidation products which are removed or flushed from the particle surfaces by percolating water.

- The water flux, or quantity of water per unit time period.

- The rate of depletion of neutralising minerals which buffer the pH of the drainage water as it percolates through the waste and passes over the surfaces of the neutralising minerals.

- The rate at which secondary metals are leached from the waste. For the

purposes of this document, secondary metals are considered to be metals which are not bound as sulphide minerals (e.g. Cd, Hg, Cr etc.) but which become soluble due to the establishment of favourable conditions for their dissolution as a result of the acid generation process.

The rates listed above are in turn dependent on a variety of secondary processes. For example, the sulphide oxidation rate is dependent on amongst other factors, the oxygen flux into the waste.

As a result of mining operations, certain fundamental changes take place which cause the sulphide-containing material, which prior to the mining operation might have had a negligible effect on the drainage water quality, to start producing contaminated drainage. The most significant physical changes which take place as a result of mining include :

- A change in the spatial distribution of various geochemical units. For example, in the case of a dragline operation, it is common for the profile to be inverted as a consequence of mining resulting in fresh sulphide minerals near the surface, overlying weathered material at depth within the pit.

- An increase in the porosity, and in particular the air-filled porosity. This in turn results in an increased air flux. The increased porosity results from the bulking process which takes place during excavation of the material from the natural state.

- An increase in the specific surface area of the rock material, thus exposing a greater quantity of fresh un-oxidised minerals.

The extent to which these changes take place, and the relative effect of these changes on various rates or processes listed above, ultimately determines the drainage water characteristics.

4 AN OVERVIEW OF THE PROCESSES WHICH GIVE RISE TO ARD IN COARSE SULPHIDE-CONTAINING WASTES

4.1 Introduction

There are a wide range of factors or processes which may influence the drainage water quality. Of these, the following are considered the most significant:

- The characteristics of the sulphide minerals.

- The characteristics of the neutralising minerals.

- The physical characteristics of the waste material including the particle size distribution, porosity, permeability etc.

- Hydrological and geohydrological factors such as the frequency and rate of flushing of water through the waste material.

- Biological factors including the presence of microbes and roots, decomposing organic matter, sulphate reducing bacteria and sulphide oxidising bacteria.

- The presence of secondary minerals, (other than those directly involved in the sulphide oxidation or neutralisation reactions), which may give rise to leaching of additional contaminants.

The above factors and processes are described in greater detail in the proceeding sections.

4.2 Sulphide Characteristics

4.2.1 Sulphide Mineralogy

Types of Sulphide Minerals

Sulphide minerals include any mineral in which sulphur is combined with a metal without oxygen. Examples of commonly encountered sulphide minerals, their chemical composition and aqueous end products after complete oxidation are summarised in Table 1(*BC AMD Task Force, Draft Technical Guide, Vol 1*).

Table 1: Common Sulphide Minerals

Mineral	*Composition*	*Aqueous End Products of Complete Oxidation*
Pyrite	FeS_2	Fe^{3+}, SO_4^{2-}, H^+
Pyrrhotite	$Fe_{1-x}S$	Fe^{3+}, SO_4^{2-}, H^+
Marcasite	FeS_2	Fe^{3+}, SO_4^{2-}, H^+
Smythite, Greigite	Fe_3S_4	Fe^{3+}, SO_4^{2-}, H^+
Mackinawite	FeS	Fe^{3+}, SO_4^{2-}, H^+
Amorphous	FeS	Fe^{3+}, SO_4^{2-}, H^+
Chalcopyrite	$CuFeS_2$	$Cu^{2+}, Fe^{3+}, SO_4^{2-}, H^+$
Chalcocite	Cu_2S	Cu^{2+}, SO_4^{2-}, H^+
Bornite	Cu_5FeS_4	$Cu^{2+}, Fe^{3+}, SO_4^{2-}, H^+$
Arsenopyrite	$FeAsS$	$AsO_4^{3-}, Fe^{3+}, SO_4^{2-}, H^+$
Galena	PbS	Pb^{2+}, SO_4^{2-}, H^+

A knowledge of the types of sulphide minerals present in the mine waste provides valuable information in predicting the types of metal contaminants likely to be released from the waste.

Sulphide Crystal Form

The crystalline form of the sulphide mineral may vary from amorphous or non-crystalline forms, such as that typically formed in near surface, low temperature environments (such as peat bogs), to massive crystalline forms which may be formed in deep, high temperature environments. Amorphous sulphides, due to their high specific surface area, will oxidise rapidly once placed in an oxidising environment, compared to massive pyrite crystals.

Alteration of one sulphide mineral form to another, may result in the formation of fine raspberry-like ball shaped crystals known as framboids. This crystal form renders the sulphide highly reactive and would be expected to result in a high rate of sulphide oxidation. The crystalline form, and in particular, the surface area of the sulphide crystals is thus a key factor affecting the rate of sulphide oxidation.

The distribution of the sulphide minerals within the host rock may further affect the rate of sulphide oxidation. The rate of sulphide oxidation in waste in which the sulphides are uniformly distributed throughout the host rock is likely to differ significantly from a waste in which the sulphides are concentrated and restricted to particular geological zones.

4.2.2 Stoichiometry of the Oxidation Reaction

The reactions of acid generation may be illustrated by examining the oxidation of pyrite. Reaction (1), represents the oxidation of pyrite to form dissolved ferrous iron, sulphate and hydrogen.

$$FeS_2 + 7/2\ O_2 + H_2O \rightarrow Fe^{2+} + 2SO_4^{2-} + 2H^+ \tag{1}$$
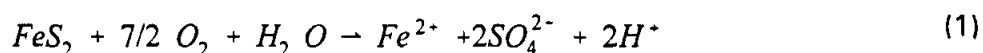
The ferrous iron, (Fe^{2+}) may be oxidised to ferric iron, (Fe^{3+}) if the conditions are sufficiently oxidising, as illustrated by reaction (2).

$$Fe^{2+} + 1/4 \ O_2 + H^+ \rightarrow Fe^{3+} + 1/2H_2O \qquad (2)$$
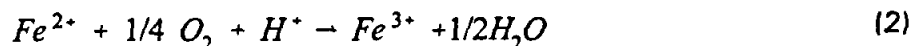
Depending on the pH, ferric iron (Fe^{3+}) may oxidise additional pyrite as illustrated by reaction (3).

$$FeS_2 + 14Fe^{3+} + 8H_2O \rightarrow 15Fe^{2+} + 2SO_4^{2-} + 16H^+ \qquad (3)$$
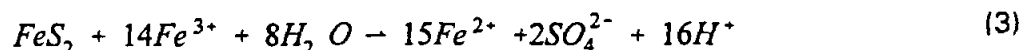
At a pH above approximately 3,5, ferric iron will precipitate as $Fe(OH)_3$, resulting in minimal Fe^{3+} remaining in solution. The precipitation reaction results in increased proton acidity as illustrated by reaction (4).

$$Fe^{3+} + 3H_2O \rightarrow Fe(OH)_3(Solid) + 3H^+ \qquad (4)$$
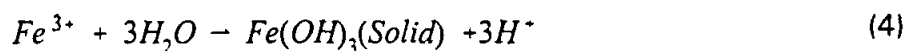
Based on the above somewhat simplified reactions, the stoichiometry of the oxidation reaction may be represented by reaction (5) or (6) depending on whether or not, $Fe(OH)_3$ precipitates.

$$FeS_2 + 15/4O_2 + 7/2H_2O \rightarrow Fe(OH)_3 + 2SO_4^{2-} + 4H^+ \qquad (5)$$

$$FeS_2 + 15/8O_2 + 13/2Fe^{3+} + 17/4H_2O \rightarrow 15/2Fe^{2+} + + 2SO_4^{2-} + 17/2H^+ \qquad (6)$$
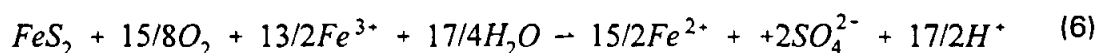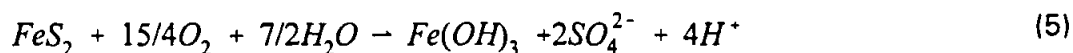
If the pH is above approximately 3,5, then more proton acidity (H^+) will be produced but the iron will tend to precipitate. At lower pH's, iron will tend to remain in the aqueous phase, and less proton acidity will be released. Irrespective of the pH range, 2 moles of sulphate are produced for every mole of pyrite oxidised.

The oxidation reaction stoichiometry is further complicated since both biological (bacterially catalysed) and abiotic (electrochemical) reactions take place. However the overall oxidation reaction of pyrite for both mechanisms is as per equation (1). Within a waste pile, the different reactions represented above may however, take place at different locations and times.

4.2.3 Limiting reagents

In many cases the rate at which the sulphide oxidation reaction takes place is primarily retarded by the rate at which the reagents (water or oxygen) are supplied to the reactive sites within the waste facility. It is useful to understand the extent to which water or oxygen may control the sulphide oxidation rate by considering the number of times that the air or water, present within the voids of the waste, must be replaced in order to supply enough oxygen and water to oxidise all the sulphide present within the material. This may be ascertained by determining whether or not the quantity of each reagent in the voids is very much less than the total quantity of reagent required to oxidise all the sulphide present in the waste. If this is the case, then it is likely that the reagent flux into the waste will control the sulphide oxidation reaction rate.

The number of times that the oxygen contained in the waste voids must be replaced in order to supply just sufficient oxygen to oxidise all the pyrite, is referred to as the number of pore volume replacements (PVR). The calculation of the PVR is given by equation (7).

$$PVR = \frac{32. \, C_{pyrite} \cdot \rho_{water} \cdot G_s \cdot Y}{e \, [\rho_{oxygen} \, (1-S) + \Upsilon_{oxygen} \cdot S]} \tag{7}$$

Where

PVR	=	pore volume replacements required to supply sufficient oxygen to oxidise the pyrite
ρ_{oxygen}	=	maximum concentration of oxygen in the atmosphere (g/m^3)
Υ_{oxygen}	=	maximum dissolved oxygen content in water (g/m^3)
Y	=	moles of O_2 required to oxidise 1 mole of the sulphide mineral
G_s	=	Specific gravity of the waste material (dimensionless)
e	=	void ratio
S	=	degree of saturation
C_{pyrite}	=	concentration of pyrite (grams/kg waste)

If, in the above expression, the value of the term $(\Upsilon_{oxygen}.S)$ is greater than the value of $\rho_{oxygen}(1-S)$, then the predominant oxygen supply mechanism is the supply of oxygen as dissolved oxygen in migrating water, or the diffusion of oxygen through the water-filled pore spaces.

The PVR for a range of degrees of saturation and void ratios are shown in Figure 1.
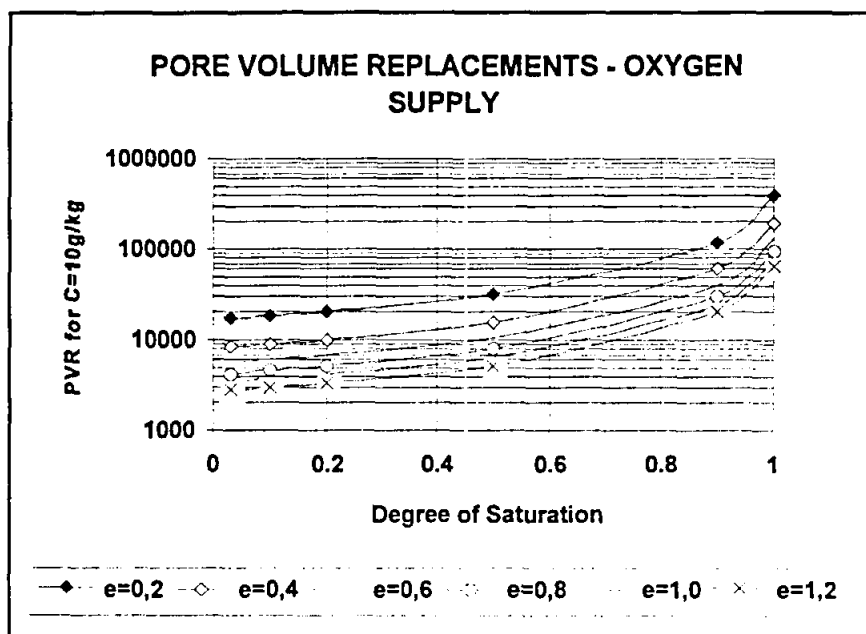
Figure 1: Pore Volume Replacements as a Function of the Void Ratio and Degree of Saturation

It should be noted from the Figure 1, that if typical values for e and S are plotted for coarse sulphide waste, relatively high values for PVR result indicating that in almost all waste facilities, the oxygen flux is likely to be the rate controlling step.

Figure 2 illustrates the relationship between the number of times that pore water, (assumed to be in the liquid phase only) must be replaced to provide just sufficient water to completely oxidise the sulphide. This is referred to as the number of pore water replacements or PWR. An equation to calculate PWR is given by:

$$PWR = \frac{R_{water} \cdot C_{pyrite} \cdot (1+e)}{w}$$

where C_{pyrite} = concentration of pyrite (g/kg bed)

w = moisture content

e = void ratio

(8)

R_{water} = stoichiometric ratio water/sulphide (g water/g sulphide)
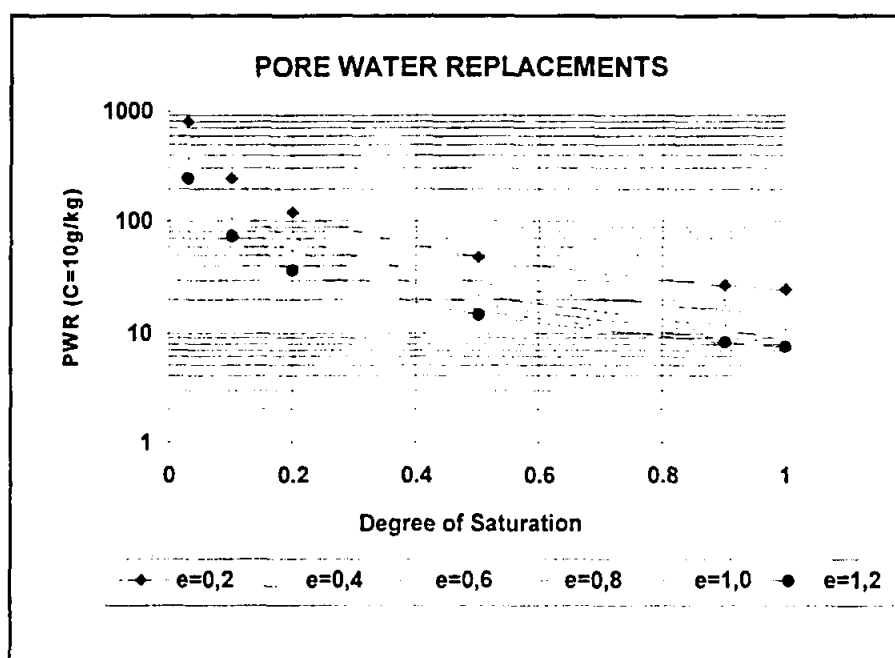
Figure 2:Pore Water Replacement as a Function of void Ratio and Degree of Saturation

From Figure's 1 and 2 it can be seen that the PWR value is always considerably less than the PVR value for any value of e or S. Even for a relatively dry material, at a degree of saturation of 0,1, the PWR value is between 100 and 500, but the corresponding PVR value, is between 6000 and 40 000. It can therefore be concluded that water will not be the limiting reagent in practically all waste piles and it is therefore not necessary to consider the water flux from the point of view of modelling the sulphide oxidation rate. Oxygen, on the other hand, could be a limiting reagent in cases where the PVR value is high and/ or, where the oxygen flux into the waste pile is low. The inclusion of an oxygen flux model is therefore generally an essential part of the prediction model.

4.2.4 Reaction Kinetics

There are many factors which affect the rate at which sulphide oxidation takes place including :

- *Temperature:-* In the case of abiotic oxidation the reaction rate approximately doubles for every 10° C increase in temperature (SRK,Mine Rock Guidelines,1989). The reaction rate for biological and abiotic oxidation is zero below 0°C. There is an optimal temperature range for bacterial oxidation in the region of 20 to 40°C (SRK,Mine Rock Guidelines,1989)

- *pH:-* The chemical reaction rate for the oxidation of pyrite and pyrrhotite has been shown to be a weak function of pH (McKibben and Barnes 1986).

- *Oxygen concentration at the sulphide mineral surface within the rock fragment:-* The diffusion of oxygen through the rock particles to the reactive front has been represented as a shrinking core model (Cathles and Apps 1975). The sulphide oxidation rate is proportional to the oxygen concentration at the surface of reactive particles.

- *Sulphide type and specific surface area:-* Sulphide minerals with a high specific surface area tend to react more rapidly compared to those with a low specific surface area.

In the case of biological oxidation, the following additional factors are important (BC AMD Task Force, Draft Technical Guide, Vol1.) :

- The availability of a source of carbon for cell growth.

- The partial pressure of carbon dioxide within the waste material.

- The availability of nutrients such as nitrogen and phosphorous.

The diversity and range of factors which influence the sulphide oxidation rate, renders the development of a mathematical model to represent all of these factors, very difficult. Even if such a mathematical model could be developed, the data requirements needed for input and calibration of such a model would prove too onerous. A preferred approach is therefore to apply some physical model or set of models to determine empirical data to represent the reaction rate under specific conditions, and model the sulphide oxidate rate using a simplified mathematical model.

The oxidation rate may be measured by monitoring the rate of consumption of oxygen with time (using a dissolved oxygen analyser) (Liljedahl 1984). The reaction rate constant is defined as :

$$k' = \frac{r_{oxygen}}{a_{sulphide} \cdot C_a}$$

(9)

Where: k' = reaction rate constant (m^3 gas/m^2 sulphide surface.s)

r_{oxygen} = oxygen consumption rate ($mol.m^{-3}$ material.s^{-1})

$a_{sulphide}$ = the sulphide surface area available for reaction (m^2)

C_a = oxygen concentration ($mol.m^{-3}$ gas)

To estimate the area of sulphide available for the reaction it is necessary to know the sulphide concentration, specific particle surface area and porosity of the sample. To avoid this complexity it is more common to determine the reaction rate k_r (m^3 gas/m^3 material.s) which is defined as :

$$k_r = k' \cdot a_{sulphide}$$

(10)

Provided that the sample tested is representative of the particle specific surface area, particle size distribution, density and sulphide concentration, the value of k_r can be used rather than k'.

The value of k_r varies and is dependent on the influence of factors such as those listed above. The simple approach described above (Liljedahl, 1984), can be applied to take cognisance of several parameters which affect the sulphide oxidation rate, such as the temperature and particle specific surface area, but it is an oversimplification in the case of coarse wastes. The proposed approach is to measure the sulphide oxidation rate on a sample of the waste which is representative with respect to as many of the parameters which influence the sulphide oxidation rate as is practically feasible. A laboratory scale test is required to facilitate the measurement of the reaction rate k_r.

4.3 The Oxygen Flux through the Waste Pile

4.3.1 Oxygen Flux Mechanisms

In most coarse wastes, the rate of supply of oxygen to the surface of reacting particles is the rate controlling step. There are several mechanisms or processes which determine the oxygen flux into a waste site, namely:

- Diffusion of oxygen through the air or water-filled portion of pore spaces.

- Advective transport of oxygen as dissolved oxygen in water through infiltrating water.

- Advective transport of oxygen through pore spaces with the driving head caused by either pressure equilibration between the atmosphere and the pressure in the air filled pore spaces of the waste material, or convection due to heating as a result of the exothermic reactions of sulphide oxidation or spontaneous coal combustion.

The relative importance of each of these mechanisms is site specific and is dependent on a number of parameters. In the case of saturated wastes or wastes under water, in which the water flux through the waste is negligible, the oxygen

flux will be controlled by the diffusivity of oxygen in water. The diffusivity of oxygen in water is approximately 10 000 times less than the diffusivity of oxygen in air. Since coarse waste typically have a relatively low degree of saturation, the contribution to the oxygen flux due to diffusion through water-filled pore spaces can generally be ignored as it represents a negligible proportion of the total oxygen flux.

Where the water flux through the waste is significant, for example, where wastes are placed below the level of the phreatic surface, the oxygen flux will be determined by the product of the water flux and the solubility of oxygen in water. This mechanism of oxygen transport will predominate, only in saturated or near saturated wastes.

Advective transport of oxygen as a result of rapid equilibration of pressure gradients caused by di-urnal and frontal atmospheric pressure changes, is particularly important in unsaturated waste materials in which the resistance to air flow, along preferential flow paths is low. This results in the rapid influx or expulsion of air from the air filled voids to equilibrate the pressure. Preferential flow paths for air flow through coarse wastes may comprise :

- settlement and shrinkage cracks

- zones where materials have segregated

- holes caused by burrowing animals and plant roots.

4.3.2 Determination of the Dominant Oxygen Flux Mechanism

A number of simple relationships have been derived to estimate the relative importance of each of the oxygen flux mechanisms described above for particular situations. These relationships are presented in Appendix A. It is essential that calculations be performed to ascertain which of the oxygen flux mechanisms will predominate since most prediction models represent only one particular oxygen flux mechanism. The predominant oxygen flux mechanism may change from time to time, as a result of changes brought about due to the application of an ARD

control, or due to natural changes which take place within the waste pile. To illustrate this point, consider a coarse waste which is covered by a plastic membrane in order to reduce the sulphide oxidation rate. Prior to the application of the cover, the predominant oxygen supply mechanism is likely to be diffusion of oxygen through air-filled void spaces. After the application of the cover, the predominant oxygen flux mechanism is likely to be advective transport driven by rapid pressure equilibration. Since the oxygen diffusion rate through the plastic membrane is negligible, air can only be driven through the holes in the membrane due to pressure gradients which are established between the air-filled void spaces under the cover, and the atmosphere, above the cover.

4.4   Neutralisation

4.4.1 Types of Neutralising Minerals

A list of common neutralising minerals is summarised in Table 2,(*BC AMD Task Force, Draft Technical Guide, Vol. 1*). Of the listed minerals, Calcite ($CaCO_3$) is the most commonly occurring mineral in nature. Should limitations need to be imposed in terms of the number of neutralising minerals which can be included in the prediction model, the selection of calcite as the neutralising mineral would therefore comprise the most reasonable choice.

Table 2: Acid Consuming Minerals and Their Neutralising Characteristics

Mineral	Composition	Acid Consuming Potential*	Buffer pH
Calcite, Aragonite	$CaCO_3$	100	5.5-6.9
Siderite	$FeCO_3$	116	5.1 -6.0
magnesite	$MgCO_3$	84	-
Rhodochrosite	$MnCO_3$	115	-
Witherite	$BaCO_3$	196	-
Ankerite	$CaFe(CO_3)_2$	108	-
Dolomite	$MgCa(CO_3)_2$	92	-
Malachite	$Cu_2CO_3(OH)_2$	74	5.1 -6.0
Gibbsite	$Al(OH)_3$	26	4,3 -3.7
Limonite/Geothite	$FeOOH$	89	3.0 -3.7
Manganite	$MnOOH$	88	-
Brucite	$Mg(OH)_2$	29	-

* Acid consuming potential is given as the weight (kg) of the mineral required to have the same neutralising effect as 100kg calcite. Note that the different minerals neutralise the acidity to different equilibrium pH's.

4.4.2 Neutralisation Reactions

The extent and direction in which a reaction proceeds is determined by the thermodynamics of the system in which the reaction takes place. The equilibrium constant defines the ratio of the concentrations of reactants and products as shown in equation (11).

$$sX + tY \rightharpoonup uZ \qquad k=\frac{[Z]^u}{[X]^s +[Y]^t} \qquad (11)$$

The equilibrium condition represents a final state or boundary condition to which reactions will proceed. The rate at which this reaction proceeds to the equilibrium point is however controlled by the reaction kinetics. From the point of view of predicting the water quality, it is necessary to select either a thermodynamic model or a kinetic model for the reactions. In general, since the equilibrium condition for neutralisation reactions is reached within a short period of time relative to the rate at which other factors change, it is reasonable to apply a thermodynamic model to the neutralisation process.

Reaction (12) presented below for the neutralising mineral calcite illustrates the typical reactions and reaction products. Under strongly acidic conditions, the acidity generated from the oxidation of sulphides is neutralised by $CaCO_3$ according to the following reaction (*Day, 1994*):

$$CaCO_3 + 2H^+ - Ca^{2+} + H_2CO_3^0 \text{ or } CO_2 \text{ (g)} + H_2O \tag{12}$$

Under mildly acidic to mildly alkaline conditions, the reaction will be as follows:

$$CaCO_3 + H^+ - Ca^{2+} + HCO_3^- \tag{13}$$
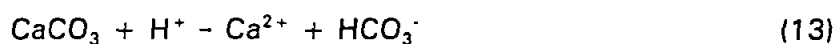
Since 2 moles of sulphate and proton acidity (H^+) are produced per mole of pyrite oxidised, the molar ratio of calcium to sulphate in the drainage water would be expected to be less than or equal to 1 under strongly acidic conditions. Uunder less acidic conditions the ratio will be greater than 1 due to the formation of bicarbonate as shown in reaction (13).

The variable rate at which calcite is consumed according to reactions (12) and (13) implies that the prediction of the mass of neutralising minerals required to neutralise the acidity generated by the oxidation of sulphide minerals is dependent on the acidity present in the pore water.

Data from eastern United States Coal mines has indicated that the ratio of neutralising potential to potential acidity in waste rock should be at least 2,4 (*Cravotta et al. 1990*). Tests using a range of mixtures of acid consuming rock

have shown that for an intimately mixed sample of limestone and acid generating rocks, the actual quantity of limestone required to prevent acid mine drainage in perpetuity would probably be at least twice that determined by conventional acid base accounting (*Day 1994*).

4.4.3 Location of Sulphide Minerals in Relation to Neutralising Minerals and the Influence Geochemical Homogeneity

The spatial relationship between acid generating and acid consuming minerals in relation to the water flow path can profoundly effect the quality of resultant mine drainage. If the neutralising minerals are located upstream of the acid generating minerals in the waste pile, then the neutralising potential of the migrating pore water, on entering the acid generating zone is limited by the extent to which the neutralising mineral will dissolve in order to reach chemical equilibrium. The prediction model needs to be able to take cognisance of the spatial variability in the location of neutralising minerals relative to acid generating minerals. An example which illustrates the effect that the relative location of acid generating and neutralising minerals can have on the rate of dissolution of neutralising minerals, is given in Appendix B.

The greater the heterogeneity of the material, the less of the total calcareous material is available for neutralisation. This may arise due to cementing of the finer calcareous material once the material above the layer of calcareous material becomes acidic (*Day et al, 1994*). It is proposed that a laboratory test procedure be developed to empirically ascertain the proportion of neutralising minerals available for dissolution.

4.4.4 Armouring of Neutralising Minerals

The extent to which neutralising minerals are available to neutralise acidity may be further reduced by armouring of the neutralising rocks. Armouring occurs when a layer of metal hydroxide precipitates or is absorbed onto the surface of the neutralising mineral thus forming a barrier between the acidic water and the neutralising mineral, thereby reducing the rate at which the neutralisation reaction

can proceed. Armouring usually occurs along flow channels where the redox potential and pH conditions change to favour precipitation of salts, such as metal hydroxides. Armouring by $Fe(OH)_3$ for example, is often observed as a reddish brown precipitate on the surface of particles and is particularly prevalent downstream of seeps. The precipitation process results in increased acidity in the resultant drainage water as illustrated by reaction (15):

$$Fe^{3+} + 3H_2O \rightarrow Fe(OH)_3 \downarrow (solid) + 3H^+ \tag{15}$$
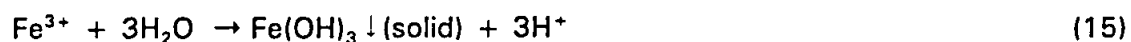
The development of a rigorous mathematical model to predict the extent to which armouring reduces the neutralisation capacity and neutralisation rate is likely to be very complex.

The conditions with respect to precipitation of solids and armouring, in a small laboratory-scale test, are generally not representative of those in the large-scale waste pile. In particular, the redox potential and pH of the pore water in a small-scale laboratory test is likely to differ significantly from that in the waste pile, or at different locations within the waste pile. The rate or extent to which neutralising minerals become armoured in a small-scale laboratory test may therefore not be relevant to the large-scale test. The armouring process could therefore present a significant added complexity in the prediction of drainage water characteristics.

4.5 Geotechnical and Physical Characteristics of the Waste Material

The geotechnical and physical characteristics of the waste, in particular, the particle size distribution, air and water permeability, moisture content, porosity and depth of the waste, have a significant influence on the other mechanisms or processes which control the drainage water characteristics.

The prediction of mine drainage characteristics requires an assessment of these parameters either through laboratory or field measurements, or by using the data from another similar site. The influence of the more important physical and geotechnical parameters on other mechanisms and processes is outlined in the

following section. The method of determining the appropriate values for the physical parameters is briefly described.

4.5.1 Particle Size Distribution

The particle size distribution has a major influence on :

- The particle specific surface area and hence the rate and extent of oxidation, neutralisation and secondary metal leaching.

- The air and water permeability, which in turn affects the water and air flux.

- The extent to which particles are flushed of stored contaminants and the development of preferential flow channels.

4.5.2 Water Permeability

The water permeability affects several parameters which influence mine drainage characteristics including:

- The quantity of mine drainage which will emanate from the waste facility, measured over a short period of time (eg. $m^3.hour^{-1}$).

- The retention time of the water within the waste facility, which can exceed several years.

- The moisture content of the waste or particular layers of the waste. Since permeability affects the retention time of moisture within the material or a layer of the material, water may either accumulate within the material during periods of high infiltration or decrease during dry periods.

The permeability of a porous medium depends on the structure of the pore system available for flow. The permeability of a saturated material is defined by D' Arcy's Law which states that:

$$q = k\frac{\Delta h}{\Delta l}$$ (16)

Where : q = water flux or flow rate $(m^3.m^{-2}.s^{-1})$

k = permeability $(m.s^{-1})$

Δh = head loss (m)

Δl = flow path length (m)

Since in most coarse wastes, unsaturated conditions prevail, cognisance must be taken of the effect of negative pore pressures and volumetric water content on the permeability. Figure 3 illustrates the relationship between the hydraulic conductivity and the pore pressure head, for a fine silty clay material and a uniform sand. As the volumetric water content decreases, so the number of connected channels available for flow decreases thus reducing the permeability of the material. The permeability of the material for degrees of saturation below unity, is usually modelled as a function of the saturated permeability and therefore requires the determination of this parameter. Methods to determine the saturated permeability of materials are briefly described in Appendix C.

4.5.3 Air Permeability

The oxygen flux, which is a function of the air permeability, may be limited or effectively cut off due to the presence of low air permeability layers above the reactive waste.

The air permeability of a porous material may be calculated from the following expression which assumes steady state conditions and a constant pressure head difference.

$$q_{air} = \frac{k_a}{\mu_a}.\frac{\Delta p}{l}$$ (18)

Where: q_{air} = air flux $(m^3.m^{-2}.s^{-1})$

k_a = air permeability of the porous material $(m.s^{-1})$

μ_a = *fluid viscosity ($Ns.m^{-2}$)*

l = *thickness of the layer (m)*

Δp = *pressure change (Pa)*

According to Corey (1954) the air permeability varies with degree of saturation as:

$$k_a \propto (1-S)^2.(1-S^2) \tag{19}$$

where S = *degree of saturation based on the effective porosity for the flow.*

The existence of preferential flow paths, such as worm holes, cracks and fissures may dramatically increase the air permeability.

Since the permeability depends on the structure of pores available for flow, the air permeability of a dry (S = 0) waste is approximately equal to the saturated water permeability.

Thus, the air permeability may be estimated from :

$$k_a = k_{a_{dry}}.(1-S)^2.(1-S^2) \tag{20}$$
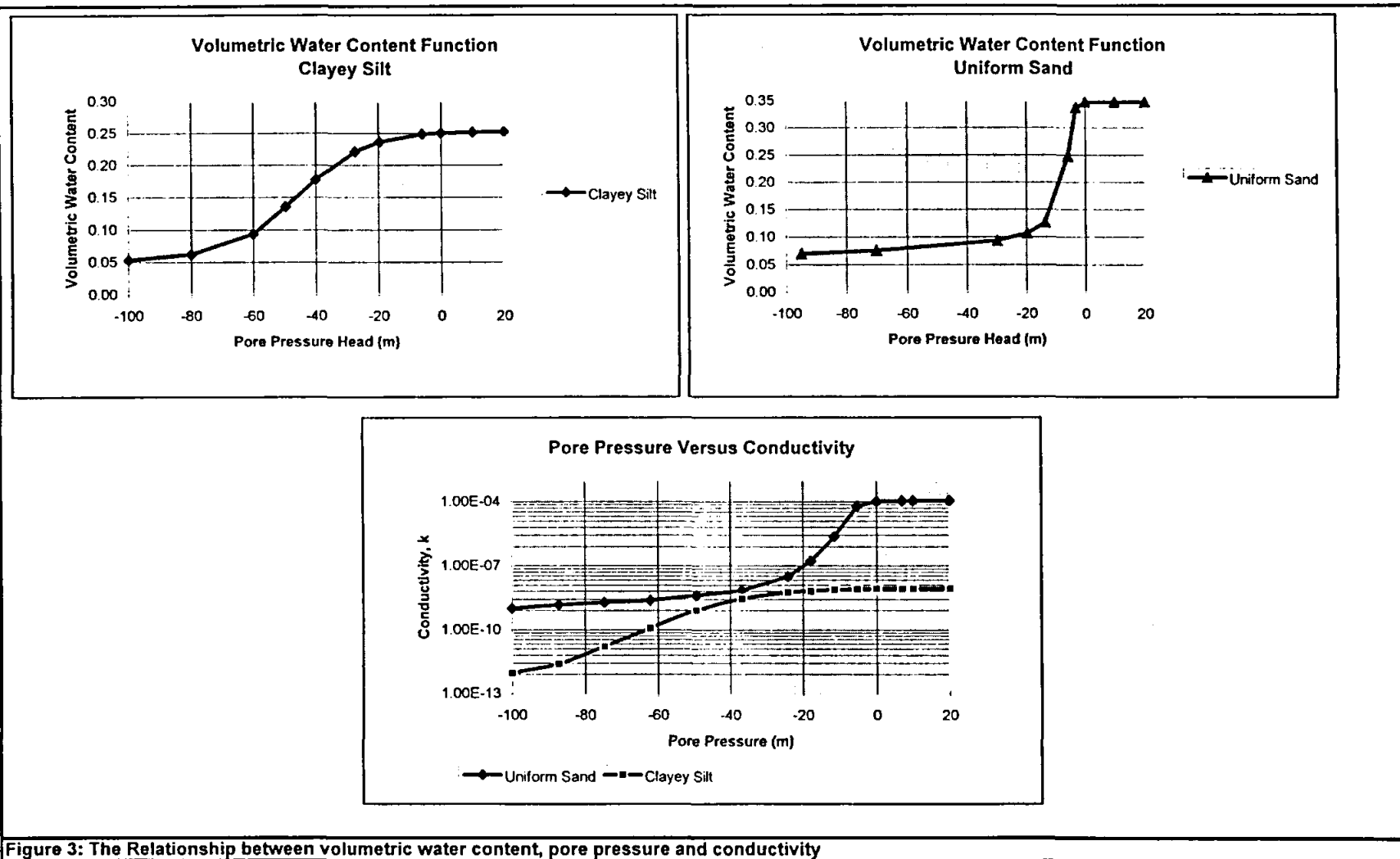
Figure 3: The Relationship between volumetric water content, pore pressure and conductivity

4.6   Hydrological Factors

4.6.1 Water Flux

The water flux may be controlled by either the permeability of the waste or the availability of water. In coarse wastes, the water flux is more often controlled by the availability of water, whereas in fine wastes, the permeability of the waste may determine the average water flux. Whereas infiltration events are typically intense and of short duration, the resulting flow rate in the drainage demonstrates considerably reduced peak flow rates due to the storativity provided by the unsaturated waste, and the limitations imposed on the flow rate by the permeability of the material. The time interval required to model infiltration due to rainfall and runoff, thus differs significantly from the time interval required to model the water flux through a waste pile.

Since the water flux through the waste pile is determined in most cases at least, by the rate and frequency of infiltration events, the net infiltration to the waste is an important parameter for the drainage prediction model.

4.6.2 Evaporation

Evaporation and capillary forces play an important role in determining the extent to which salts accumulate on the surface, and in the uppermost layers of the waste. Salts which accumulate on the ground surface during extended periods of net exfiltration (eg. the dry season) are flushed from the surface as surface runoff during the first rains of the wet season.   The first rains of a season typically give rise to the highest contaminant loads and concentrations from surface runoff.

4.7   Contaminant Mobility

4.7.1 Effectiveness of Contaminant Flushing

Preferential channels for water flow are particularly prevalent within coarse wastes and result in less frequent flushing of some surfaces and more frequent flushing of

others. It is estimated (Morin et al 1994) that for waste rock piles exceeding a few metres in height, only 5 to 10% of the surface area may be regularly flushed by infiltration events. The remaining rock surfaces may only be flushed under conditions of extreme rainfall or submergence. There is currently no direct test method available to measure the extent to which surfaces are flushed. The effectiveness of flushing may be indirectly estimated by monitoring the leachate water quality, leachate volume and sulphide oxidation rate in a column test or kinetic test apparatus.

The degree of saturation, S, is an indicator of the extent to which surfaces will come into contact with flushing water.

The following statements would apply to any waste containing readily soluble salts on the surfaces of particles:

- The total proportion of particle surfaces which are flushed per unit time period, tends to increase as the degree of saturation of waste increases.

- If the rate of removal of soluble salts exceeds the rate of generation of salts, then the concentration of contaminants in the mine drainage may decrease, once the particle surfaces along the flow channels become cleansed of previously accumulated salts.

- If the rate of removal of soluble salts is less than the rate of generation of salts, then the mass of soluble salts which accumulate within the waste will tend to increase, as will the concentration of contaminants in the resulting drainage. At some point, chemical saturation with respect to one or more precipitates will be reached and the concentration of contaminants in the drainage water will tend to remain constant until either the solubility changes (due for example, to a change in the pH), or until the rate of generation of salts decreases.

4.7.2 Frequency of Flushing

The time lapse between infiltration events is significant since it affects the extent to which oxidation products accumulate within the waste, on the particle surfaces and within the flow channels. If prolonged periods with little infiltration prevail, the concentration of contaminants in the drainage would be expected to be considerably higher (excluding the effect of chemical saturation), than would be the case if the material were subject to more frequent flushing. This peak in the contaminant load and concentration is often observed in South Africa and elsewhere at the start of the wet season. The prediction model needs therefore to be capable of simulating variations and temporal changes in the net infiltration rate.

Concentration gradients develop outwards from the most frequently flushed flow paths. During wetter periods, the number of flow paths along which movement of water takes place, increases as flow paths adjacent to and draining into the most frequently flushed paths, become active. The high salt loads typically observed in seepage at the start of the wet season, can be explained by the increased number of flow paths subject to flow and hence flushing. The preferential flow paths can therefore not be represented as a separate entity with respect to the prediction of the drainage characteristics. The water quality along the preferential flow paths is a complex function of the water quality in waste surrounding the preferential flow path, and vise versa.

4.8 Biological Factors

4.8.1 Sulphide Oxidising Bacteria

The accelerated rate of acid generation as a result of certain bacteria, for example, *Thiobacillus ferrooxidans* may exceed the chemical oxidation rate several fold (Scharer et al, 1994). For bacteria to thrive, the environmental conditions for the bacteria must be suitable. Optimal environmental conditions vary from one type of bacteria to another, for example, in the case of *Thiobacillus ferrooxidans*, the ideal pH range is in the region of 3,2 , whereas for *Thiobacillus novellus*, the ideal pH range is in the neutral to alkaline range (Scharer et al, 1994). Both of the above species of bacteria are sulphur oxidising. Additional factors which influence the rate

of acid generation in situations where bacterially enhanced oxidation is prevalent include:

- The nitrate, phosphorus, ammonia and carbon dioxide concentrations.
- Organic carbon availability.
- The intensity of intra-specific competition.
- The bacterial population growth rate.
- The moisture content.
- Dissolved oxygen status.
- The concentrations of any bacterial inhibitors.
- The temperature and changes in the temperature.

The number and complexity of factors affecting the rate of biologically assisted sulphide oxidation implies that a rigorous mathematical model to represent these processes would also be very complex. An approach which incorporates some of the more important factors into a semi-empirical model, possibly based on data collected from a simple small-scale laboratory test, is likely to be the most appropriate in the case of coarse wastes.

4.8.2 Oxygen Consumption due to the Degradation of Plant Roots and Other Organic Matter

The presence of microbes which assist in the degradation of organic matter leads to the consumption of oxygen in the upper layer of soil where plant roots or other organic matter is present. This phenomenon can be used to assist in reducing the sulphide oxidation rate (such as in the case of composted organic wastes used as a cover to reduce the oxygen flux into the waste). The respiration rate due to the presence of microbes in the root or topsoil zone, should therefore be included in the drainage prediction model as this could significantly reduce the oxygen flux to the underlying sulphide-containing waste. Rates quoted in the literature range from 10^{-6} to 10^{-7} mole O_2 /m³/second.(Jaynes, 1983)

4.9   **Secondary Minerals**

Secondary metals and minerals are those which are not directly associated with the sulphide or neutralising mineral, but are present within the waste and which can be leached from the waste. In general, the solubility of metals such as nickel, copper, cadmium , lead, manganese and magnesium increases with decreasing pH. At the onset of acidic drainage, secondary metals may be leached from the rock at rates several orders of magnitude higher than would be the case under neutral drainage conditions. Additional factors which influence the rate of leaching or concentration of secondary metals in the drainage water include:

- The type of minerals containing the metals and their solubility under various pH / Eh conditions.

- The distribution and surface area of the secondary metal containing minerals.

- The pH of the solubilising mine drainage water and any changes in the pH along the path of flow. Note that an increase in the pH along the path of migration of the mine drainage water may result in re-precipitation of the metals (usually as a metal hydroxides under high Eh conditions).

Figure 4 presents the calculated metal sulphide and hydroxide solubilities for a range of metals (After Bhattacharrya et al., 1981).

The prediction of secondary metal concentrations therefore requires a prediction of in particular:

- The type, distribution and concentration of secondary metals within the waste.

- The pH and Eh conditions in the waste pile and at various locations within the waste pile.

- The extent to which migrating mine drainage water comes into contact with

minerals containing secondary metals

- The kinetics and thermodynamics of the secondary metal dissolution process.

Table 3 presents the pH of hydrolysis (hydroxide precipitation) of some elements from dilute solutions (*Britton, 1955*).

Table 3: pH of Hydrolysis for Selected Elements from Dilute Solutions

Element	pH	Element	pH	Element	pH	Element	pH
Fe^{3+}	2,0	Al^{3+}	4,1	Cd^{2+}	6,7	Pr^{3+}	7,1
Zr^{4+}	2,0	U^{6+}	4,2	Ni^{2+}	6,7	Hg^{2+}	7,3
Sn^{2+}	2,0	Cr^{3+}	5,3	Co^{2+}	6,8	Ce^{3+}	7,4
Ce^{4+}	2,7	Cu^{2+}	5,3	Y^{3+}	6,8	La^{3+}	8,4
Hg^{+}	3,0	Fe^{2+}	5,5	Sm^{3+}	6,8	Ag^{+}	7,5 -8,0
In^{3+}	3,4	Be^{2+}	5,7	Zn^{2+}	7,0	Mn^{2+}	8,5 -8,8
Th^{4+}	3,5	Pb^{2+}	6,0	Nd^{3+}	7,0	Mg^{2+}	10,5
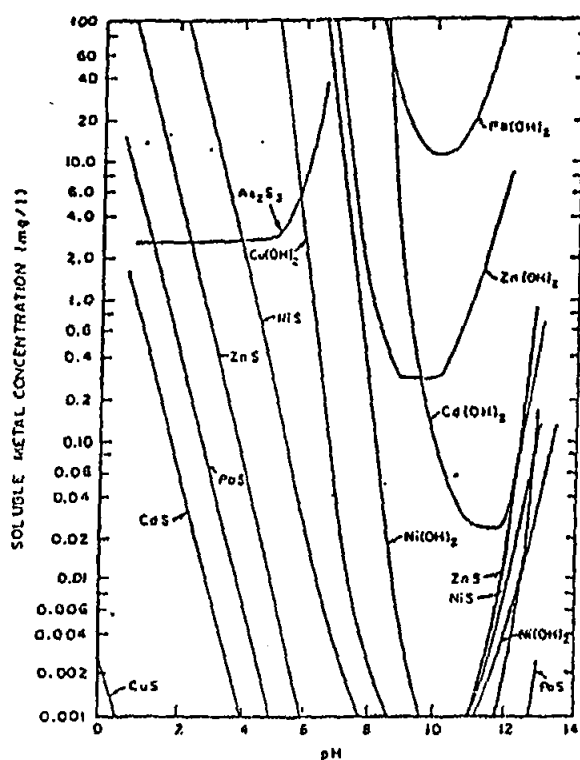
Calculated Metal Sulphide and Hydroxide Solubilities (Bhattacharrya et al., 1981)

Figure 4: Metal Sulphide and Hydroxide Solubilities

The type and concentration and distribution of secondary metals or minerals can be determined from laboratory analysis of waste samples.

The latter factors are to a large extent dependent on the ability to predict drainage water quality due to the combination of al the other factors discussed previously. If the pH and Eh within the waste pile can be predicted, it is proposed that a simple laboratory-scale leach test be applied under specific pH and possibly Eh conditions, to determine the propensity of the waste to release secondary metals into the drainage water.

5 THE PREDICTION OF POLLUTION LOADS AND THE APPLICATION OF GEOCHEMICAL TESTS AND COMPUTER MODELS

This section outlines a proposed method of approach to the prediction of pollution loads from coarse sulphide-containing wastes and shows the relevance of acid base accounting tests (ABA), kinetic tests and computer models, to the prediction of contaminant loads.

It is necessary to carry out prediction modelling to determine whether the pollution loads or drainage water quality is likely to exceed some required target value. The target value may be an effluent standard or a waste load allocation. Should it be found that the target value will be exceeded, then it is necessary to either ensure that the contaminated water is not discharged, or reduce the extent to which the water becomes contaminated in the first place. The prediction method needs therefore to be able to predict the effect of the application of a particular control, or a combination of drainage control measures. The approach outlined below uses a combination of physical tests and a computer model(s) to predict the drainage characteristics.

The stages in the approach are summarised below:

Step 1: Characterisation of the Waste Material

The waste should be characterised in terms of its acid generating and neutralising potential. This involves :

- Definition of the mass and extent of units of similar geology and mineralogy. Samples should be taken from the borehole logs (pre-mining) or from the waste material (post mining) for ABA testing. The ABA test results can be used to classify the material in terms of its acid generating and neutralising

potential. The ABA test provides an indication as to whether the drainage from a particular unit is likely to become acidic. This is based on the relative proportions of the mass of acid generating and neutralising minerals present in the rock. ABA tests cannot be used to predict process rates such as the rate of sulphide oxidation and can therefore not be used to predict drainage water quality.

• Representative samples should be selected for laboratory analysis to determine the elemental composition of the rock. This is useful in assessing the types of metals which might be leached from the waste.

Further information relating to acid base accounting tests is given in Appendix D. The detailed test procedure is documented in *BC AMD Task Force, Draft Technical Guide, Vol 1*.

Step 2 : Characterisation of the Mining Induced Mineralogical and Physical Changes

The physical, mineralogical and geochemical changes which take place as a result of mining should be predicted. The characteristics of the waste which need to be predicted include:

• The particle size distribution of the waste material.

• The relative location or distribution of the geochemical units with respect to one another in waste.

• Geochemical changes which might take place as part of the mineral processing operation, such as lime addition.

Step 3 : Characterisation of the Kinetics of the Oxidation and Neutralisation Processes

Kinetic tests can be used as a first estimate of the drainage water quality. The proposed kinetic test procedure described in Part 2 is designed to create optimal

oxidation conditions, and to measure a number of parameters relating to the oxidation, neutralisation and contaminant flushing processes. By "optimal oxidation conditions", it is meant that the oxidation rate in the test cell should be similar to the maximum oxidation rate which might occur in the field. To achieve optimal conditions, the sample may be inoculated with sulphide oxidising bacteria to ensure that bacteria are present and have the opportunity to develop. In addition, humidified oxygen-rich air, is pumped through the sample to ensure that rate of supply of oxygen, to the reactive surfaces, does not limit the rate of oxidation. The resulting oxidation reaction rate in the test cell, is therefore primarily controlled by the particle specific surface area, mineralogy and particle size distribution. It is therefore important that the test be carried out on samples of the material which are representative of the waste in the pile with respect to :

- Particle size distribution or particle specific surface area.

- Sulphide content and neutralising mineral content. (grams/kg sample)

- Mineralogy of the sulphide minerals and neutralising minerals.

- The average temperature within the waste pile.

Step 4: The Prediction of Drainage Characteristics

The drainage water quality from the kinetic test can be used as a first estimate or approximation of the water quality from the waste pile. There are however, a number of factors which operate in the field which cannot be simulated in the kinetic test, and therefore cause the water quality in the waste to differ significantly from that of the drainage from kinetic test. In order to predict the water quality emanating from a waste pile, it is necessary to either carry out a test on a larger scale (e.g. field test pile) so that the conditions in the test are more representative of the field conditions, or apply mathematical models to simulate the sulphide oxidation, contaminant flushing, neutralisation and the other processes which play a significant role in the determination of water quality on a large scale. The advantage of a large-scale physical model is that it is more representative of site

specific conditions such as the seepage regimes, flushing paths, thermal and convective air effects, which cannot be simulated using a small-scale test, such as the kinetic test cell. The disadvantages of large-scale physical models are that they are costly, case specific and time consuming. There is also very limited flexibility in the extent to which alternative drainage control measures can be evaluated. A mathematical model on the other hand, has the advantage of being able to make predictions quickly and cost effectively. It has the disadvantage that since the processes which are modelled are complex and not necessarily fully understood, many simplifying assumptions are necessary, and these processes are not accurately represented. The proposed approach for coarse sulphide- containing wastes is to use a combination of a small-scale physical model and a computer model in an attempt to get the best of both worlds. The small-scale physical model is used to ascertain the values of those parameters for which the current state of development of mathematical models is inadequate, or data collection requirements too onerous. The small-scale test presents a more reliable method of determining these parameters. A mathematical model, developed to simulate the processes which are influenced by the size of the waste pile, or take place over too long a time span to model using a physical test, is then applied to model the remaining processes.

Step 5 : Identification of Candidate Mine Drainage Control Options

Should the prediction modelling carried out as step 4, indicate that the pollution loads or concentrations are unacceptable, it will be necessary to implement control measures to reduce the pollution load to an acceptable level. A range of candidate mine drainage control measures should be evaluated based on the available knowledge regarding site conditions. Priority should be given to control measures which either reduce the rate of oxidation of the sulphide minerals, or which prevent the migration of contaminants from the waste pile, as the application of these measures usually results in the most cost effective and reliable long term control.

Consideration should be given to the effect of controls at different stages during the life of the waste pile. Emphasis should be placed on ensuring that the design is appropriate to the post closure phase as it is usually some time after mining, that

the worst conditions with respect to mine drainage quality, often occur.

Since the level of uncertainty associated with predicted mine drainage quality is generally high, consideration should be given to a stage-wise implementation of controls which enables the mine to implement additional control measures during the life of the mine should the initial selection of controls prove inadequate.

Step 6: Selection of a Combination of Suitable Control Measures for Detailed Evaluation, Design and Implementation

The effectiveness of the selected controls should be evaluated in terms of the extent to which they are likely to reduce the pollution load or concentration of the resulting drainage. This may involve:

• Kinetic tests to evaluate the effect of specific control measures such as blending, lime addition and segregation.

• Mathematical modelling, column tests or field trials as appropriate, to predict the effect of controls or combinations of controls.

Step 7 : Monitoring and Assessment of the Effectiveness of the Applied Drainage Controls.

Since extended lag times (often decades) are required before the effect of the application of a particular control, can be observed in the water quality monitoring results, it is necessary to include long-term monitoring. This should involve not only the water quality, but also the acid mine drainage parameters which the control is intended to modify. For example, if a control is intended to reduce the oxygen flux into a waste pile, it is necessary to monitor not only the drainage quality, but also the parameters which provide the information necessary to evaluate the extent to which the oxygen flux and sulphide oxidation rate is reduced by the control. This is required because the water quality need not necessarily change significantly for several years, until such time as the accumulated oxidation products within the waste pile have been effectively flushed out.

6   CONCLUSIONS

The following conclusions, relevant to the prediction of drainage characteristics from coarse wastes, may be drawn from the description of the processes described in this chapter:

- The prediction methodology applied to a problem involving a coarse material should be capable of taking into consideration the spatial variability of coarse wastes, and should be capable of predicting the likely range of contaminant concentrations or loads, rather than a single finite value.

- The extent to which changes in the material characteristics take place, as a result of the mining operation, affects the relative rate at which the drainage characteristic determining processes take place.

- Since the equilibrium condition for neutralisation reactions is reached within a short period of time, relative to the rate at which other factors change, it is reasonable to apply a thermodynamic model to model the neutralisation process.

- Should limitations need to be imposed in terms of the number of neutralising minerals which can be included in the prediction model, the selection of calcite, to represent all neutralising minerals, is considered the most reasonable choice, given its abundance in most wastes.

- The prediction model needs to be able to take cognisance of the spatial variability in the location of neutralising minerals relative to acid generating minerals.

- It is proposed that a laboratory test procedure be developed to determine empirically, the proportion of neutralising minerals available for dissolution.

- The armouring process, and the effect that this has on the drainage

charateristics, is recognised. It is envisaged that the incorporation of armouring into either a small-scale laboratory test or a rigorous mathematical model, would prove very complex.

- The physical and geotechnical properties of the waste have a significant influence on a number of processes which influence drainage charateristics. Data for most of these parameters is best obtained through published literature, laboratory and field tests. Since the parameters are generally highly variable within the waste pile, it is essential that the prediction model is capable of taking account of the spatial variablity.

- It is recognised that for coarse wastes in particular, the net water flux through the waste is in most cases determined by the net infiltration rate, rather than the permeability of the waste material.

- The extent to which particle surfaces are flushed by migrating water, can have a significant effect on the drainage characteristics and variations in the drainage characteristics. This factor needs to be included in the prediction model.

- The prediction model needs to be able to simulate variations and temporal changes in the net infiltration rate.

- The influence of sulphide oxidising bacteria on the sulphide oxidation rate is considered best represented using a semi-empirical model, possibly based on data collected using a simple small-scale laboratory test procedure.

- The respiration rate due to the presence of microbes in the root or topsoil zone, should be included in the drainage prediction model, as this could significantly reduce the oxygen flux to the underlying sulphide-containing waste.

- The proposed approach to model the drainage characterisics from coarse wastes, involves a combination of a small-scale physical model, and a

computer based, mathematical model. The physical model(s) should be developed to determine empirical site specific values for a range of parameters representing complex processes, for which rigorous mathematical models do not exist, or for which the data aquisition requirements for existing models are considered too onerous. The computer model uses the empirical data acquired from the physical model, and integrates this data into a series of integrated mathematical models, which model those processes which can most appropriately be modelled using a mathematical model. This approach is likely to provide a practical useable model, which can be applied to evaluate a range of drainage control measures and assist in the design of improved mining and rehabilitation methods.

SECTION TWO

A MODEL TO PREDICT POLLUTION LOADS FROM COARSE SULPHIDE-CONTAINING WASTES

Contents

CHAPTER ONE

THE PREDICTION MODEL - *SALMINE*

1   INTRODUCTION

1.1   Layout of Chapter 1

This chapter provides a technical description of the model *Salmine version 1.0*, developed to predict the pollution loads from coarse sulphide-containing materials. The information is intended to provide users with sufficient background information to decide on the applicability of the model for the particular problem under consideration. The layout of this chapter is as follows:

☞   Part 1 introduces the model and describes layout of the chapter and the intended application of the model.

☞   Part 2   provides a general overview of the model and describes the processes and manner in which the processes are represented. Part 2 does not provide details of the modelling of each individual process, but describes how the processes are integrated in the model.

☞   The latter parts of this chapter are concerned with specific processes, represented in *Salmine* as sub-models or routines. For each sub-model the following aspects are addressed:

•   The specific objective of the sub-model is described.

•   Selected models which have been developed by others to represent specific processes are reviewed and discussed for the purpose of

ascertaining their relevance, usefulness and applicability to the *Salmine* model.

- The mathematics which has been applied in the *Salmine* model is documented.

- The limitations particular to the sub-model are documented.

- The data requirements for the sub-model are described.

1.2   The Applicability of the *Salmine* Model to Coarse Wastes

Salmine is intended to predict the drainage characteristics from coarse sulphide - containing waste material. There are a number of simplifying assumptions which may limit its applicability in certain instances.   The most important of these assumptions may be summarised as follows:

- The oxygen flux into the waste is assumed to be driven primarily by diffusion of oxygen through the air-filled pore space. As discussed in Section 1, this is the predominant mechanism of oxygen supply in most coarse wastes such as spoil piles. There are however coarse waste materials or conditions under which this assumption is no longer valid. A method of assessing the validity of this assumption in site specific instances was presented in Section 1.

- It is assumed that water enters at the surface and migrates in a vertical downward direction only, ultimately emanating from the base of the waste. The model can therefore not be used to predict the rate of accumulation of salts on the surface of the waste pile due to capillary rise driven by evaporation.

- The model applies to the unsaturated zone only. If a phreatic surface develops within the waste, then the model can only be used to predict pollution loads from the zone above the phreatic surface. This limitation is

generally not of concern since the rate of sulphide oxidation below the phreatic surface is usually several orders of magnitude lower than that above the phreatic surface. The limitation may be significant in terms of the *drainage quality where significant neutralisation of the drainage takes place* below the phreatic surface.

• Acid generating and neutralising minerals are represented in the model by the specific minerals pyrite and calcite. The contribution to the acid generating or neutralisation process from other minerals must be calculated by expressing the quantity of these minerals as the pyrite equivalent or calcite equivalent mass. The selection of pyrite and calcite to represent all the acid generating and neutralising minerals respectively is based on the fact that these two minerals comprise the most abundant acid generating and neutralising minerals encountered in nature.

• *Salmine* version 1.0 does not include a sub-model to predict secondary metal leaching. The concentrations of metals other than iron, cannot therefore be predicted.

• *Salmine* represents a combination of experimental and analytical methods to simulate the processes active in a sulphide deposit. Both a physical model, comprising the kinetic test and a computer based mathematical model are required in order to predict the leachate water quality.

2   AN OVERVIEW OF THE MODEL

2.1   Description of the Typical Situation to be Modelled

Figure 1 illustrates the features associated with the development of ARD from a typical coarse sulphide-containing waste facility such as a rock pile, spoil pile or discard dump.

Infiltration /evaporation
Evapotranspiration

Migration of Contaminants

Oxygen Flux

Fissures/ cracks

Inflow to
waste facility

Surface Runoff

Neutralising
Minerals

Sulfide

Waste
Facility

Phreatic Surface

Variable particle size distribution

Ground water seepage

Seeps

Natural Ground

Reactions take place along the
path of migration

COARSE SULPHIDE-CONTAINING DEPOSIT ILLUSTRATING THE
PHYSICAL AND CHEMICAL PROCESSES WHICH GIVE RISE
TO CONTAMINATION AT A POINT OF CONCERN

SCHEMATIC REPRESENTATION OF A TYPICAL COARSE SULPHIDE-CONTAINING DEPOSIT	FIGURE 1

2.2   Modelling Zones

Given the complexity and diversity of chemical and physical processes operating within and outside the waste pile, and the differences in modelling time frames, a single mathematical model to predict the water quality at the point of concern is not considered practical. Rather, a range of models are required at different sections along the path of migration of water.

Figure 2 shows the typical physical problem divided into five zones namely:

- Zone 1 represents the surface of the waste material. The prediction of the runoff quality requires both a model to predict the rate of accumulation of contaminants on the surface due to capillary rise and evaporation, and a surface runoff or hydrological model, capable of predicting a range of hydrological factors such as flow depths, surface flow rates etc.

- Zone 2 represents the zone above the phreatic surface which is characterised by unsaturated flow, generally in the vertical direction. This is the primary zone of generation of acidity and other contaminants.

- Zone 3 represents the zone below the phreatic surface, which is characterised by saturated flow, generally in the horizontal or near horizontal direction. The rate of generation of contaminants in zone 3 is considerably less than that in zone 2. Solute transport models and saturated flow models would generally be used to predict the drainage characteristics of water passing through zone 3. In certain cases, it may be necessary to include a thermodynamic model to represent the neutralisation of the drainage as it passes through this zone.

SALMINE applies only to Zone 2

Zone 1

Zone 2

Waste Facility

Zone 3

Ground water seepage

Un-mined Ground

Zone 4

Zone 5

Zone 1 – Surface water Runoff
Zone 2 – Primary Source of Contaminants
Zone 3 – Below Phreatic Surface
Zone 4 – Groundwater Zone
Zone 5 – Environment (surface Water)

Phreatic Surface

Point of Concern

POSSIBLE PATHS OF MIGRATION
zone 1 – zone 2 – zone 3 – zone 4 – zone 5
zone 1 – zone 2 – zone 3 – zone 5
zone 1 – zone 2 – zone 4 – zone 5
zone 1 – zone 2 – zone 1 – zone 5
zone 1 – zone 5
zone 1 – zone 4 – zone 5

	SCHEMATIC REPRESENTATION OF COARSE SULPHIDE–CONTAINING DEPOSIT ILLUSTRATING MODELLING ZONES	FIGURE 2

- Zone 4 represents the groundwater zone downstream or beneath the waste facility. A similar set of models to those in zone 2 might be applied

- Zone 5 represents the surface flow downstream of seeps. This zone is beyond the scope of this document but it is important to recognise that changes in the drainage characteristics might occur within a short distance of the seep due to a variety of processes active in this zone.

Of these zones, the most significant in terms of the generation of contaminants is zone 2. It is within this zone that the primary (but not necessarily the only) source of contamination arises. Without the ability to predict the quality of water leaving zone 2, it is unlikely that any further useful prediction of the water quality elsewhere along the path or at the point of concern may be made. It is for this reason that the *Salmine* model focuses entirely and is indeed limited to zone 2, the initial source of the contaminants. The specific objective of the *Salmine* model may therefore be stated as: *"To predict quality and quantity (hence contaminant load) of water leaving the base of the unsaturated zone of the waste."*

The remaining discussion in this chapter relates only to zone 2, the source of contamination.

2.3   Model Skeleton

2.3.1   Representation of Physical Situation in the Model

Figure 3 illustrates the representation of the physical situation in the computer model. The computer model represents a vertical section through the waste with the upper boundary comprising the surface of the waste. The lower boundary would comprise the higher of :

- the level of the phreatic surface, or

- in the absence of a phreatic surface within the waste, the lower extremity of the waste material.

Ten layers are used to represent changes in the characteristics of the material with depth. Properties can only change across the boundary of layers and are assumed to be homogeneous within each layer.

SALMINE MODEL REPRESENTING A COLUMN
OF MATERIAL IN ZONE 2

Oxygen Flux through surface

Infiltration of Rain/runoff

LAYER 1

LAYER 2

LAYER 3

LAYER 4

LAYER 9

LAYER 10

Vertical Downward migration of
water and contaminants only

Partially saturated flow and
Pseudo-karst flow mechanisms

Oxidation of Sulfides and release
of contaminants

Neutralisation of acidity, dissolution
of calcite, precipitation of specific
salts

Leachate leaves zone 2

Direction of
movement of
water

Vegetation

Waste Material
with specific
geotechnical
properties

Neutralising
Material (calcite)

Sulfide containing
Material (pyrite)

Flushing and
migration of
contaminants

Oxygen flux
(diffusion through
air filled pore
speces)

SCHEMATIC REPRESENTATION OF THE SALMINE MODEL	FIGURE 3

All data is entered and results calculated per square metre of surface area, measured perpendicular to the column.

Modelling of a waste profile therefore requires that the characteristics of the typical profile(s) within the waste be estimated. Layer 1 represents topsoil or a layer containing organic matter, in which consumption of oxygen due to microbes which break down organic matter such as plant roots, is assumed to be the predominant oxygen consumption mechanism. In the underlying layers, it is assumed that consumption of oxygen through sulphide oxidation is the predominant oxygen consumption mechanism.

2.3.2   Summary of Data Requirements

The data requirements for *Salmine* version 1.0 are summarised in Table 1. With the exception of the atmospheric properties, all parameters must be specified for each layer but need not necessarily differ across layer boundaries. Excessive or unrealistic changes in the values of parameters across layer boundaries can lead to numerical instability.

Further details of data requirements, assumptions, limitations, and a description of the mathematics for each sub-model is given in next section.

2.3.3   Physical and Chemical Processes Included in the Model

The physical and chemical processes represented in the model, together with the sequence of calculations, are shown in Figure 4. The rectangles in the figure represent each of the sub-models and the arrows the sequence of calculations. Each of the sub-models may briefly be described as follows:

TABLE 1: PARAMETERS REQUIRED FOR SALMINE

Parameter	Units	Default	Data Source
ATMOSPHERIC PROPERTIES			
Atmospheric Pressure	N/m^2	101325	Weather stations
Atmospheric Oxygen Concentration	$moles/m^3$	8,15	Perry et al (1973)
Ambient Temperature	Kelvin	288	site conditions
Diffusion coefficient of Oxygen in Air	$m^2.s^{-1}$	$1,90 \times 10^{-5}$	Perry et al (1973)
PHYSICAL PROPERTIES			
Layer thickness	m	-	Site specific
GEOTECHNICAL PROPERTIES			
layer porosity	N/A	-	See App. C Table 1
layer averaged specific gravity	N/A	2,7	Laboratory tests
Layer averaged saturated water permeability	m/s	-	See Appendix
Proportion of flow to rapid flow paths	N/A	0,2	Field calibration data
Layer averaged initial degree of saturation	N/A	-	Laboratory tests
Residual degree of saturation	N/A	-	Laboratory tests, field measurements or literature
Empirical pore size distribution factor	N/A	3	Literature
Calibration constant for flow velocity		1	Field or laboratory test calibration
SULPHIDE PROPERTIES			
Initial pyrite concentration	g/kg waste	-	ABA test
Initial oxidation rate	g/kg/week	-	Kinetic test
NEUTRALISING MINERAL PROPERTIES			
Initial calcite concentration	g/kg waste	-	ABA test
MICROBIAL RESPIRATION (ORGANIC MATTER DECOMPOSITION)			
Average microbial respiration rate (layer 1)	$moles/m^3/s$	$0-10^{-6}$	Literature
INFILTRATION			
Net infiltration into layer 1	$litres/m^2/$ time step	-	Rainfall - runoff
COMPONENT SOLUBILITIES AND pH (Optional)			
pH	-	0-14	Thermodynamic chemical equilibrium models e.g. MinteqA2
$[SO_4]$, $[CO_3^{2-}]$, $[Ca^{2+}]$ and $[Fe_{total}]$	moles/litre	-	
COMPONENT CONCENTRATIONS FOR INFILTRATING WATER			
pH			Thermodynamic chemical equilibrium model e.g. MinteqA2
$[SO_4]$, $[CO_3^{2-}]$, $[Ca^{2+}]$ and $[Fe_{total}]$	moles/litre		

CALCULATIONS

Diffusion

| Next time Step |

Calculate the Oxygen Concetration
Profile and oxygen flux based
on the diffusion mechanism
dC/dx

RESULTS

Sulfide Oxidat.

Calculate the mass of sulfide
(pyrite) consumed during the time
step in each layer

Store the current Sulfide
reaction rate (assuming
excess reactants) for each
layer

Calculate the quantity of oxidation
products released in each layer
during the time step.

Store the current sulfide
balance (g/kg) for each
layer.

Water Quality

Total mass of chemical
components in each layer
= sum of aqueous and solid
phase components

Neutralisation

Chemical equilibrium calculation
to determine the mass of
chemical components in the
aqueous phase in each layer

Store the chemical component
concentrations for all
aqueous phase components

Concentration of aqueous
chemical components present
in each layer

Store the masses of chemical
components in the solid phase

Percolation

Calculation of the total inflow &
outflow from each layer, change
in moisture content and outflow
from layer 10 during the time
step.

Store the volume of leachate
produced in layer 10 and the
degree of saturation of each
layer

Calcite Mass

Store the mass of calcium
and carbonate in the solid
phase in each layer.

Calculation of the mass of
neutralising minerals dissolved
in each layer during time step.

| SALMINE
SEQUENCE OF CALCULATIONS | FIGURE 4 |

Oxygen Supply Sub-Model

The key features of the oxygen supply sub-model are as follows:

- The oxygen concentration gradient across each layer is calculated using a model for diffusion through air-filled pore spaces only. Oxygen is assumed to be supplied from the surface, downwards through the waste to the underlying layers. The oxygen flux due to other oxygen transport mechanisms discussed in Section 1 are ignored. (See the discussion of oxygen flux mechanisms, Section 1 for explanation).

- The oxygen concentration gradient is calculated based on the oxygen consumption rates due to decay of organic matter in layer 1, and due to sulphide oxidation in layers 2 through to 10.

Sulphide Oxidation Sub-Model

The key features of the sulphide oxidation sub-model are :

- The maximum rate of oxidation of sulphides is determined from kinetic laboratory tests carried out on samples of the material. The kinetic tests are performed in a humid environment in which the concentration of oxygen within the sample voids is maintained at atmospheric concentration throughout the test period by pumping air through the sample. The test should be carried out in a room in which the temperature is representative of the mean temperature in the waste pile. The sample may be inoculated with bacteria to enhance the rate of oxidation. The rate of oxidation for the sample is estimated by either measuring the concentration of contaminants in the leachate, or by direct measurement of the oxygen consumption rate. Conditions in the test should closely resemble those in the field with respect to :

    - the particle size distribution and specific surface area.

- the mineralogy of the waste.

- the average temperature within the waste.

- the presence and activity of sulphide oxidising bacteria.

This aspect is documented in further detail in Chapter 2 of this section.

- The reaction rate determined from kinetic tests is used in *Salmine* to calculate the oxygen concentration profile within the waste pile and hence the rate of production of contaminants in layers 2 to 10, for each time step. The quantity of sulphide oxidised is proportional to the oxygen concentration.

- The rate of production of chemical components Fe^{2+} and SO_4^{2-} due to the oxidation of pyrite is calculated based on the assumed stoichiometry of the reaction.

Infiltration and Water Flux

The key features of the water flux sub-model are :

- Net infiltration rates per time step must be specified as input to the model. Exfiltration due to evaporation from the upper layers of material or evapotranspiration is not modelled. Either a steady state or non-steady state net infiltration rate may be modelled.

- Rapid flow paths (RFP's) and slow flow paths (SFP's) are represented by assigning a proportion of the flow to the SFP's and the remainder of the flow to the RFP's. The proportion assigned to the SFP's is based on empirical results which must be gathered from field data. A simple Darcian type approach is applied to model the flux through the RFP's and the SFP's. This approach requires as inputs an estimate of the residual degree of saturation, the moisture content, and the saturated water permeability for both the RFP's and SFP's respectively. Commercially available computer packages such as FLAC, SEEP/W or AQUA, which are specifically intended to model unsaturated flow, may be used to calibrate the water flux submodel used

in *Salmine*.

Chemical Equilibrium, Neutralisation, Precipitation, Dissolution Sub-Model

It is assumed that chemical equilibrium conditions are reached during each time step.

The chemical speciation sub-model provides two options to estimate the pH of the pore water within each layer and the concentration of considered components as follows:

- *Salmine*'s neutralisation and chemical equilibrium routine provides a simplified approach to solve the mass action and mass balance expressions simultaneously for an aqueous system containing the chemical components Ca^{2+}, CO_3^{2-}, H^+, Fe^{2+} and SO_4^{2-}. The routine enables the concentration of species and the pH of the pore water to be estimated based on a particular set of assumptions. The influence of secondary metals (e.g. Mn, Ni, Cu, Mg, Al etc.) is not taken into account in this model.

- Alternatively, should the routine prove unsuitable for the particular problem under consideration, it is possible to use the results determined by experiment or by applying an independent model to determine the trends in the aqueous component concentrations. Although this option provides greater flexibility and allows for the precipitation of other solids, it is more time consuming.

The rate of depletion of calcite is estimated by calculating the mass of calcite which would need to dissolve within each time step to maintain the aqueous concentrations of calcium and carbonate in the pore water at the equilibrium concentration.

Mixing and Flushing Sub-model

The proportion of contaminants available for migration in each time step is assumed to be dependent on the effective degree of saturation of the waste, raised to a power term which is a function of the pore size distribution index. It is assumed that complete mixing of the oxidation products and neutralising minerals is able to take place during each time step. Only aqueous phase components are considered to be mobile and able to pass from one layer to the next.

2.3.4 Simulation Process

The sequence of calculations is illustrated in Figure 4. An appropriate time step interval (one for which there is some change but generally not too large a change over the time step interval) has been found to be of the order of one week or one month. Since several time steps are required for the contaminants generated at the top of the waste pile to exit as leachate from the base of the pile, the calculations must be repeated a sufficient number of times until pseudo-steady state conditions are reached with regard to:

- the degree of saturation within each layer, and

- the water quality and quantity of leachate.

Since both acid generating and neutralising minerals are depleted with time, the leachate quality also varies with time. By extrapolating the trends in the rate of depletion of pyrite and calcite within each layer, the rate of accumulation of less soluble salts such as gypsum and Fe_2O_3 , together with the change in leachate quality may be predicted. This type of simulation is useful in evaluating the time required for a particular control measure to have an effect.

The operating manual for the Salmine programme is enclosed as Appendix E to this report. The manual describes the use of programme icons and dialog boxes specific to *Salmine*.

2.4   Programme Language and Computer Software Requirements

Salmine operates in a Windows environment and requires Excel version 5.0 or later. System resources are as required for the Windows and Excel programmes. Operating instructions are written in Visual Basic.

3   THE OXYGEN SUPPLY ROUTINE

3.1   Objective of the Routine

The objective of this routine is to calculate the oxygen concentration gradient in the waste pile which is established as a result of the diffusion of oxygen from the surface of the waste pile through the pore spaces to the reactive particle surfaces.

3.2   Description of the Oxygen Flux Routine

The oxygen flux through a porous homogenous media composed of both water and air-filled voids may be derived from Fick's first law and is given by :

$$J = -D_p.n.(1-S+H.S).\frac{dC_a}{dz} = -D\frac{dC_a}{dz} \qquad (1)$$

Where : J =   *flux calculated per unit cross sectional area of the porous material (mol.m^{-2}. s^{-1})*

   D_p =   *pore diffusivity (m^2.s^{-1})*

   C_a =   *oxygen concentration in the gas phase (mol.m^{-3} gas)*

   D =   *effective diffusion coefficient based on the concentration in the gas phase (m^2.s^{-1})*

   n =   *porosity of the waste*

   S =   *degree of saturation*

   H =   *equilibrium constant for oxygen in water at a particular temperature.*

The transient diffusion and consumption of oxygen in a porous medium may be described by the following differential equation for a first order chemical reaction:

$$n(1-S+H.S).\frac{\partial C_a}{\partial t} = D.\frac{\partial^2 C_a}{\partial z^2} - k_r.C_a \qquad (2)$$

Accumulation = diffusion - consumption

Scharer, Garga, Smith & Halbert (1991) have shown, using a model to predict acid generation in pyritic mine tailings, that steady state conditions develop within unsaturated tailings within a few days. This assumption would also hold true for coarse wastes, since they generally have a higher air permeability than fine wastes. At steady state, equation (2) simplifies to:

$$D.\frac{d^2 C_a}{dz^2} - k_r.C_a = 0 \qquad (3)$$

Steady state conditions with respect oxygen flux are assumed for each discrete time step.

The general solution to this equation is:

$$c_a(z) = B_1.\exp[z.\sqrt{\frac{k_r}{D}}] + B_2.\exp[-z.\sqrt{\frac{k_r}{D}}] \qquad (4)$$

Where $c_a(z)$ = *concentration of oxygen at depth z (mole/m³ gas)*

B_1 *and* B_2 *are constants which depend on the boundary conditions*

D = *effective gas diffusivity for gas-filled pore space*

Oxygen consumption in the topsoil or rehabilitated cover (layer 1), due to microbes acting on organic matter such as plant roots, is modelled as a zero order reaction as shown in equation (5). Oxygen consumption rates due to the breakdown of organic matter such as plant roots have been measured by *Currie (1970)*. It has been found that rates vary considerably between seasons and depend largely on

vegetation.

$$D.\frac{d^2c_a}{dx^2} = A_a \qquad \text{where } A_a \text{ is the oxygen consumption rate} \qquad (5)$$

$$(mole/m^3 \text{ bed, sec})$$

In the top layer, equation (5) applies and in the lower nine layers equation (4) applies. The following boundary conditions are applied at the interface of each layer:

• At surface, the oxygen concentration equals the atmospheric concentration.

$$c_a(at \ surface) = c_{atmospheric} \qquad (6)$$

• The oxygen concentration gradient across each layer boundary, immediately on either side of the boundary is the same, therefore:

$$\frac{dc_a}{dz_{layer\ i}} = \frac{dc_a}{dz_{layer\ i+1}} \qquad (7)$$

• The concentration on either side of the boundary between two layers is the same:

$$c_a\big|_{z_i, L} = c_a\big|_{z_{i+1}, 0} \qquad (8)$$

• Finally, it is assumed that there is no diffusion across the base of the spoil pile, implying that the diffusion gradient at this point is zero.

$$\frac{dc_a}{dz_{layer\ n}}\bigg|_{z=L_n} = 0 \qquad (9)$$

A matrix of 19 equations with 19 unknowns is solved analytically at each time step.

Various methods of estimating the effective diffusivity D have been proposed. The method described below has been found to best represent the results of laboratory experiments for non-aggregated media (*Collin 1987*).

A function to estimate the effective diffusivity of partially saturated aggregated and non-aggregated material which accounts for the diffusion in the gas and water-filled pore spaces, is presented in equation (10), (*Millington and Shearer, 1971*). This approach assumes that the material is composed of solid spherical particles of non-porous media. The diffusibility for non-aggregated media may be estimated from :

$$\frac{D}{D_a^o} = (1-S)^2.[n(1-S)]^{2x_a} + H.\frac{D_w^o}{D_a^o}.S^2.(n.S)^{2x_w}$$

(10)

where : D = *effective diffusivity (m^2.s^{-1})*

D_a^o = *binary diffusion coefficient in air (m^2.s^{-1})*

D_w^o = *binary diffusion coefficient in water (m^2.s^{-1})*

And the exponents x_a and x_w are given by :

$$[n(1-S)]^{2x_a} + [1-n(1-S)]^{x_a} = 1$$

(11)

$$[n.S]^{2x_w} + [1-n.S]^{x_w} = 1$$

(12)

A graph of the non-dimensional effective diffusivity (D/D_a^o) as a function of the degree of saturation is shown in Figure 5.

In the derivation of Figure 5, diffusion through air-filled and water-filled pore spaces has been taken into account. A porosity of 0,3 was assumed in the calculation. The contribution to the diffusivity from the water-filled pore spaces is negligible except for values of S close to 1,0, and may therefore be ignored since the degree of saturation in most coarse wastes is considerably less than 1,0. Equation (10)

therefore simplifies to:

$$\frac{D}{D_a^o} = (1-S)^2.[n(1-S)]^{2x_a}$$
(13)
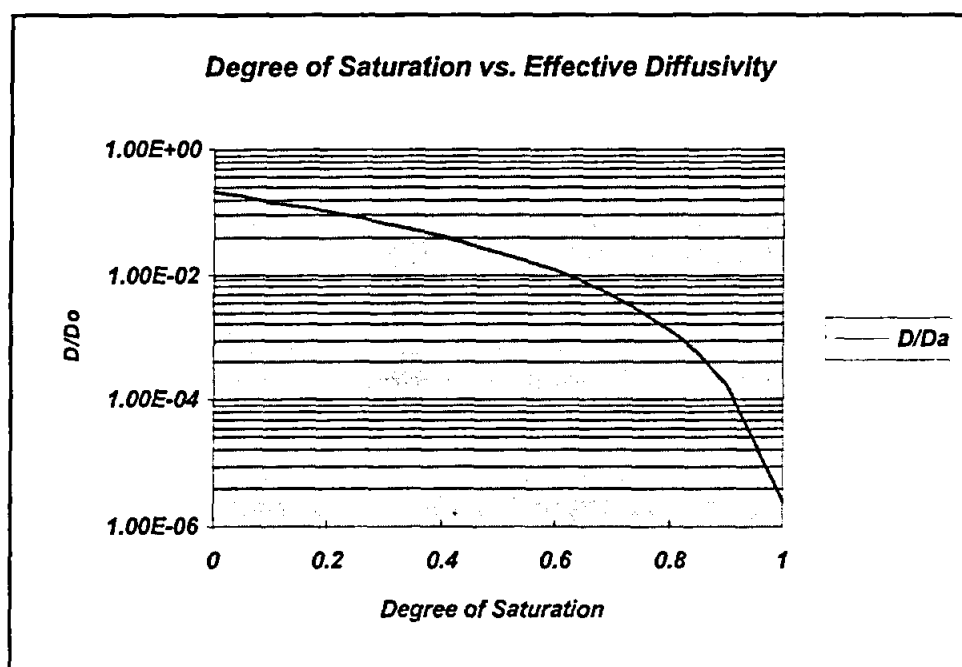
Figure 5 : Effective Diffusivity versus Degree of Saturation

3.3   Summary of Key Limitations

The following limitations apply to the oxygen flux model:

- Oxygen diffusion is assumed to be limited to the air-filled pore spaces. Diffusion through liquid and solid phases (pore water and solid particles) is ignored. Air-filled voids are assumed to be interconnected and continuous.

- The model estimates the oxygen flux due to diffusion only and is limited to the vertical downward direction. Under certain circumstances, other oxygen supply mechanisms including rapid pressure equilibration due to atmospheric pressure changes, convection due to heating or spontaneous combustion of coal, or infiltration of oxygen rich water may contribute to and possibly exceed the oxygen flux due to diffusion. The contribution of other oxygen

flux mechanisms should be compared with the oxygen flux calculated using the diffusion model to ensure the validity of this assumption. Simple evaluation procedures to estimate the upper bound limits for oxygen flux due to other mechanism are presented in Section 1.

• The oxygen flux across the lower boundary of layer 10 is assumed to be zero.

3.4   Options

Should the oxygen flux due to other oxygen transport mechanisms be significant, then the default value for the diffusivity of oxygen in air can be increased to account for the influence of the other oxygen supply mechanisms.

4   SULPHIDE OXIDATION

4.1   Objective of the Sulphide Oxidation Routine

The objective of the sulphide oxidation routine is to calculate the quantity of primary oxidation products produced in each layer during each time step as a direct consequence of the oxidation of sulphides.

4.2   Insights from the Literature Review

Various models exist to simulate the chemical and biological oxidation of sulphide minerals. The primary output from many of these models is the rate of oxidation of the sulphide minerals or the rate of production of contaminants.

An expression for the rate of production of sulphate is given in the following equality which is derived from the overall reaction stoichiometry for the complete oxidation of pyrite.(SRK, 1989)

$$\frac{1}{2}\frac{d[SO_4^{2-}]}{dt} = \frac{-d[FeS_2]}{dt} = -\frac{1}{3.5}\frac{d[O_2]}{dt}$$ (14)

Where: $[SO_4^{2-}]$ = moles of sulphate per unit volume

                  $[FeS_2]$ = moles of pyrite per unit volume

                  $[O_2]$ = moles of oxygen per unit volume

The rate of depletion of sulphide in a fragment of sulphide containing rock may be controlled by one of three rates as follows:

•   the rate at which oxidant (oxygen or Fe^{3+}) is supplied to the surface of the rock fragment, or

•   the rate at which oxidant diffuses through the rock fragment towards the sulphide grains and the rate at which oxidation products diffuse out of the rock fragment, or

•   the surface reaction rate for the sulphide minerals.

The transport of oxygen through the macro-pore spaces is generally regarded as the overall rate controlling process (*Cathles and Schlitt, 1980; Scharer et al, 1991*) within the waste pile.

The mass balance of oxygen in the pore space has been described as follows for diffusive oxygen transport into the pore space :

$$n_a \cdot \frac{dC}{dt} = D_e \frac{d^2C}{dz^2} + r_{oxygen}$$ (15)

where n_a = *air-filled porosity (m^3/m^3)*

      C = *concentration of oxygen in the pore space (moles /m^3)*

      t = *time (s)*

D_e = effective diffusivity of oxygen in the pore spaces (m^2/s)

z = depth from the surface (m)

r_{oxygen} = volume averaged oxygen consumption rate (moles O_2 $/m^3.s$)

The shrinking core model (Levenspiel, 1972) has classically been used to model the concentration of oxygen from the rock surface to the moving reaction front within a rock fragment. This model assumes that rock fragments are spherical and that sulphide crystals are homogenously distributed throughout the rock fragment. Under this condition, the concentration of oxygen from the rock surface to the moving reaction front within the rock fragment is given by :

$$D_e^* \frac{d^2 C^*}{dr^2} + \frac{2dC^*}{rdr} = -k'a^* C_s^*$$

(16)

Where : D_e^* = effective diffusion coefficient of oxygen within the particle $(m^2.s^{-1})$

C^* = concentration of oxygen within the particle $(mol.m^{-3})$

r = radial distance within the particle (m)

k' = first order reaction rate constant per unit surface area of sulphide $(s^{-1}.m^{-2})$

a^* = surface area of the reacting front (m^2)

An expression for the fraction of un-reacted pyrite at any time t in the presence of the oxidants oxygen and ferric iron has been derived (Jaynes et al, 1984; Ohio State University Research Foundation, 1970; Levenspiel, 1972) and is as follows:

$$\frac{dX}{dt} = -\frac{1}{t_D(O_2)(1-X)+t_C(O_2)} - \frac{1}{t_D(Fe^{3+})(1-X) + t_C(Fe^{3+})}$$

(17)

Where : X = the mass fraction of sulphide remaining in rock at time t (kg/kg)

t_d = the total time required to oxidise all the sulphide assuming that the diffusion rate of reactants and

products is the rate controlling step

t_c =   *total time required to oxidise all the sulphide assuming that the resupply rate of oxidant to the reaction front is much faster than the chemical oxidation of pyrite*

(O_2)& (Fe^{3+}) *refer to the oxidants oxygen and ferric iron respectively.*

If $t_d >> t_c$ then diffusion through the rock fragment will never be the rate controlling step, the rock fragment will weather uniformly across its diameter. If $t_d << t_c$, diffusion will become the rate controlling step and a more clearly defined oxidation front will be observed in the rock fragment.

The oxygen consumption rate, r_{oxygen}, given in equation (15) is the product of the reaction rate of the sulphide minerals or rock surfaces and the concentration of oxygen at the surface of the rock particle as shown in equation (18) below:

$$r_{oxygen} = k_r . C \qquad (18)$$

where k_r = *overall specific reaction rate measured at the rock surfaces* $(mol.m^{-2}. s^{-1})$

The reaction rate k_r is dependent on two factors namely the rate of chemical oxidation and the rate of biological oxidation. The chemical oxidation rate may be modelled by the following relationship (*Moses and Herman, 1991; McKibben and Barnes, 1986*):

$$k_c = A(0.33pH)^{0.7} e^{-\frac{E_a}{RT}} [O_2] \qquad (19)$$

where: k_c =   *chemical surficial reaction rate constant* $(mol\ m^{-2}\ s^{-1})$

E_a =   *Arrhenius activation energy* (J/mol)

$[O_2]$ =   *Oxygen concentration* (mol/m^3)

A =   *Arrhenius pre-exponential factor*

R =   *molar gas constant* $(J\ mol^{-1}\ K^{-1})$

$$T \quad = \quad temperature \ (K)$$

The pre-exponential factor A, for the chemical rate constant is dependent on the sulphide content.

The biological oxidation rate can be modelled in the following manner (*Scharer et al, 1991*) :

$$k_B = B[\frac{1}{1+10^{2.5-pH}+10^{pH-4}}]e^{-\frac{E_a}{RT}} \tag{20}$$

Where : B = *a biological scaling factor used to fit site specific data*

k_B = *biological surficial reaction rate constant (mol.m^{-2}.s^{-1})*

The biological scaling factor (*SENES and Beak, 1988*) is a function of the moisture content, nutrient levels and the partial pressure of oxygen and carbon dioxide. The biological reactivity as predicted by this model is plotted as a function of pH in Figure 6.

Biological Reactivity as a Function of pH
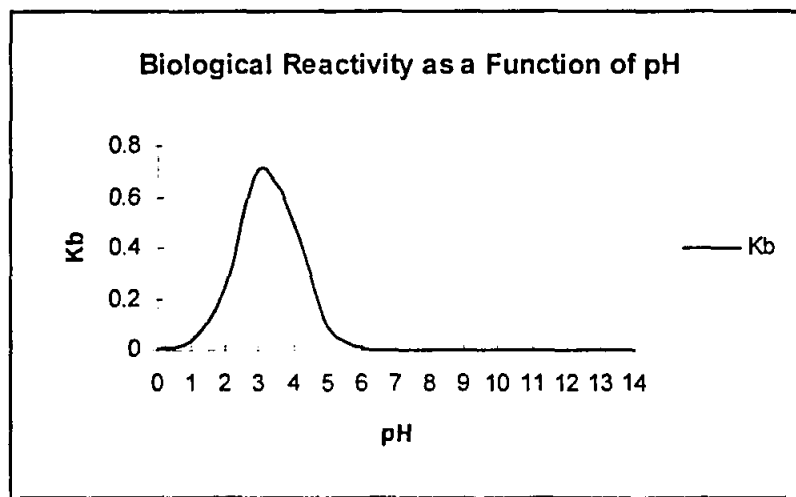
Figure 6 : Biological Surficial Reaction Rate Constant as a Function of the pH

The specific reaction rate for fine particles (less than 2mm) for the combination of biological and abiotic oxidation may be calculated as follows:

$$R_{s,p} = (k_c + k_B)a/\rho \qquad (21)$$

where : $R_{s,p}$ =   overall specific reaction rate (mol $kg^{-1} \cdot S^{-1}$) for fine particles

a =   the specific surface area of sulphide minerals ($m^2 \cdot m^{-3}$)

ρ =   density of the sulphide mineral ($kg \cdot m^{-3}$)

In the case of coarse particles, a shrinking core type of model can be used to represent the oxidation process. It can be shown (Scharer et al, 1994) that the overall oxidation rate per unit surface area is given by the combination of two phenomena namely:

•   the transport of oxygen through the reaction products to the sulphide and

•   the temporal shrinking of the reactive front as the sulphide is oxidised.

The overall reaction rate is presented as equation (22).

$$k_r = \frac{C}{\gamma}\left[\frac{1}{\dfrac{C}{\gamma(k_c + k_B)} + \dfrac{\Delta x}{D}}\right] \qquad (22)$$

Where : k_r =   overall specific reaction rate of the rock surfaces (mol $sulphide.m^{-2}.s^{-1}$)

Υ =   stoichiometric constant relating oxygen uptake to mineral oxidation

Δx =   the thickness of the layer surrounding the particle (m)

C =   local concentration of oxygen in the pore space ($mol.m^{-3}$)

D =   diffusion coefficient of oxygen through the liquid film and layer of reaction products.

Since the temperature at the reaction site has a significant effect on both the biological oxidation rate and the chemical oxidation rate, attempts have been made to model temperature increments resulting from enthalpies of sulphide oxidation reactions. Equation (23), (*Scharer et al, 1994*) has been used to model temperature changes on a monthly basis :

$$\rho_b C_P \frac{\partial \Delta T}{\partial t} + k \frac{\partial^2 \Delta T}{\partial z^2} + F_w C_w \frac{\partial \Delta T}{\partial z} = Q_{RX} - \Delta H_V E_W \qquad (23)$$

Where :

ΔT	=	temperature rise in the material (K)	
C_P	=	heat capacity of the solids($J.kg^{-1}.K^{-1}$)	
ρ_B	=	bulk density of the material(kg/m^3)	
k	=	thermal conductivity($J.m^{-1}.K^{-1}.s^{-1}$)	
F_w	=	vertical water flux($mol.m^{-2}.s^{-1}$)	
C_w	=	molar heat capacity of water ($J.mol^{-1}.K^{-1}$)	
Q_{RX}	=	sulphide reaction enthalpy generation($J.m^{-3}.s^{-1}$)	
ΔH_{Γ}	=	enthalpy of evaporation(J/mol)	
E_w	=	evaporation water loss($mol.m^{-3}.s^{-1}$)	

4.3   Description of the Sulphide Oxidation Sub-model

Given the profound spatial variability of sulphide minerals in coarse wastes, and the fact that reactive sites tend to be concentrated at relatively localised "hot-spots" within the waste facility, the approach used above to predict temperatures at reaction sites in coarse waste facilities is not considered practical. Although the influence of temperature on the reaction rate is significant, the model described above is considered unrealistic for the purpose of modelling the behaviour of coarse wastes. Furthermore, the approach to represent biological and chemical oxidation described above represents a mathematically eloquent model for sulphide oxidation, however the data requirements are considered too onerous for coarse wastes given the practical difficulty in determining the parameter values. Coarse wastes such as

spoils, typically exhibit a wide variety of particle sizes and shapes. The assumption of the above model that particles are spherical and evenly sized is considered inapplicable for most coarse wastes.

After due consideration of the detailed mathematical model, it is proposed that a simple empirical approach be adopted comprising a small-scale laboratory reactor test. The test is used primarily to estimate the likely maximum sulphide oxidation rate. The sample should be selected such that it is representative with respect to particle size distribution and mineralogy. The proposed kinetic test method is described in Chapter 2. An empirical expression for the rate of depletion of the mass of sulphide dS/dt, is considered for the purpose of the *Salmine* model, to be a simple function of the time since the start of the kinetic test, the maximum observed oxidation rate, and a decay constant, shown as equation (24):

$$\frac{dS}{dt} = K_0.e^{-k_1.t} \tag{24}$$

Where $\dfrac{dS}{dt}$ = the rate of oxidation of the sulphide material (g/kg bed/week)

K_0 = maximum measured oxidation rate (grams sulphide/kg bed /week)

k_1 = decay constant (per week)

t = time since the start of the kinetic test (weeks)

The maximum oxidation rate, K_0 (grams pyrite/kg bed/week), is determined from the kinetic test which is described in Chapter 2.

The stoichiometry of the sulphide oxidation reaction is assumed to be as per reaction (25)

$$FeS_2 + \frac{7}{2} O_2 + H_2O \rightarrow Fe^{2+} + 2SO_4^{2-} + 2H^+ \tag{25}$$
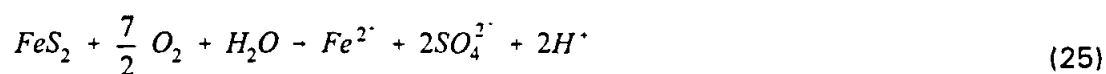
The initial specific reaction rate, k_r (m^3 gas/ m^3 waste rock per second) is

calculated from equation (26), and is derived from the assumed stoichiometry of the sulphide oxidation reaction.

$$k_r = \frac{112.K_0.R.T.\rho_{dry}}{120.32.P_{atm}}$$

(26)

Where R = *universal gas constant*

T = *temperature (Kelvin)*

P_{atm} = *atmospheric pressure (Pa)*

In practice, the reaction rate would not follow this equation directly due to the influence of in particular, biologically assisted oxidation, changes in temperature and changes in pH.

The quantity of sulphide oxidised during each time step is calculated from:

$$\sum_{layers} k_r(t^*).C_a(z).\Delta t.\frac{120}{3,5.\rho_{dry}}$$

(27)

where $k_r(t^*)$ = *reaction rate constant (m^3 O_2 / m^3 waste/sec)*

$C_a(z)$ = O_2 *concentration at depth z (moles/m^3 gas)*

Δt = *time step in seconds*

ρ_{dry} = *dry density of material*

The oxygen concentration, $C_a(z)$, is determined from the oxygen flux model.

The reaction rate constant is a function of the kinetic test equivalent oxidation time, t^*.

The calculation is repeated for each time step and each layer. The kinetic test equivalent oxidation time t^*, is calculated at each real time step and for each layer from equation (28), which is derived by integrating equation (24) with respect to time and solving for t, given the boundary conditions at $t^* = 0$, $S_i = 0$ and at $t^* = \infty$, S_t = total initial pyrite content of the waste.

$$t^* = -\frac{1}{k_1}.Ln(S_t.\frac{k_1}{K_o})$$

(28)

where t^* = *kinetic test equivalent reaction point (weeks)*

S_t = *pyrite balance at time step t (g pyrite/kg bed)*

The new reaction rate for the following time step for each layer is calculated by substituting the value for t^* into equation (24).

4.4   Key Assumptions and Implications

The assumptions implicit in the sulphide oxidation model may be summarised as follows:

- A single specific reaction stoichiometry is assumed, which remains constant throughout each layer and each time step. The implication of this assumption is that the model is limited to pyrite. The model may be applied to wastes containing predominantly other sulphide minerals, by calculating a pyrite equivalent mass.

- The maximum oxidation rate is assumed to occur at the kinetic test equivalent time, t^* =0. In reality, the maximum oxidation rate need not necessarily occur immediately once the sulphide-containing rock fragments are exposed to air, but may require a period of time to establish optimal conditions for biological and chemical oxidation. However, since the peak oxidation rate derived from the kinetic test is used, and since the kinetic test is carried out at "optimal" conditions for chemical and biological oxidation, the error arising from this assumption is relatively small.

- Since intermediate oxidation products (e.g. Fe^{3+}) are not considered in the assumed stoichiometry of the oxidation reaction, it is implied that the complete oxidation reaction is assumed to take place within each discrete layer. From the point of view of predicting drainage water quality at the

base of the waste pile, this assumption is considered reasonable since the averaged stoichiometry of the reaction over the entire depth of the pile and over the time step interval is represented by the assumed stoichiometry.

5   INFILTRATION AND WATER FLUX

5.1   Objective of the Water Flux Routine

The objective of the infiltration and water flux model is to simulate the net infiltration of water into the waste pile and the vertical downward movement of water through the unsaturated zone.

5.1.1 Unsaturated Flow Equations - Homogeneous Material

The governing differential equation for one dimensional flow can be written as per equation (29), *(SEEP/W version 3.0)* which states that the difference between the flow entering and leaving and elemental volume over a discrete time interval is equal to the change in volumetric water content.

$$\frac{\partial}{\partial z}(k_z \frac{\partial H}{\partial z}) + \frac{\partial}{\partial y}(k_y \frac{\partial H}{\partial y}) + Q = \frac{\partial \Theta}{\partial t} \qquad (29)$$

where k_z *and* k_y =   *hydraulic conductivity in the z and y directions respectively*

H =   *total head*

Q =   *water flux into the discrete volume*

t =   *time*

Θ =   *volume water/ total volume = volumetric water content*

The total head, H, is the sum of the elevation head, z, and the pore water pressure head u_w/γ_w. This gives :

$$u_w = \gamma_w(H-z) \qquad (30)$$

The volumetric water content is a function of the pore pressure and the nature of the material. Figure 7 illustrates typical volumetric water content functions for two different materials, namely a sand and silty clay.

The slope of this curve, designated m_w, represents the rate of change in the amount of water retained by the soil as a result of a change in pore pressure. The slope of the curve steepens with increasing coarseness of material. For very coarse materials such as a poorly graded gravels, the slope of the curve may be near vertical for pore pressures less than zero. The slope of the soil water characteristic curve is defined by equation (31):

$$m_w = \frac{\partial \Theta}{\partial u_w} \tag{31}$$

Since the elevation of the elemental volume is constant, equation (29) may be re-written as per equation (32) by substituting for the term $\partial \Theta$:

$$\frac{\partial}{\partial z}(k_z \frac{\partial H}{\partial z}) + \frac{\partial}{\partial y}(k_y \frac{\partial H}{\partial y}) + Q = m_w \gamma_w \frac{\partial H}{\partial t} \tag{32}$$

This governing differential equation may be solved using a numerical technique such as the finite difference or finite element method. In most waste piles, the component of flow in the horizontal direction within the unsaturated zone is negligible and may therefore be ignored. In this case, equation (32) simplifies to the one dimensional case as shown in equation (33)

$$\frac{\partial}{\partial z}(k_z \frac{\partial H}{\partial z}) + Q = m_w \gamma_w \frac{\partial H}{\partial t} \tag{33}$$

Volumetric Water Content Function
Clayey Silt

Volumetric Water Content Function
Uniform Sand
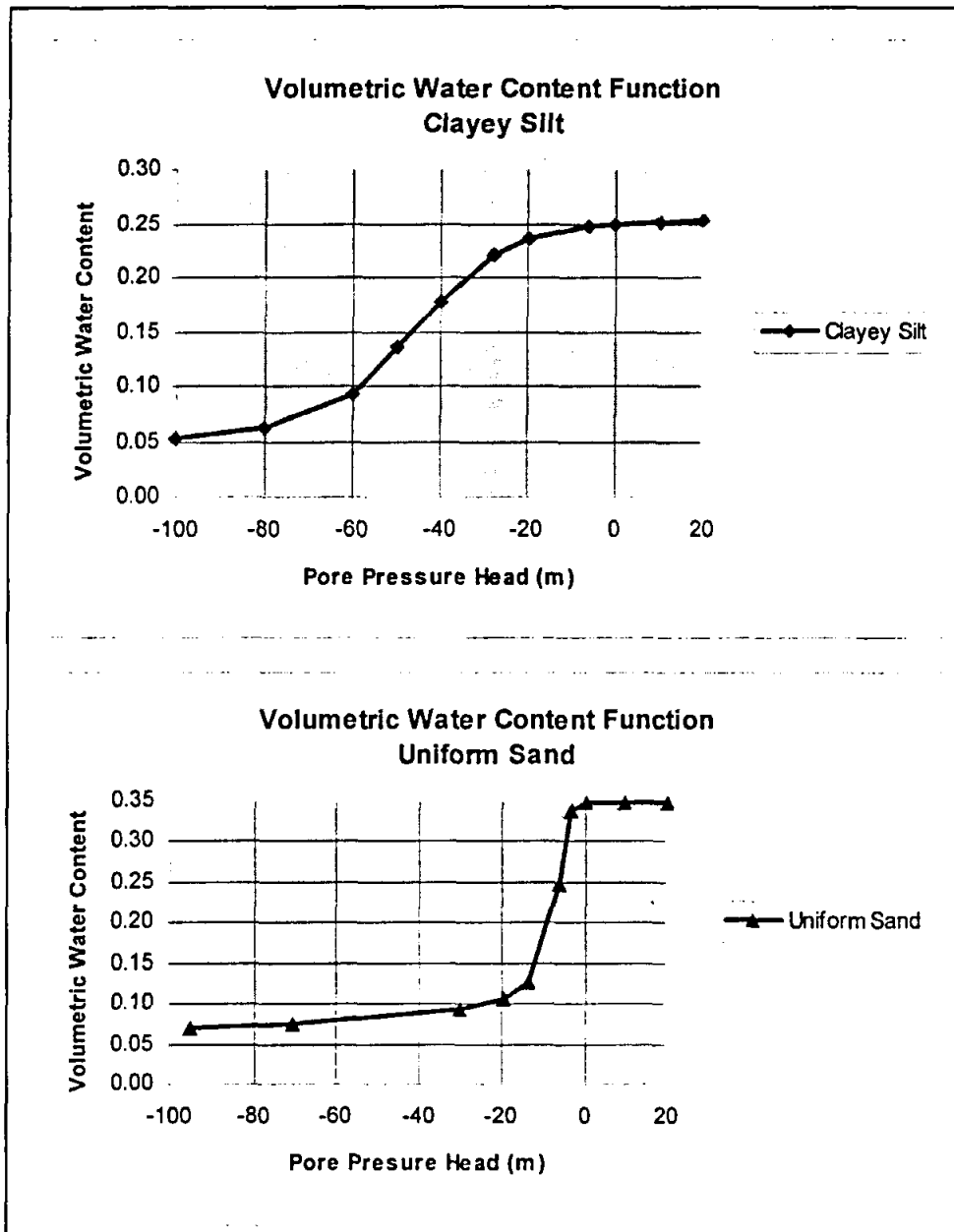
Figure 7 : Examples of Volumetric Water Content Functions

Since water flows along a web of interconnected conduits, decreasing the volumetric water content has the effect of decreasing the size and number of conduits available for flow thereby reducing the conductivity. The effective degree of saturation, S_e, may be defined as:

$$S_e = \frac{S - S_r}{1 - S_r}$$

(34)

Where : S   =   degree of saturation

S_r =   residual degree of saturation or degree of saturation above which a significant increase in the matric suction does not produce a significant decrease in the degree of saturation.(determined by laboratory test)

For negative pore pressure values above the air entry value, the water permeability may be calculated as :

$$k_z = K_{sat} . S_e^{\delta}$$ (35)

Where δ =   an empirical constant dependent on the pore size distribution.

There are a number of commercially available computer programmes to model unsaturated flow such as *FLAC.*, *UNSAT2* and *SEEP/W*. A limitation of the programmes is that they do not take cognisance of the heterogenous nature typically found in many coarse waste piles, which gives rise to preferential flow paths.

5.1.2 Preferential Flow Paths

In the case of heterogenous coarse waste, high permeability channels or preferential flow paths may be the primary controls of water movement. This implies that a large part of the total flow may take place through a small proportion of the cross sectional area. This gives rise to the double or multi-peaked solute plumes which have been reported in the field (*Jury et al, 1989; Butters et al, 1989; Roth et al, 1991; Sassner et al, 1994*). The concept of preferential flow paths can be described by a bi-model or multi- modal probability distribution of the residence time in the waste pile (*Destouni et al, 1994*), which recognises the existence of two (or more) populations of residence times within the waste pile and satisfies the continuity equation. The continuity equation for bi-modal flow may be written as:

$$q = \upsilon q_{SFP} + (1 - \upsilon) q_{RFP}$$ (36)

Where   q   =   *mean water flow per unit cross sectional area*

q_{SFP} & q_{RFP} =   *the mean water flux along the slow flow paths,(SFP),*
and the preferential or rapid flow   paths, (RFP),
respectively.

υ   =   *probability that the flux is dominated by the slow flow*
paths.

The residence time of an ideal tracer can be represented by(*Eriksson et al, 1994*):

$$f(T) = \upsilon PDF(T_1) + (1-\upsilon)PDF(T_2) \quad \quad (37)$$

Where $f(T)$ =   *bi-modal distribution for the residence time in*
the waste material

$PDF(T_1)$, $PDF(T_2)$ =   *probability distributions for the residence time*
for the slow and fast flow paths respectively

The water flux routine applied in Salmine requires that the proportion of flow along the SFP's be specified as input data.   Thus if the net infiltration to the layer during the time step is Q, the proportion which passes through the SFP's is given by υQ and the proportion which passes along the RFP's is given by $(1-\upsilon)Q$. The model further assumes that the residence time within each layer for flow along the RFP's is much shorter than the time step Δt, and that water leaving layer j during a time step will be distributed throughout the lower layers during the time step. It is therefore assumed that no water accumulates along the RFP's and the volumetric water content remains unchanged from that at the beginning of the time step.

The volume of water flowing from layer j, along the RFP's is distributed to the layers $j+1$ through to layer 10 according to the weighting factors calculated such that equation (38) is satisfied:

$$1 = \sum_{i=1}^{10} \left[\frac{\frac{1}{d_{ij}}}{\sum_{j=i+1}^{j=10} \frac{1}{d_{ij}}} \right] \quad \quad (38)$$

Where d_{ij} =   distance from the top of layer I to the top of layer j

The weighting factor, f_{ij} used to determine the quantity of flow from layer I which will enter layer j along the RFP's is given by equation (39):

$$f_{ij} = \frac{\frac{1}{d_{ij}}}{\sum_{j=i+1}^{j=10} \frac{1}{d_{ij}}}$$

(39)

The total flow passing the top surface of layer I, $Q_{RFP\,I}$, along the RFP's is thus calculated from equation (40) as follows:

$$Q_{I}(1-\upsilon) = Q_{RFP_{I}} \cdot \sum_{j=i+1}^{10} f_{ij}$$

(40)

Where $Q_{RFP\,I}$ =   *volume of water flowing from layer I along the RFP's.*

    $.Q_{I}$ =   *total volume of water leaving layer I .*

The user is required to decide for each layer of material, the proportion of the total inflow to the layer, υ, that will pass through the layer along the slow flow paths. An indication of the correct value may be obtained by observing the response of a waste pile or kinetic test cell to an infiltration event by plotting the inflow and outflow hydrographs.

5.1.3 Routine for the Calculation of the Flux along the SFP's and the Volumetric Water Content

The spatial variability in the particle size distribution of coarse wastes has a profound effect on the pore pressure distribution within the unsaturated zone resulting in dramatic changes in pore pressure over short distances within the waste. Typical coarse wastes often demonstrate a sharp change in the gradient of the negative pore pressure versus volumetric water content or permeability curves

for relatively small changes in the negative pore pressure.   This   often results in mathematical instability if the rigorous finite difference or finite element approach is applied to solve equation (32). Furthermore, given the variability of the material, the finite element or finite difference solution procedure does not necessarily result in a significantly more accurate prediction of the actual volumetric water content or water flux, than would a simplified approach.

The approach used in *Salmine* to model temporal changes in the   volumetric water content and the water flux along the SFP's, is to   assume that each layer comprises an independent compartment with respect to flow. An imaginary "wetting front" is assumed to form in a layer, whenever the   degree of saturation is greater than S_r. S_r must be specified as an input parameter and may be determined from laboratory tests on a sample of the waste. The rate at which the wetting front moves through the layer is a function of the permeability of the waste, k, which is determined from equation (35). The distance that the imaginary wetting front moves during the time step, Δt, is calculated as follows:

$$q_i^* = k_z.\Delta t \tag{41}$$

Where q_i^* =   vertical downward distance moved by the imaginary wetting front in time Δt, (m/m^2)

Substitution for k_z from equation (32), gives:

$$q_i^* = K_{sat}.(\frac{S-S_r}{1 - S_r})^6.\Delta t \tag{42}$$

In addition to equation (42) above, a mass balance condition must be satisfied for each layer and at each time step.   The mass balance equation is given below:

$$\Delta V_{storage} = V_{inflow} - V_{outflow} \tag{43}$$

Where V_{inflow} and $V_{outflow}$ *represent the volume of water infiltrating through the top and exiting at the lower boundary of the layer respectively, during the time step.*

At the start of the time step, the distance from the upper boundary of the layer to the wetting front is $q^{*}_{r=0}$. If the degree of saturation in the layer is greater than S_r, then it is assumed that the excess moisture is situated in a wetting front which comprises a saturated zone of thickness $\theta^{*}_{r=0}$. The remainder of material in the layer is assumed to have a degree of saturation of S_r.

The routine for calculating the flow rate and volumetric water content in each layer may be summarised as follows:

❶   At the start of the time step, just prior to infiltration, the following calculations are performed for each layer:

> ► The degree of saturation $(S_{r=0})$ and depth to the wetting front $(q^{*}_{r=0})$ at the end of the previous time step, are retrieved from the data base.

> ► The thickness of the imaginary wetting front is calculated from equation (44)

$$\theta^{*}_{r=0} = \frac{(S_{r=0} - S_r)}{n.l} \tag{44}$$

Where $\theta^{*}_{r=0}$ = thickness of the wetting front prior to infiltration

$S_{r=0}$ = the degree of saturation at the start of the time step

$n.l = V_v$ = volume of voids in the layer

❷   Water is then allowed to infiltrate the layer. The total quantity of water which infiltrates layer j is assumed equal to the quantity of water which flowed out of layer j-1, during the previous time step.

The infiltrated water results in an additional "wetting front" located just below the top surface of the layer, of thickness :

$$\theta^{\bullet}_{infilt} = \frac{\upsilon q_t}{S_r.n(1-S_r)}$$ (45)

To simplify the calculation, the two wetting fronts are combined to form a single equivalent imaginary wetting front in each layer. This is achieved by taking moments about the upper boundary of each layer of the wetting front thickness, to calculate the depth to the lower extremity of an equivalent single wetting front. The depth to the lower extremity of the single wetting front $q^{\bullet}_{new}$ is calculated as follows:

$$q^{\bullet}_{new} = \frac{q^{\bullet}_{t=0}.\ \theta^{\bullet}_{t=0} + 0.5.(\theta^{\bullet}_{infilt})^2}{\theta^{\bullet}_{t=0} + \theta^{\bullet}_{infilt}}$$ (46)

where $q^{\bullet}_{new}$ =   *depth to the combined wetting front (m)*

$\theta^{\bullet}_{t=0}$ =   *thickness of the wetting front in the layer at the end of the previous time step (m)*

$\theta^{\bullet}_{infilt}$ =   *thickness of the wetting front associated with the infiltrated water (m)*

The thickness of the combined wetting front is calculated as follows:

$$\theta^{\bullet}_{new} = \theta^{\bullet}_{t=0} + \theta^{\bullet}_{infilt}$$ (47)

❸   The thickness $(\theta^{\bullet}_{new})$, and depth $(q^{\bullet}_{new})$, of the combined new wetting front in each layer has been calculated. Next, the distance that the wetting front moves down through the layer is calculated based on the effective permeability of the waste as follows:

$$q_t^{\bullet} = K_{sat}.(\frac{S-S_r}{1 - S_r})^{\delta}.\Delta t$$ (48)

Where S =   *degree of saturation ≤ 1*

At the end of the time step, the new depth to the wetting front is calculated from:

$$q^{\bullet}_{t_{end}} = q^{\bullet}_{t} + q^{\bullet}_{new}$$ (49)

❹   The quantity of water which flows out of the layer during the time step is calculated as follows:

• If $q^{\bullet}_{t\,end} - \theta^{\bullet}_{new} >$ *layer thickness* then the entire wetting front volume passed out of the layer and will be available during the next time step as infiltration to the next lower layer. The degree of saturation at the end of the time step will be S_r

• If $q^{\bullet}_{t\,end} <$ *layer thickness* then no water passes out of the layer. The degree of saturation in the layer will be increased due to the net inflow of water to the layer during the time step.

• If $q^{\bullet}_{t\,end} - \theta^{\bullet}_{new} <$ *layer thickness,* then the outflow is calculated as follows:

$$Q_{SFP} = [\frac{q^{\bullet}_{t\,end} - l}{\theta^{\bullet}_{new}}](S-S_r)$$ (50)

❺   At the end of the time step, after water has been allowed to flow out of the layer, the new depth to the wetting front and new degree of saturation is written to a spreadsheet for use in the next time step.

❻   At the end of the time step, the quantity of water remaining in the layer is calculated from equation (51) below, thus satisfying the condition of mass balance:

$$V_{t=t} = V_{t=t-1} + Q_{inflow} - Q_{RFP} - Q_{SFP}$$ (51)

where Q_{inflow} = *total inflow to layer j from layer j-1 during time step i*

Q_{RFP} = *total outflow from layer j during the time step i due to flow along the RFP's*

Q_{SFP} = *total outflow from layer j during the time step i due to flow along the SFP's*

$V_{i=i}$ = *volume of water in layer j at the end of time step i*

$V_{i=i-1}$ = *volume of water in layer j at the end of time step i-1*

❼   The total volume of water available to infiltrate the next lower layer at the start of the next time step is given by equation (52):

$$Q_{inflow_{j-1}} = Q_{SFP_j} + Q_{RFP_j} \qquad (52)$$

Where j refers to the layer number.

5.2   Key Assumptions and Implications of the Water Flux Model

The assumptions relating to this model are as follows:

•   Since flow occurs in the vertical downward direction only, evaporation losses or losses due to capillary rise are not considered.

•   Water can only migrate from a layer to the next lower layer during a single time step. The time step selected must be sufficiently short to ensure that this limitation is realistic. The minimum residence time for water in the waste pile is therefore 10 time steps.

•   Since evaporation losses are not considered, the degree of saturation cannot decrease below the residual degree of saturation for each respective layer.

---

6   CHEMICAL PRECIPITATION, DISSOLUTION AND NEUTRALISATION

6.1   Objective of the Chemical Precipitation, Dissolution and Neutralisation Routine

The objectives of this model are as follows :

- To estimate the pH of the pore water in each layer.

- To estimate the concentration of aqueous chemical components in each layer including sulphates, carbonates, iron and calcium.

- To estimate the concentration of chemical species.

6.2   Description of the Thermodynamic Chemical Equilibrium Model

Whereas sulphide oxidation reactions are typically modelled on the basis of reaction kinetics, thermodynamic models are commonly applied to model neutralisation in waste rock piles. The thermodynamic model represents the end condition or boundary condition to which the system will move, given sufficient time. The time that the system will take to achieve the species concentrations predicted in the thermodynamic model is however a function of the kinetics of the reactions. For the purpose of this model, a routine has been developed in which the reactions are assumed to proceed sufficiently rapidly such that equilibrium conditions are achieved within each time step. This assumption can result in errors which may be evident from field measurements. For example, with regard to the redox couple Fe^{2+}/Fe^{3+}, at pH < 5, the thermodynamic model would predict that Fe^{2+} is almost entirely converted to Fe^{3+}. However, field observations show that this is not the case since the rate at which Fe^{2+} is oxidised is relatively slow compared to the rate at which water migrates through the waste pile, resulting in the release of Fe^{2+} from the waste pile under circumstances in which a thermodynamic model would indicate complete conversion of Fe^{2+} to Fe^{3+}. The rate of oxidation of Fe^{2+} to Fe^{3+} has been

shown to be strongly dependent on the alkalinity of the water (*Department of the Interior, Federal Water Quality Administration, 1970*).

The chemical speciation model comprises a thermodynamic model, which is used to calculate the aqueous species concentrations, pH, and the mass of secondary minerals which precipitate.

There are two mathematically equivalent approaches to solve multi-component thermodynamic problems (*USEPA, 1991*), namely :

- minimisation of the systems free energy under mass balance constraints, or

- simultaneous solution of the non-linear mass action expressions and linear mass balance relationships.

The majority of computer models such as MINTEQA2, (*USEPA, 1991*), use the latter approach which is briefly described below:

A system of n independent components can combine to form m species, represented by the set of mass action expressions of the form :

$$[S_i] = \frac{k_i}{\gamma_i} \cdot \prod_j X_j^{-a_{ij}}$$

(50)

where: $[S_i] = Ci$ = concentration of species i

k_i = equilibrium constant for the formation of species i

γ_i = activity coefficient of species i

X_j' = activity of component j

a_{ij} = stoichiometric coefficient of component j in species i

For example, for a solution of $CaCO_3$ dissolved in water, the chemical components selected for the problem would include H_2O, Ca^{2+}, CO_3^{2-} and H^+ . These components would combine to form a set of chemical species according the

reactions shown below:

Table 2 : Reactions and Log Equilibrium Constants for a 0.001M solution at 25° C.

Reactions	Mass Action Constraints	Log K
$H_2O \rightharpoonup H_2O$	$[H_2O] = \{H_2O\}k'_1$	1,0
$H^+ \rightharpoonup H^+$	$[H^+] = \{H^+\}k'_2$	1,0
$CO_3^{2-} \rightharpoonup CO_3^{2-}$	$[CO_3^{2-}] = \{CO_3^{2-}\}k'_3$	1,0
$Ca^{2+} \rightharpoonup Ca^{2+}$	$[Ca^{2+}] = \{Ca^{2+}\}k'_4$	1,0
$H_2O - H+ \rightharpoonup OH-$	$[OH\cdot] = \{H_2O\}\{H+\}^{-1} k'_5$	-14,0
$CO_3^{2-} + H+ \rightharpoonup HCO_3^-$	$[HCO_3\cdot] = \{CO_3^{2-}\}\{H+\}k'_6$	10,2
$CO_3^{2-} + 2H^+ \rightharpoonup H_2CO_3^-$	$[H_2CO_3\text{-}] = \{CO_3^{2-}\}\{H^+\}^2 k'_7$	16,5
$Ca_{2+} + H_2O - H+ \rightharpoonup CaOH+$	$[CaOH+] = \{Ca_{2+}\}\{H_2O\}\{H+\}^{-1} k'_8$	-12,2
$Ca^{2+}\ CO_3^{2-} +H^+ \rightharpoonup$ $CaHCO_3^+$	$[CaHCO_3^+] = \{Ca^{2+}\}\{CO_3^{2-}\}\{H^+ \}k'_9$	11,6
$Ca^{2+}\ CO_3^{2-} \rightharpoonup CaCO_3$	$[CaCO_3] = \{Ca^{2+}\}\{CO_3^{2-} \}k'_{10}$	3,0

Note: the terms in { } brackets represent the activities of the components
the terms in [] represent the concentrations

In addition to the mass action expressions, the set of n independent components are governed by n mass balance equations of the form:

$$Y_j = \sum_i a_{ij}.C_i - T_j \tag{51}$$

where T_j = *total dissolved concentration of component j*

In the example above, the mass balance expressions required to complete the set of equations which define the $CaCO_3$ system are as follows:

$$Y_{ca} = [Ca^{2+}] + [CaOH^+] + [CaHCO_3^+] + [\ CaCO_3\ ] - T_{ca} \tag{52}$$

$$Y_{CO_3} = [CO_3^{2-}\ ] + [\ HCO_3^-] + [\ H_2CO_3^-\ ] + [CaHCO_3^+] + [CaCO_3] - T_{CO_3} \tag{53}$$

$$Y_{H+} = [\ H^+] - [OH^-] + [HCO_3^-\ ] + [H_2CO_3^-] + [CaOH^+] + [\ CaHCO_3^+] - T_{H+} \tag{54}$$

Where Y_j = *error in the mass balance equation*

T_j = *total analytical concentration of component j*

The solution to the problem is the set of component activities, X, which result in the set of component concentrations, C, such that each individual set of mass balance differences, Y, are equal to zero or some small error.

The solution to the set of equations for the calcite system may therefore be found by substituting the expressions for the mass action constraints into the mass balance equations and then solving the system of non-linear equations using a numerical solution procedure.

The chemical speciation problem described in *Salmine* is similar to that of the calcite system described above, except that in addition to the components listed above, the components Fe^{2+} and SO_4^{2-} are also included. The matrix of stoichiometries for the reactions included in *Salmine*, together with the log K values, is shown in Figure 8.

In the case of the components H^+, Fe^{2+} and SO_4^{2-}, the total analytical concentration T_j, are calculated from the mass of each component produced due to the oxidation of pyrite. The component masses are calculated from the aqueous phase and solid phase masses present in the layer. The total component masses are calculated as follows :

$$T_j = M(aq)_j + M(s)_j \qquad (55)$$

where M(aq) refers to the aqueous phase mass and M(s) the solid phase mass

In the model Salmine, it is assumed that the proportion of chemical components which can contribute to the leachate water quality is dependent on the degree of saturation and pore size distribution factor. The balance of the mass of chemical components is assumed to lie off the interconnected discrete flow channels and is therefore unable to significantly alter the leachate chemistry. The net concentration

of each chemical component j is calculated as per equation (56) below.

$$T_j = \frac{M(aq)_j + M(s)_j}{V_j}.S^\delta$$

(56)

where Vj = volume of water in layer j

Thus for spoils with a low degree of saturation, a smaller proportion of the total stored products can be leached from the waste. Likewise, for lower degrees of saturation, a smaller proportion of the total mass of calcite will be available for neutralisation. For saturated spoils, the concentration (and hence load) of each contaminant will be limited only by the chemical saturation concentrations with respect to solid species.

The Davies equation(57), (USEPA, 1991), is used to calculate the activity coefficient γ_i for each species.

$$\log \gamma_i = -AZ_i^2 \left[\frac{I^{0.5}}{1 + I^{0.5}} + 0.24I\right]$$

(57)

where I =   *solution ionic strength*
          A =   *constant* $= 0,52$
          Z_i =   *charge on species i*

ACTIVITY species	Ca2+ 1.60E-04	CO32- 2.44E-07	H+ 4.36E-10	e- 7.04E+04	H2O 1.00E+00	Fe2+ 5.02E-23	SO42- 2.22E-15	log K
Ca2+	1							0
CO32-		1						0
H+			1					0
e-				1				0
H2O					1			0
Fe3+				-1		1		-13.03
Fe2+						1		0
SO42-							1	0
OH-			-1		1			-13.998
HCO3-		1	1					10.33
H2CO3		1	2					16.681
CaOH+	1		-1		1			-12.598
CaHCO3+	1	1	1					11.33
CaCO3	1	1						3.15
Fe(OH)3-1			-3		3	1		-31
Fe(OH)2			-2		2	1		-20.57
Fe(OH)+			-1		1	1		-9.5
Fe(SO4)						1	1	2.25
Fe(SO4)+				-1		1	1	-9.11
Fe(OH) +2			-1	-1	1	1		-15.22
Fe(OH)2 +1			-2	-1	2	1		-18.7
Fe(OH)3			-3	-1	3	1		-26.63
Fe(OH)4 -			-4	-1	4	1		-34.63
Fe(SO4)2 -1				-1		1	2	-7.61
Fe2(OH)2 4+			-2	-2	2	2		-28.88
HSO4 -			1				1	1.987
CaSO4(aq)	1						1	2.309
Fe2O3 (s)			-6	-2	3	2		-24.61
calcite	1	1						8.475
gypsum	1				2		1	4.848

Figure 8 : Assumed Stoichiometric Matrix applied to the Chemical Speciation Sub-model in Salmine

The solution ionic strength is calculated as:

$$I = \frac{1}{2}\sum_{i=1}^{m} Z_i^2 C_i$$ (58)

where Z_i = charge on species i

Only three solid species are considered, namely calcite, haematite and gypsum. During the solution procedure the saturation index is calculated for each solid phase. The solid species with the highest positive saturation index is then allowed to precipitate. For every solid species that precipitates, one degree of freedom is lost

and one component activity becomes dependent on the activity of another. For example, if calcite precipitates the activity of carbonate may be calculated from:

$$(CO_3^{2-}) = \frac{1}{k_{CaCO_3} \cdot (Ca^{2+})}$$

(59)

In the event that gypsum precipitates, the sulphate activity is fixed as follows:

$$(SO_4^{2-}) = \frac{1}{k_{CaSO_4} \cdot (Ca^{2+})}$$

(60)

Similarly, if Fe_2O_3 precipitates, the activity of Fe^{2+} is fixed according to equation (61).

$$(Fe^{2+}) = \frac{(H^+)^3 (e^-)}{k_{Fe_2O_3}}$$

(61)

where the terms in brackets represent the component activities

In order to estimate the electron activity *(e⁻)* a relationship for the electron activity is assumed which is based on the Eh- pH relationship for Fe^{2+}/Fe^{3+}. Figure 9 presents a framework for the Eh-pH diagram in which the most usual limits of Eh and pH in the near surface environments have been plotted. The upper limit of the weathering environment is considered to be in direct contact with air whereas the lower limit is considered to be the water table.

Assumed Eh vs. pH Diagram for Fe2+/Fe3+
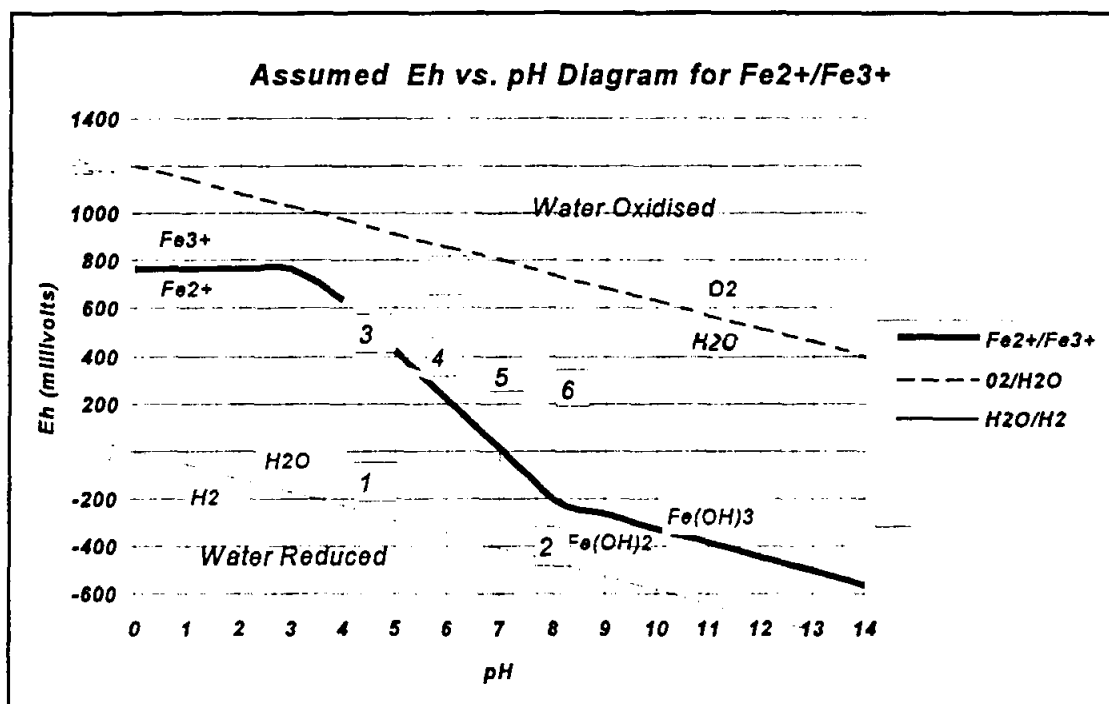
Figure 9 : Eh -pH Relationship Assumed in Salmine

The zones marked 1 to 7 on the figure represent the Eh-pH conditions typical of the following environments :

①   bogs and waterlogged soils

②   reducing marine sediments

③   acid mine waters

④   rain water

⑤   river waters

⑥   ocean waters

⑦   oxidising lead sulphide deposits

The Eh-pH function assumed in the model *Salmine* is shown as a thick solid line. The horizontal portion of the curved line (Fe^{2+}/Fe^{3+}) represents the reaction :

$Fe^{2+} - Fe^{3+} + e^-$

The steeply sloping portion of the curved line represents the reaction:

$Fe^{2+} + 3H_2O - Fe(OH)_3 + 3H^+ + e^-$
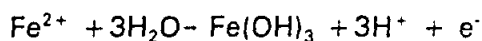
The flatter portion of the curved line to the right of pH = 8 represents the reaction:

$Fe(OH)_2 + OH^- - Fe(OH)_3 + e^-$
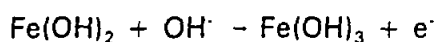
The pH is calculated as follows:

$$pH = -\log(H^+) \tag{62}$$

Where   *(H⁻)*   =   *H⁺ activity*

Should the saturation index fall below zero for a particular solid then the solid re-dissolves. The saturation index is defined as :

$$Saturation\ Index = \log[\frac{IAP}{k_i}] \tag{63}$$

Where IAP   =   *ion activity product for the species*

The system of non-linear equations is solved using the Excel add-in programme, *Solver* supplied by Microsoft with Excel version 5 or later. The approach used to solve the equations is to initially assume the saturation indices for each solid to be less than zero and then to solve the equations. On completion of the solution procedure the saturation indices are re-calculated. The solid with the highest positive saturation index is then allowed to precipitate by setting the saturation index for that solid equal to zero. The solution procedure is then repeated and once the numerical solution technique has converged to a solution, the assumed saturation index values are compared with the new calculated saturation index value for each solid. If the calculated saturation indices differ from the assumed values, then the solid with the highest positive saturation index is allowed to precipitate and any solids with a negative saturation index are allowed to re-dissolve, the solution procedure is then repeated. Once the calculated saturation indices are the same as the assumed values, the solution procedure is terminated.

The objective function for the solver routine is set to minimise the least squares function shown as equation (64) subject to the constraints shown as equation (65):

$$Objective\ function = Minimise \sum_{j=1}^{n} (T_j - \sum_{i=1}^{m} a_{ij}c_i)^2 \tag{64}$$

The charge balance for the electron component is excluded from the above expression.

$$M(s)_j \geq 0 \hspace{4cm} (65)$$

Where $M(s)_j$ =   *mass of solid species j*

On completion of the above solution procedure, the concentrations of aqueous species [Ca], [CO$_3$ $^{2-}$], [Fe^{2+}] and [SO$_4$$^{2-}$]   are calculated together with the mass of solid species CaCO$_3$, Fe$_2$O$_3$ and CaSO$_4$.

6.3   Key Assumptions and Implications

The limitations applicable to the model are as follows:

- The chemical components considered are restricted to Ca^{2+}, CO$_3$$^{2-}$, Fe^{2+}, SO$_4$$^{2-}$ and H$^+$.   The model cannot therefore be used for the analysis of situations involving other metals. The validity of the model may therefore be limited in cases where secondary metals are likely to be present at concentrations which significantly alter the thermodynamic problem, or where sulphides composed primarily of metals other than iron, may be present in significant quantities.

- The solid species considered in the model are calcite, gypsum and haematite. A single solid species is therefore included for each chemical component in the model. The choice of the solid species, haematite and gypsum, was based on the results of modelling carried out using MinteqA2, which predicted that these minerals were the predominant minerals formed under a wide range of cases, involving the components Fe^{3+} and SO$_4$$^{2-}$.

- The mass of chemical components available to be leached is assumed dependent on the pore size distribution factor and the degree of saturation.

- It is assumed that the calcite does not become armoured during the

precipitation process, rendering it unavailable for neutralisation.

6.4   **Options**

The chemical equilibrium module may be switched on or off at the start of each simulation. It is generally not necessary to run the chemical equilibrium module at every time step since the change in water quality from one time step to the next is usually small. If the chemical speciation module is switched off, the chemical equilibrium conditions present in each layer are trended, based on the results obtained when the module was last applied. If the results of the chemical speciation routine indicate that components were present in the solid phase at the end of the previous time step, then it is assumed that the solution remains saturated with respect to the component throughout all future time steps while the chemical speciation sub-module is switched off. The aqueous phase concentration, is therefore assumed to remain constant throughout all future time steps, until the chemical speciation sub-model is switched on again. A mass balance equation is solved during each time step to calculate the solid phase component mass, at the end of each time step. Likewise, if the chemical speciation sub-model indicates that the component under consideration is not present in the solid phase, then it is assumed that for proceeding time steps, while the chemical speciation sub-module is switched off, no solid phase will precipitate. The mass balance equation is solved for the component under consideration by assuming that the entire mass of the component is present in the aqueous phase.

The approach described above considerably simplifies the computational effort and time required to execute temporal analyses. Provided that the chemical speciation routine is applied at reasonable frequency for each layer, such that the significant changes in the component concentrations are detected, the approach would not result in significant deviations in the predicted water quality.

A further option has been provided which enables the user to specify saturation concentrations with respect to solid species. The data may be obtained from

laboratory or field tests, or from other chemical equilibrium models such as MinteqA2. In this case, saturation concentrations and the pH must be specified for each chemical component. The values for saturation concentrations and pH may be specified for each layer and may be changed after each time step or as frequently as desired. The method of trending results between each time step is similar to that previously described.

7   CALCITE DEPLETION

7.1   Objectives

To calculate the calcite mass balance in each layer after each time step.

7.2   Description of the Calcite Depletion Routine

The calculation sequence to estimate the mass of calcite remaining after each time step, for each layer, is as follows:

❶   The mass of calcite dissolved/precipitated in each layer, in order to maintain the aqueous concentration of CO_3^{2-} and Ca^{2+} at the predicted equilibrium concentration without allowing inflow or outflow from the layer under consideration is calculated.

❷   The additional mass of calcite which must be dissolved or precipitated in order to re-establish the equilibrium concentration after infiltration, is calculated. For example, if 12 litres of water flow into layer j from layer $j-1$ with a Ca^{2+} concentration of 0.020moles/litre, and if the equilibrium concentration for Ca^{2+} in layer j is 0,05mole/litre, then:
(0,050-0,020)mole/litre x 12 litres x 100 g/mole $CaCO_3$ = 36g $CaCO_3$ would need to dissolve in layer j in order to re-establish equilibrium.

❸   The mass of calcite remaining in the layer after dissolution or precipitation

is calculated by subtracting the mass of calcite dissolved during the time step from the mass of calcite at the start of the time step.

The initial available mass of calcite present in each layer is required as input to the model. The calcite equivalent mass of neutralising minerals present in a sample of the waste may be determined from laboratory analysis. The proposed method to determine the neutralising potential is documented in Appendix D. Since only a proportion of the neutralising potential of the material is generally available for neutralisation in coarse wastes, it is proposed that the total calcite equivalent content applied in the model be less than that determined by the net neutralisation potential test. The kinetic test procedure discussed in Chapter 2, may be used to estimate the proportion of the total calcite equivalent content of the waste which is available for neutralisation.

7.3   Key Assumptions and Implications

A key assumption implicit in the routine described above is that the water passing through the layer comes into contact with calcite minerals for a sufficient period of time for dissolution to occur.

8   CONTAMINANT TRANSPORT

8.1   Objectives of the Contaminant Transport Routine

The objective of the contaminant transport routine is to calculate the quantity of aqueous phase components which are flushed from each layer to the next lower layer due to migrating water.

8.2   Description of the Contaminant Transport Routine

Mathematical models to predict the proportion of aqueous phase contaminants

which are flushed from the waste particle surfaces, were not found in the literature. This is apparently an aspect of ARD prediction modelling which has not been addressed in detail but which can be particularly significant in the case of coarse wastes, given the presence of preferential flow paths and the fact that the coarse waste are generally unsaturated throughout most of their life. The approach described in this section, has been developed for the *Salmine* model, and is based on the following premise:

- In a saturated waste pile, all soluble species present in the waste pile are considered to be situated on a flow path and will therefore be able to migrate from one layer to the next as seepage.

- Since coarse waste piles are usually only partially saturated, aqueous phase species stored on rock fragment surfaces which are not in contact with discrete flow channels, remain immobile. The proportion of particle surfaces which are not flushed, increases as the degree of saturation decreases. Once the residual degree of saturation S_r is reached, no flushing or transport of dissolved aqueous phase species can takes place since there are effectively no discrete flow channels along which water can flow.

- Since the permeability k_u , is a measure of the area available for flow, it is assumed that the proportion of aqueous species available for flow would be proportional to k_u/K_{sat}.

- Since $k_u = K_{sat}.S_e^{\delta}$, the proportion of aqueous phase chemical components available for movement from one layer to the next is calculated as:

$$\xi_j = \frac{k_{u_j}}{K_{sat_j}} = S_{e_j}^{\delta_j} \tag{66}$$

where ξ_j = *proportion of aqueous phase chemical components available for movement in layer j*

The subscript j refers to the layer number.

The empirical constant, δ, is related to the pore size distribution index (*Fredlund et al. Soil Mechanics for Unsaturated Soils*) :

$$\delta = \frac{2+3\lambda}{\lambda} \tag{67}$$

Where : λ =   *the pore size distribution index, defined as the negative slope of the effective degree of saturation, S_e versus matric suction, $(u_a - u_w)$, curve.*

Typical values for λ are as follows(*Fredlund et al., 1993*):

Uniform sand	∞
Soil and porous rocks	2,0
Natural sand deposits	4,0
Volcanic sand	2,29
Fine sand	3,70
Silt loam	1,82
Glass beads	7,30

Soils with a wide range of pore sizes have a small value of λ. The more uniform the particle distribution, the higher the value of λ. The value for λ, may be determined from laboratory measurements by measuring the hydraulic conductivity of the soil at various negative pore pressures.

The proportion of conservative aqueous species which are available for transport during a unit time interval may therefore be estimated from S^δ, and the proportion which remains stationary during the time interval will be $(1-S^\delta)$.

8.3   Key Assumptions and Implications

No distinction is made between the percentage of aqueous phase components flushed from the SFP's and the percentage flushed from the RFP's. Since the degree

of saturation applied in the above routine is the average degree of saturation over the entire layer, the model tends to over-estimate the proportion of aqueous phase products flushed from the waste along the RFP's and under estimate the proportion flushed from the SFP's. In a waste pile, preferential flow paths are typically discontinuous from the top of the pile to the bottom, and a tracer would be expected to follow a path which passes along the SFP's and RFP's at different stages on route to the bottom of the waste pile. This implies that contaminants generated along the SFP's migrate into the RFP's thus resulting in the establishment of a contaminant concentration gradient which decreases in the direction away from the RFP's. The steepness of the concentration gradient is a measure of the error implicit in this assumption. If the actual mass of contaminants along the RFP's is similar to that in an adjacent SFP zone then the error implicit in the assumption is negligible. As the concentration difference increases, so the error increases.

9   WATER QUALITY

9.1   Objectives of the Water Quality Routine

The objective of the water quality routine is to calculate the concentrations of aqueous species and the mass of solid species in each layer at the end of each time step. The concentration of chemical components leaving the lowest layer represents the concentration of contaminants released from the unsaturated zone of the waste.

9.2   Description of the Water Quality Routine

The total mass of component i, in layer j, is the sum of the mass of the component bound in solid phase and aqueous phase species, as shown in equation (68):

$$M_{ij} = M(aq)_{ij} + M(s)_{ij} \tag{68}$$

The mass of the component in the aqueous phase may be differentiated into two groups, namely that which is available for transport and that which is not, as given by equation (69):

$$M(aq)_{i,j} = \xi M(aq)_{i,j} + (1-\xi)M(aq)_{i,j} \tag{69}$$

where $\quad M(aq)_{i,j}$ $\quad$ = $\quad$ *total mass of aqueous phase component i in layer j*

$\xi M(aq)_{i,j}$ $\quad$ = . $\quad$ *mass of aqueous phase component available for transport*

$(1-\xi)M(aq)_{i,j}$ $\quad$ = $\quad$ *mass of aqueous phase component not available for transport*

The concentration of the chemical component in layer *j* is calculated as follows:

$$C_{i,j} = \frac{\xi M(aq)_{i,j}}{V_j} = C(out)_{i,j} \tag{70}$$

where $C(out)_{i,j}$ = *concentration of component i in the outflow from layer j*

V_j $\quad$ = $\quad$ *total water volume in layer i*

$C_{i,j}$ $\quad$ = $\quad$ *concentration of component i in layer j*

The load of component *I*, to pass out of layer *j-1*, and into layer *j* during the time step is calculated as :

$$M(out)_{i,j-1} = \frac{\xi M(aq)_{i,j-1}}{V_{j-1}} = C(out)_{i,j-1} \cdot q_{j-1} \tag{71}$$

Where $M(out)_{i,j-1}$ $\quad$ = *mass of component i passing out of layer j-1*

q_{j-1} $\quad$ = $\quad$ *flow volume from layer j-1 during the time step*

The concentration of the component in layer j, at the start of the next time step, $t=t+1$, is calculated as follows :

$$C_{i,j,t+1} = \frac{\xi_{j-1,t} \cdot M(aq)_{i,j-1,t} \cdot q_{j-1,t} + \xi_{j,t} \cdot M(aq)_{i,j,t} \cdot V_{j,t}}{q_{j-1} + V_j} \tag{72}$$

The aqueous phase mass of component i, at the start of the next time step, $t=t+1$, after infiltration to layer j from layer $j-1$, and outflow from layer j to layer $j+1$, is calculated as follows:

$$M(aq)_{i,j,t+1} = C_{i,j,t+1} \cdot (V_{j,t} + q_{j-1,t} - q_{j,t}) + M(aq)_{i,j,t} \cdot (1 - \xi_{j,t}) \qquad (73)$$

CHAPTER TWO

KINETIC TEST TRIALS AND THE DEVELOPMENT OF A PROPOSED NEW KINETIC TEST PROCEDURE FOR COARSE WASTES

1 INTRODUCTION

The second objective of the project was to evaluate kinetic laboratory test methods to determine the propensity of coarse wastes to generate acidity. This chapter addresses this objective and describes :

- The field and laboratory tests which were carried out to evaluate a kinetic test method to determine the propensity of coarse wastes to develop acidity.

- Based on observations made during the kinetic test trials, and with the knowledge of the data requirements for the *Salmine* model, modifications to the kinetic test method and apparatus are proposed to improve the prediction methodology.

2 DESCRIPTION OF THE KINETIC TEST APPARATUS AND TEST PROCEDURE APPLIED DURING THE RESEARCH PROJECT

2.1 Test Materials

Arthur Taylor Opencast Mine and Middelburg Mine agreed to participate in the project by providing the necessary sample material and carrying out some of the test work.

Samples were collected from specific lithologies from each mine. In the case of Middelburg Mine, the sample was collected from the parting material between the No. 1 and No. 2 coal seams. This material comprised sandstone and contained pyrite nodules of diameter up to 10cm. The pyrite mineral represented approximately 40% by volume within the nodules. The remainder of the nodules comprised quartz grains and other accessory minerals, varying in size and shape. Acid Base Accounting (ABA) test results on samples of the parting material are summarised in Table 1 below:

TABLE 1: ACID BASE ACCOUNTING RESULTS - MIDDELBURG MINE MATERIAL

Depth (m)	Lithology	Base Potential (meq.g)	Acid Potential (meq.g)	NNP (meq.g)
28.88 -29.31	Sandstone	0,5317	0,7722	-0,241

In the case of Arthur Taylor Opencast Mine, ABA testing previously undertaken by the Mine had indicated that the spoil had a relatively high positive net neutralising potential (NNP). One particular lithology, designated T_2, was however considered potentially acid generating and was sampled for the kinetic test trials.

2.2   Test Apparatus and Test Methodology

Six 220 litre uPVC plastic drums, were used initially as containers for the tests. Each drum was fitted with a tap near the base of the drum for collection of leachate.

Each sample from each mine was split into three parts and each part re-sampled and placed loosely in each of the drums as follows:

- One drum was left at each of the mines for testing by mine personnel at the site.

- The second set of drums were tested in Johannesburg and placed outside

where they were exposed to normal weather cycles similar to those at the Mine sites.

- The third set of drums were placed inside and irrigated artificially once every week using distilled water.

The sample left at the mine was exposed to normal rainfall and evaporation, the applied test procedure for collecting leachate samples is described in Appendix F.

This test procedure was continued in the case of the outside drums for a period of 77 weeks.

During the course of the project, it was recognised that improvements could be made to the kinetic test apparatus which could potentially speed up the reaction rate and enable additional parameters, useful for the prediction of drainage water quality to be measured. The revised kinetic test apparatus, shown as Figure 10, was constructed and the material from the inside drums was transferred to the new apparatus, referred to as the humidified kinetic test cell.

THERMOMETER

DISSOLVED OXYGEN METER

OUTLET AND VALVE

LEACH WATER TANK

OUTLET AND VALVE

AIR TIGHT LID

THERMOCOUPLES ON INSIDE OF HUMIDITY CELL

FILTER - GEOTEXTILE

ROCK

AIR TANK TO MEASURE AIR FLUX

EXHAUST AIR OUTLET

IRRIGATION ARM

PUMP

PERFORATED PLATE

STRAIN GAUGE AND PROVING RING

VALVE

LEACHATE COLLECTION TANK
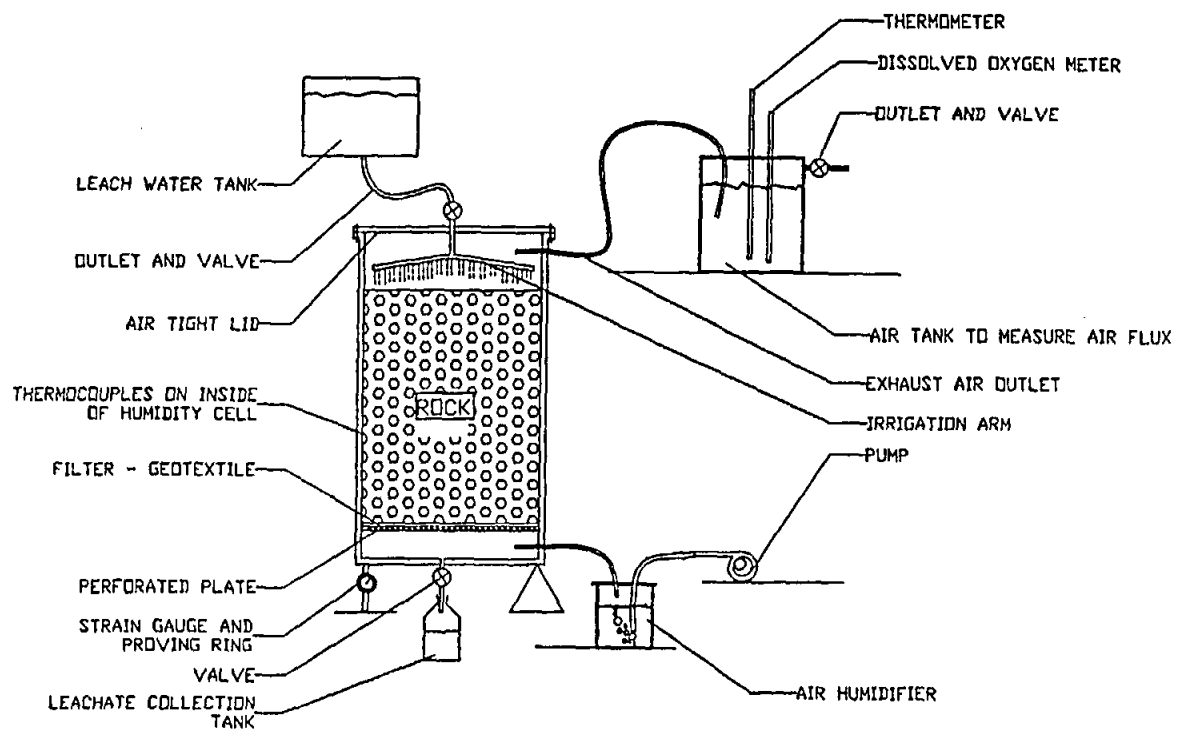
AIR HUMIDIFIER

Figure 10 : Revised Kinetic Test Apparatus

The modifications to the kinetic test apparatus key features of the humidified kinetic test apparatus may be summarised as follows:

- Since problems had been experienced with the outlet taps on the first set of drums in so far as the joints between the tap and the drum leaked and frequently resulted in inadvertent loss of leachate, it was decided to make the drums more robust by constructing them of PVC piping material.

- A test cell with a smaller diameter was used. During the initial trials using the 220 litre drums it was recognised that a considerable quantity of distilled water was required in order to be able to collect a sample of leachate. In the case of the Arthur Taylor test, the distilled water tended to evaporate

before reaching the base of the drum, resulting in only two samples being collected over a period of several months of testing. The 300 mm diameter cell was selected primarily because less distilled water would be required to carry out the test. The smaller size was considered adequately large to contain a sample of material which was representative of the waste with respect to particle specific surface area.

- An inlet was provided at the base of the test cell to enable humidified oxygen rich air to be pumped through the sample. A fish tank pump was used for this purpose. The air was humidified prior to pumping into the base of the test cell. The use of humidified air reduced the evaporation losses thereby reducing the total volume of distilled water required to pass through the test cell. The air pump, ensured that a pressure gradient was maintained between the base of the cell and the top surface of the spoil material, so as to cause oxygen-rich air to be driven upwards through the sample.

- The perforated base plate ensured that the entire sample remained unsaturated at all times during the test. Previously, water could collect at the base of the drum after rainfall events and this would partially inundate the sample thus affecting the drainage water quality by potentially reducing the oxidation rate, changing the availability of neutralising minerals and the proportion of contaminants flushed from the sample. This lack of control over the degree of saturation was overcome by ensuring that all leachate could drain into a separate collection sump located at the base of the column.

The waste from the "inside" drums, was transferred to the new humidified kinetic test cells in January 1995. The humidified kinetic test was run for 18 weeks thereafter.

2.3 Test Results

The test results are documented in Appendix G and are briefly summarised below:

pH

The leachate pH for each test is plotted against time in Figure 11 below.

Arthur Taylor (Kinetic Test)

Middelburg Mine (Kinetic Test)

Arthur Taylor (Drum Test)

Middelburg Drum Test
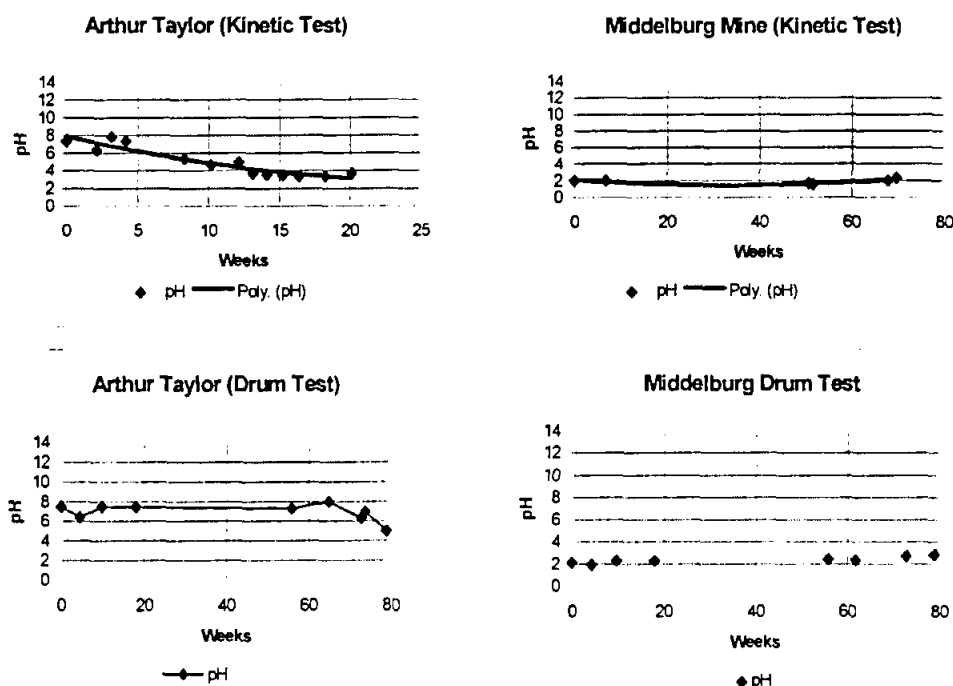
Figure 11 : Test Results - pH

In the case of the Middelburg Mine humidified kinetic test, the drainage pH remained between 2,25 and 1,1 throughout the test period. The pH of the drainage from the drum test was similar, in the range 2,85 to 1,8.

The time taken to the onset of acidic drainage was significantly shorter in the case of the Arthur Taylor humidified kinetic test than was the case for the corresponding drums subjected to the natural environment.

Sulphate Concentrations

The sulphate concentrations are shown as a function of time for Arthur Taylor and Middelburg Mine in Figure 12.

Arthur Taylor (Kinetic Test)

Middelburg Mine (Kinetic Test)

Arthur Taylor (Drum Test)

Middelburg Drum Test
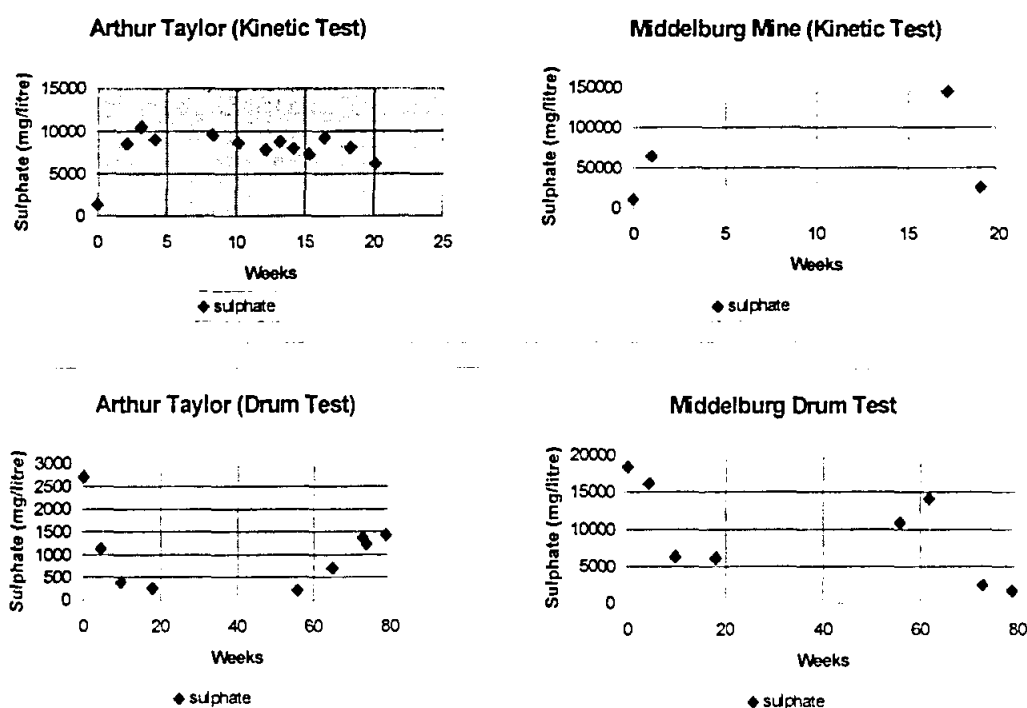
Figure 12 : Test Results - Sulphate Concentrations

The results demonstrate the following :

- The sulphate concentration in the leachate from the Middelburg test results is in the region 1 600 to 144 000 mg/litre, whereas the sulphate concentration from the Arthur Taylor test remained in the range 7 000 to 10 000mg/litre. The significantly higher sulphate concentration in the case of the Middelburg Mine test indicates that either the sulphide content or sulphide oxidation rate is significantly higher in the case of the material taken from Middelburg Mine.

- The drum tests showed an initial decrease in sulphate concentration for a period of between 10 and 20 weeks. This is believed to be attributable to the initial flushing of stored oxidation products which were already present on the surface of the rock fragments at the start of the test.

- In the case of the Arthur Taylor humidified kinetic test, the sulphate concentration remained relatively constant at approximately 7 000 to

10 000 mg/litre.

Iron Concentrations

Iron concentrations in the leachate are plotted as a function of time in Figure 13 for each test.
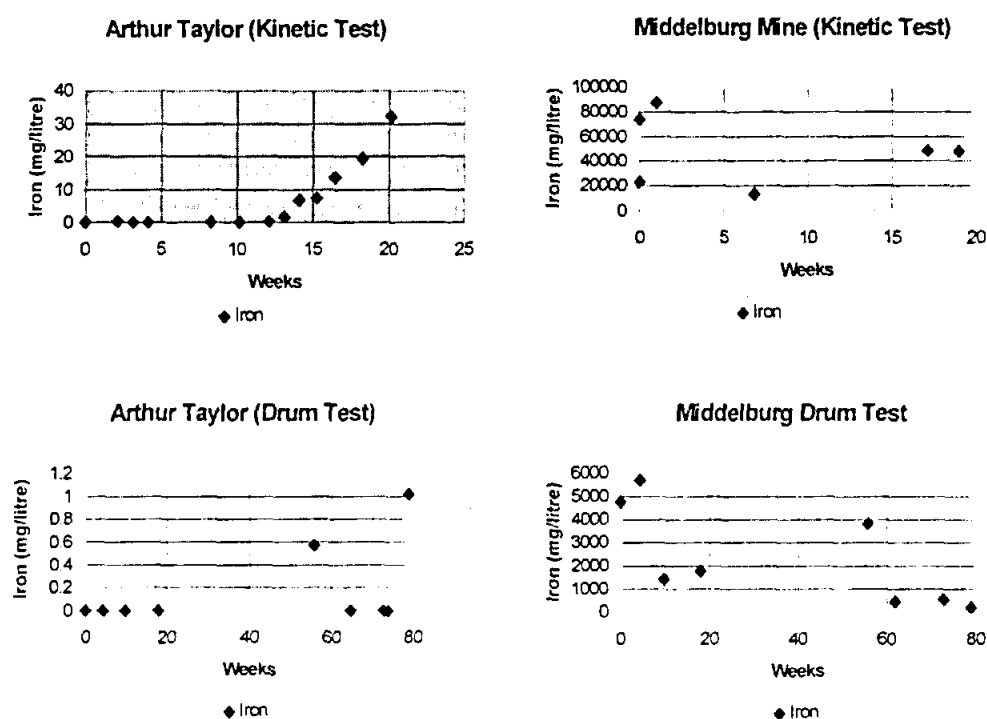
Figure 13 : Test Results - Iron Concentrations

The following observations are noted with respect to iron concentrations:

- In the case of the Arthur Taylor test, iron was leached from the sample once the alkalinity reduced to zero.

- The Middelburg Mine results show iron concentrations several orders of magnitude higher than the Arthur Taylor results.

- The humidified kinetic test resulted in iron concentrations more than an order of magnitude higher than the drum test results for both the Middelburg and

the Arthur Taylor Mine samples.

2.4   Discussion

The significantly reduced time to the onset of acidic drainage and the increased concentrations of contaminants in the leachate, is believed to be attributable to the following :

- The application of humidified air results in an increase in the rate of slaking of the rock fragments which results in an enhanced particle surface area.

- The enhanced reactant flux ensures that both water and oxygen are available on all particle surfaces throughout the test cell.

- The mobility of contaminants was enhanced since the rock particle surface remains wet throughout the test and a much smaller portion of the applied water is lost to evaporation.

The leachate quality from the humidified kinetic test would generally be expected to differ from the leachate quality in the field for the following reasons:

- Where the oxygen flux to particle surfaces is limited due to low air-permeability, the contaminant load would generally be less than the contaminant load obtained using the kinetic test and visa versa, provided that chemical saturation with resect to solid species is not reached.

- The time to the onset of acidic drainage would generally be significantly longer since the acidity produced in the zone of oxidation will be neutralised by available alkalinity in the waste pile below the zone of oxidation.

- Temperature differences between the field and the kinetic test may result in significant differences in the oxidation rate.

Notwithstanding the deficiencies of the humidified kinetic test, the procedure provides a useful indicator of the maximum likely rate of sulphide oxidation, contaminant production and neutralisation.

Since the rate of consumption of oxygen is not measured directly, the rate of oxidation of the sulphides must be inferred from the rate of production of oxidation products, as measured from the weekly sulphate load in the leachate. Errors in the interpretation of the sulphide oxidation rate may therefore arise for the following reasons:

- The concentration of aqueous products in the leachate sample, could be governed by the solubility of specific salts such as gypsum, rather than the rate of sulphide oxidation. The concentration of sulphate in the leachate might therefore lead to a significant under-estimation of the actual rate of oxidation of the sulphide.

- The initial mass of stored oxidation products may result in an over-estimation of the sulphate oxidation rate.

To overcome the above difficulties, it is proposed that the test apparatus be designed to facilitate measurement of the oxidation rate by direct measurement of the oxygen consumption rate, rather than estimating the sulphide oxidation rate from the sulphate load in the leachate.

The proposed modifications to address the above shortcomings in the test procedure are described in the proceeding section.

3   PROPOSED HUMIDIFIED KINETIC TEST PROCEDURE

3.1   Objectives of the Proposed Humidified Kinetic Test

The proposed approach to the prediction of contaminant loads from coarse wastes was documented in detail in Section 1. Essentially, this approach involves a combination of a small-scale laboratory model, and a mathematical model. The small-scale laboratory model (humidified kinetic test) is used to determine values for specific parameters which are then used in the mathematical model to scale the results to the field situation. The mathematical model was described in detail in Chapter 1 of this Section. The humidified kinetic test may be regarded as a "black box" in so far as the test takes account of many variables which affect the rate of the reaction. These variables include amongst others:

- The type of sulphide, its grain size, surface area, shape and distribution within the host material.

- The characteristics of the host material including the particle specific surface area, slaking characteristics and micro porosity.

- The effect of bacteria such as *Thiobacillus ferro-oxidans*

- The effect of temperature on the reaction rate.

The proposed modifications to the humidified kinetic test are described below.

3.2   Description of the Test Apparatus

Figure 13 illustrates the proposed apparatus for kinetic testing of coarse wastes. The apparatus is similar to that used in the humidified kinetic test trial, with the following additional features :

- The concentration of oxygen in the exhaust air and the air flux are measured to provide a direct indication of the rate of oxygen consumption.

- The water balance within the sample can be monitored as the test apparatus is constructed as a lysimeter.

- Insulation may be provided to the test cell to simulate the insulating effect of the spoil. This might assist in better simulating actual temperature conditions within the waste pile, thus ensuring that the test is carried out at a temperature which is representative of the actual temperature within the waste pile.

- The cell may be equipped with thermocouples on the inside of the cylinder to measure temperature changes.

- The cell may be inoculated with sulphide oxidising bacteria to ensure that the bacteria are present in the sample.

Since the water flux can affect the pH and rate of dissolution of neutralising minerals, it is proposed that the infiltration volume in the test be equivalent to the average water flux in the actual waste pile. Since a certain minimum volume of water is required for analysis by laboratories, the minimum required diameter of the kinetic test apparatus can be calculated based on the equation (74). This ensures that the average water flux through the sample is equal to the average water flux in the field, and that there is sufficient water available for laboratory analyses.

$$d_{test} = 1000. \sqrt{\frac{4.V_{sample}.\lambda}{1000.\pi} \cdot \frac{n_{sample}.\omega}{MAI}} .$$

(74)

where : d_{test} =   minimum required diameter of cylinder (mm)

V_{sample} =   minimum volume of leachate required for the

laboratory analysis (ml)

MAI = *mean annual field infiltration rate (mm/annum)*

n_{sample} = *average sampling rate (samples/annum)*

λ = *factor to account for evaporation and absorption losses (approx 1,05)*

ω = *number of times that the leachate collected is re-circulated prior to laboratory analysis*

Water would thus be added to the sample at an average rate of $V_{sample}\lambda$.

In addition to the above requirement, it is proposed that the diameter and depth of test cell should not be less than 3 to 4 times the maximum size of rock fragment in the sample. Typically, a test cell diameter of 0,5m is sufficient for most coarse wastes.

3.3   Proposed Test Procedure

As was the case for the kinetic test trials undertaken, the sample should be selected such that it is representative with respect to the geochemical characteristics and particle specific surface area. The material should be placed in the kinetic test cell at a dry density similar to that in the field.

Humidified air is pumped through the base of the sample to saturate the air-filled void spaces with oxygen-rich air, thereby ensuring that the rate of supply of oxygen and water to the reactive particle surfaces are not the rate controlling steps.

The sample is irrigated with distilled water by evenly applying the distilled water to the top surface at a rate Q (l/week). The distilled water is allowed to percolate through the waste and is collected as leachate in the void at the base of the column. The valve at the base of the column is opened to decant the leachate collection void at the required intervals, either for re-circulation of the leachate through the column, or for laboratory analysis, or both.

3.4   Determination of Parameters values from the Proposed Humidified Kinetic Test

The proposed test can be used to estimate the value of a number of parameters and process rates including:

- The permeability of the waste.

- The oxygen consumption rate and hence the rate of sulphide oxidation under "ideal" conditions.

- The leachate quality and presence of secondary minerals.

- The rate of flushing of contaminants and the flushing effectiveness.

- The rate of accumulation of oxidation products.

The proposed method of evaluating each of the above parameters is briefly summarised below.

Water permeability

The water permeability may be determined by completely saturating the sample from the base and then measuring the water flux under the application of a constant pressure head. The water permeability may be calculated from equation (75).

$$K_{sat} = Q \cdot \frac{L}{\Delta h.A} \tag{75}$$

Where $Q = $ *flow rate* $(m^3.s^{-1})$

$A = $ *cross sectional area of the kinetic test cell* (m^2)

$L = $ *depth of the kinetic test cell* (m)

$\Delta h = $ *difference between reservoir levels* (m)

Oxygen Consumption and Sulphide Oxidation Rates

The oxygen consumption rate can be measured directly by measuring the change in concentration between the exhaust and inlet air, and the air flux. A dissolved oxygen metre and air flow metre is required for this purpose. The concentration of oxygen in the air is calculated using the solubility ratio for oxygen in water. The rate of sulphide oxidation may be estimated based on the assumed stoichiometry of the complete oxidation reaction, which for the pyrite oxidation reaction is as follows:

$$\frac{dS}{dt} = \frac{119.V_{O_2}.\Delta C_a.\frac{2}{7}}{M} \tag{76}$$

Where dS/dt = *rate of depletion of pyrite in the sample (grams/kg waste/week)*

V_{O_2} = *air flux (m³/week)*

Δc_a = *difference between the inlet atmospheric oxygen concentration and the exhaust atmospheric oxygen concentration. (mole/m³)*

M = *sample mass (kg)*

Alternatively, if the oxygen consumption rate cannot be measured directly, the sulphide oxidation rate may be estimated from the sulphate production rate as follows:

$$\frac{dS}{dt} = \frac{2.119.Q.C_{SO_4}}{1000.M} \tag{77}$$

Where Q = *Water flux (litres/week)*

C_{SO_4} = *Sulphate concentration (mg/litre)*

Leachate Quality

It is proposed that leachate samples be tested as follows:

Prior to re-circulation   -   pH and TDS

On a weekly basis   -   pH, TDS, acidity/alkalinity, Ca, dominant metals associated with the sulphides and SO_4^{2-}

On a monthly basis   -   pH, TDS, acidity/ alkalinity and a full cation and anion balance.

The volume of leachate entering and leaving the test cell should be monitored in each case.

A chemical equilibrium programme such as MinteqA2 can be used to check for chemical saturation with respect to solid species and to identify the types of salts which may accumulate in the waste.

Rate of Accumulation of Oxidation Products

The net rate of accumulation of oxidation products within the test cell is calculated as the difference between the rate of production and the rate of flushing of a particular contaminant. The ratio between the rate of production (g/kg) and rate of flushing (g/kg) of contaminants, referred as ζ, provides useful information in understanding the types of controls which may be applied should it be necessary to reduce the contaminant load. For example :

- If $\zeta \approx 1$ then a reduction in the oxidation rate can be expected to render a proportional reduction in the concentration of the contaminant in the leachate. Reducing the water flux 10 fold alone on the other hand would

at worst have no effect either on the contaminant load or concentration.

- If $\zeta \gg 1$, then contaminants will tend to accumulate within the waste material. Increasing the water flux is likely to result in an increase in the contaminant load and possibly, (but not necessarily), an increased contaminant concentration. Reducing the water flux is likely to result in a reduced contaminant load, (but not necessarily), a reduced concentration. In this case, it would be necessary to reduce the sulphide oxidation rate by up to several orders of magnitude.   Only after some time, once the accumulated contaminants have been flushed from the waste pile, will a significant change in the water quality be observed.

- If $\zeta \ll 1$, then the quantity of stored contaminants would tend to deplete with time. In this case, reducing the water flux may result in an increased concentration of contaminants. Increasing the water flux on the other hand, could result in a reduced concentration of contaminants, but would probably result in an increased contaminant load. The application of controls which reduce the oxidation rate are unlikely to have an effect on the contaminant load in the short term.

CHAPTER THREE

MODEL DEMONSTRATION, CONCLUSIONS

AND RECOMMENDATIONS

1   MODEL DEMONSTRATION

1.1   Description of the Problem

The following example is intended to demonstrate the application of the model. In this example, an attempt has been made to predict the drainage water quality from the field drum tests carried out on the spoil material from Middelburg Mine. In the model, infiltration has been assumed constant at 10 mm/week. The height of material in the drum was assumed to be 0,5 m. The material properties for each layer in the model were regarded as homogeneous throughout the depth of the drum.

1.2   Input Data

The data is summarised in Table 1 below:

1.3   Simulation Setup

Each simulation was run over a period of 35 weeks using a time step interval of 1 week. The chemical component concentration trend routine was applied to extrapolate the results of the thermodynamic equilibrium model over several time steps.

1.4   Results

The detailed results of the model simulation are presented in Appendix G. Figure 14

illustrates the predicted oxygen concentration as a function of depth. The figure shows that the oxygen concentration reduces by 0,0062% between the top surface of the drum and the base of the drum thus indicating that oxygen supply to the rock fragment surfaces is not likely to limit the sulphide oxidation rate.

TABLE 1: SUMMARY OF INPUT DATA

Parameter	Units	Symbol	Middelburg Mine -T2 seam
layer thickness (assumed uniform)	m	l	0,05
Porosity	-	n	0,4
Saturated water permeability	m/s	K_{sat}	1×10^{-2}
Initial degree of saturation	_	S_{init}	0,2
Residual Degree of saturation	_	S_r	0,05
SFP proportion of flow	-	U	.8
Empirical pore size distribution coefficient	-	δ	2
Initial Pyrite Concentration	g/kg waste	c_p	20
Initial max oxidation rate	g/kg/week		0,376
Initial calcite equivalent content	g/kg waste		5
Net Infiltration rate	mm/week		10
Microbial respiration rate layer 1			0,0
Average particle specific gravity		SG	2,7

OXYGEN CONCENTRATION PROFILE
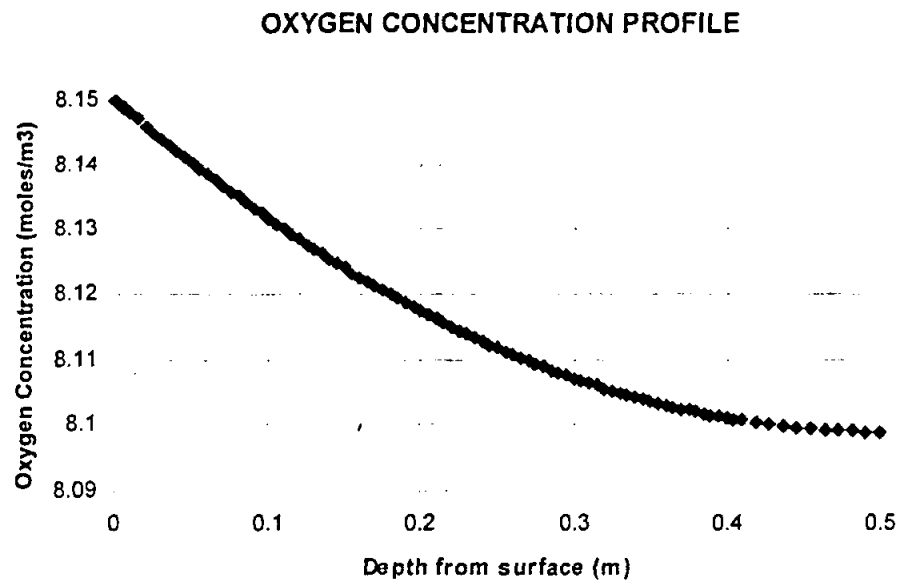
Figure 14 : Predicted Oxygen Concentration Profile for Drum Test

Figure 15 illustrates the predicted temporal variation in the quantity of sulphide remaining in the drum for each layer. The model predicts that 50% of the total initial sulphide mass is depleted after 19 weeks.

There is no significant difference in the quantity of sulphide consumed in each layer.
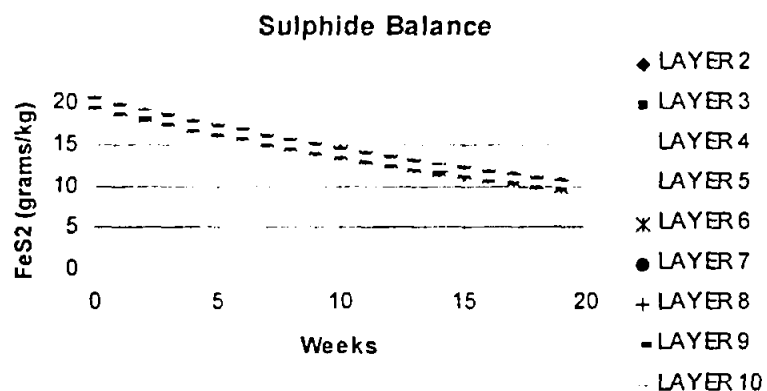
Figure 15 : Sulphide Balance

The exponential decay function assumed in the model is illustrated in Figure 16,

in which the sulphide reactivity is plotted as a function of time. From the results of the simulation, the reactivity of the sulphide reduced to 35% of its initial value after 30 weeks.

Sulphide Reactivity
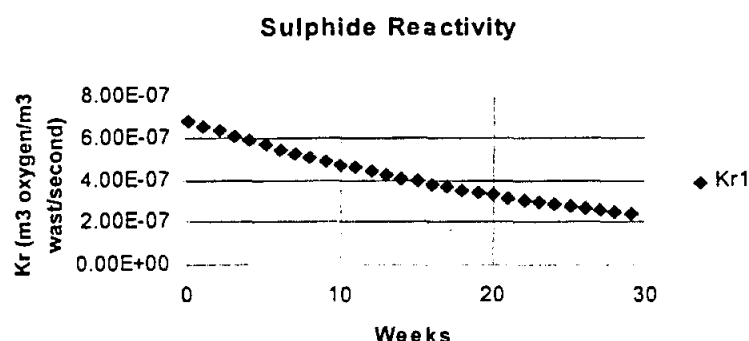
Figure 16 : Sulphide Reactivity versus Time

The temporal variation in the mass balance for each chemical component and pyrite is illustrated in Figure 16. The following trends are predicted by the model:

• Calcium tends to remain in the spoil as while calcite is dissolved, gypsum is precipitated.

• Carbonate is depleted relatively rapidly, 99,98% of the initial carbonate content is removed from the spoil by week 37.

• Iron tends to accumulate in the spoil as Fe_2O_3.

• The rate of generation of sulphate exceeds the rate at which sulphate is flushed from the sample giving rise to a net accumulation of sulphate in the spoil.

Figure 17 presents a series of graphs which summarise the leachate quality predicted by the model. The following trends may be observed :

• The model predicted an initial pH in the pore water in region of 7,0 falling at week 18 to between 0,3 and 0,5.

• The model predicted a rapid increase in the concentration of iron from week 18 onwards with the iron concentration increasing to 75 000mg/litre.
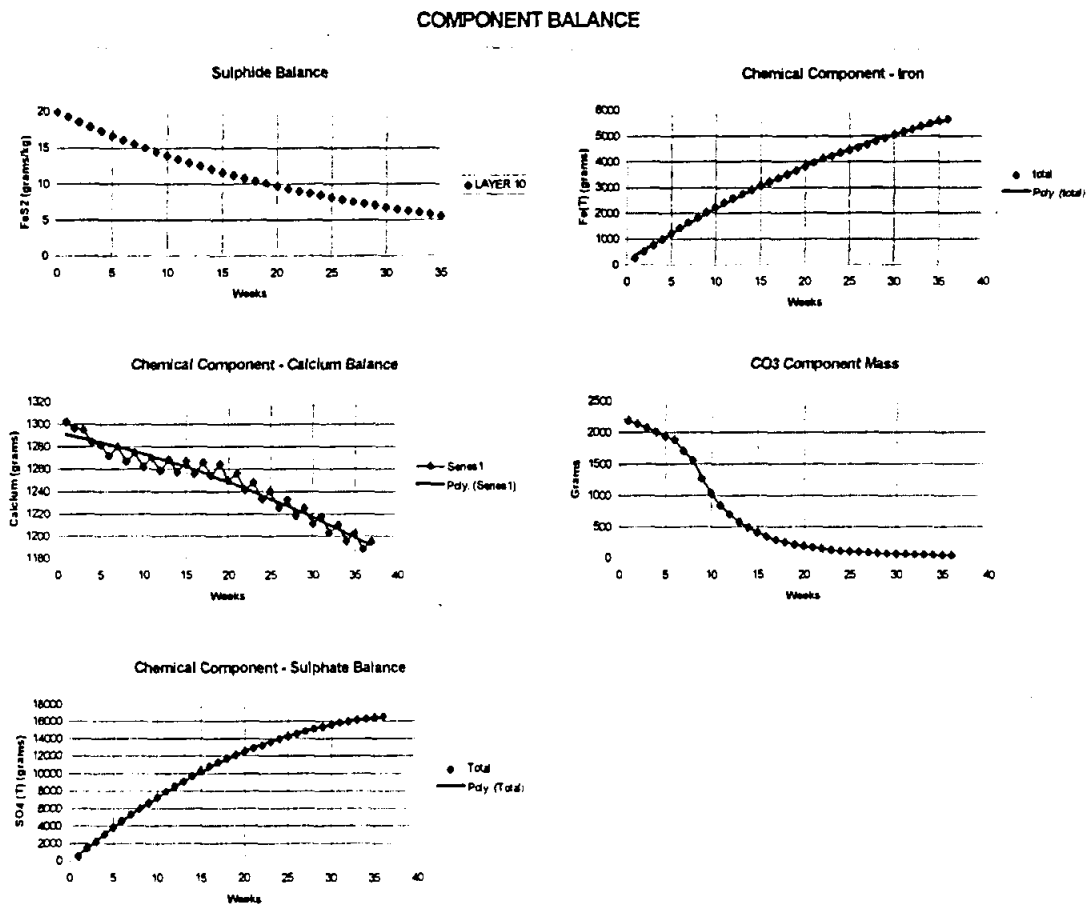
Figure 16: Predicted Mass Balance

• The predicted sulphate concentration increased at a decreasing rate throughout the simulation period. The maximum sulphate concentration was 227 180mg/litre. The convex slope of the curve is attributable to the decrease in the rate of sulphide oxidation and hence sulphate production.

• The carbonate concentration decreased relatively rapidly as the available calcite was depleted.

- The calcium concentration in the leachate remained relatively constant throughout the period of simulation. The calcium concentration in the leachate was in the region of 82 to 219 mg/litre throughout most of the simulation period.

- The pH of the leachate dropped to in the region of 0,3 to 0,5 from week 18 onwards.

The predicted concentrations of the chemical components, namely SO_4, Ca, CO_3 and Fe are shown in Figure 17.
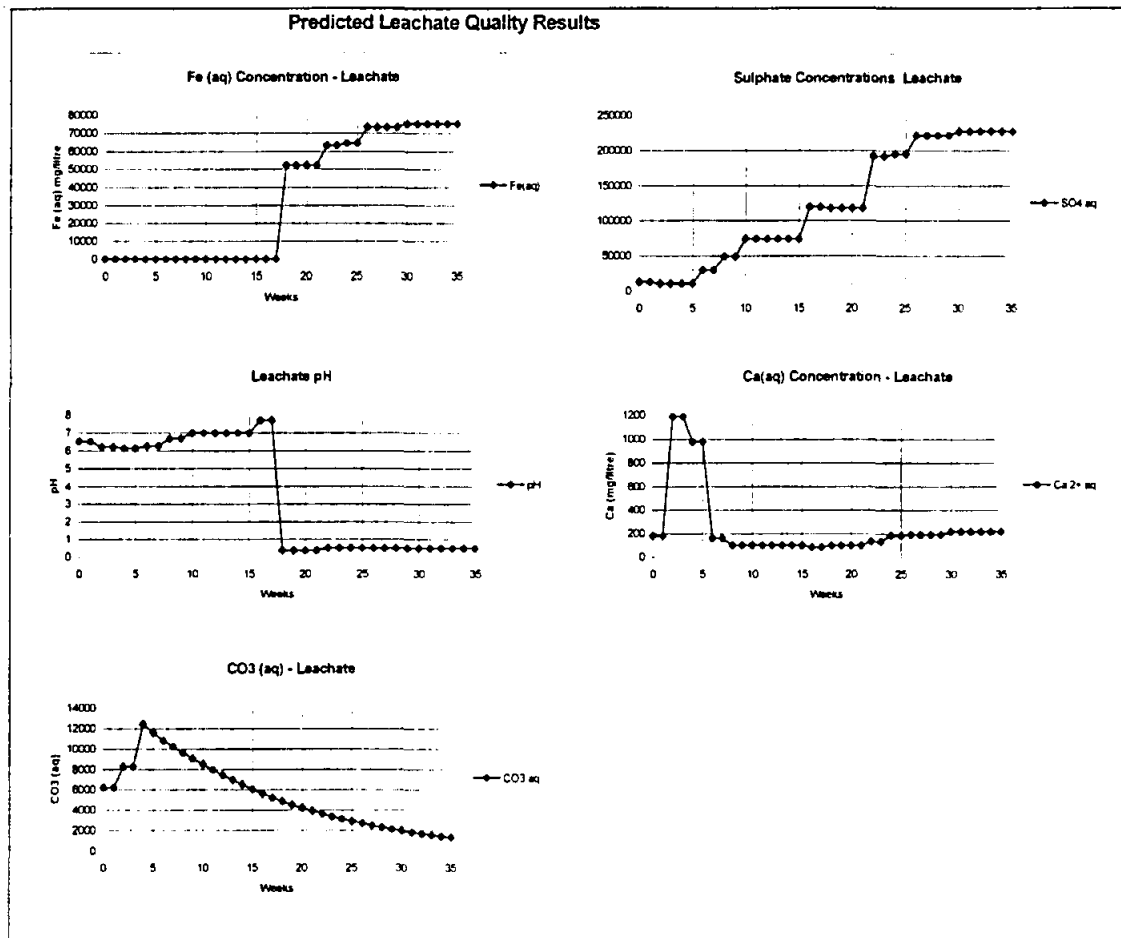
Figure 17 : Predicted Leachate Quality

An example of the results of the thermodynamic chemical equilibrium programme is presented as Figure 18 below. The analytical concentrations shown on the left represent the input to the model and includes components in the solid and

aqueous phases.   The predicted species concentrations are shown on the right for each species included in the model.   The mass of each component in the solid phase and the predicted concentrations of the components in the aqueous phase is shown at the bottom of the Figure.   The volume of water in the layer was 1,01 litres.

The chemical equilibrium routine proved problematic at times in so far as convergence was often difficult to achieve particularly if the initial guessed values were far from the final solution.

Thermodynamic Chemical Equilibrium Model

ANALYTICAL CONCENTRATIONS (solids plus aqueous) mol/litre	
Ca2+	8.09E-01
CO32-	1.58E-02
Fe2+	1.63E+00
SO42-	4.18E+00

PREDICTED SPECIES CONCENTRATIONS mol/litre	
Ca2+	8.8411E-05
CO32-	3.2633E-17
H+	1.1099E-01
e-	9.6483E-14
H2O	1.0000E+00
Fe3+	1.6112E-04
Fe2+	2.4621E-04
SO42-	8.5893E-02
OH-	7.7419E-14
HCO3-	1.0585E-07
H2CO3	1.5794E-02
CaOH+	2.3503E-16
CaHCO3+	1.2793E-10
CaCO3	3.9024E-18
Fe(OH)3-1	1.8010E-32
Fe(OH)2	3.2233E-23
Fe(OH)+	8.2022E-13
Fe(SO4)	3.6012E-03
Fe(SO4)+	2.9405E-01
Fe(OH) 2+	1.2813E-05
Fe(OH)2 +	4.4696E-08
Fe(OH)3	2.4246E-15
Fe(OH)4 -	3.6463E-22
Fe(SO4)2 -1	8.6361E-01
Fe2(OH)2 4+	3.1899E-09
HSO4 -	1.2647E+00
CaSO4(aq)	1.4813E-03
Fe2O3 (s)	*2.35E-01*
calcite	*0.00E+00*
gypsum	*8.07E-01*

RESULTS		Ca2+	CO3 2-	Fe 2+	SO4 2-
Solid Phase Mass	grams	0.807328	0	0.46909486	0.807328419
Aqueous Conc	mol/litre	0.00157	0.015794	1.16167689	3.37696293

Figure 18 : Example of the Thermodynamic Chemical Equilibrium Model

2   CONCLUSIONS

Development of the *Salmine* model has highlighted the complexity of the processes which give rise to pollution loads from coarse sulphide-containing wastes. These processes which are described in broad outline in Section 1, have been modelled as described in Section 2, using a considerable number of simplifying assumptions. Furthermore, there are a number of additional processes which have not been included in the model which could be significant in determining the pollution loads from wastes, but which have proved too complex to include in this model. A kinetic test method has been proposed to model some of the more complex processes active in the waste. This procedure takes cognisance of a range of variables, and comprises a small-scale physical model which enables empirical data to be acquired. Some of this can be used as input data for the computer model *Salmine*.

The effects of scale make the use of a small-scale test, such as the drum test unsuitable for the calibration and verification of the model. Data from large-scale tests needs to be gathered to enable the verification of the model.

Coarse wastes typically demonstrate considerable variability in parameter values. Furthermore the uncertainty associated with these values is relatively high and a deterministic approach can therefore not be expected to give confident predictions of the water quality. The sensitivity of the pollution load predicted by the model to various parameters should always be assessed. The model should be applied with caution and it use at present limited to "order of magnitude" estimates of pollution loads and drainage water quality.

The selection of a combination of a small-scale physical model and a mathematical model provide a prediction method which has much of confidence of a large-scale physical model but at a considerably reduced costs and reduced time requirement. The mathematical model offers the advantage of being used to evaluate alternative methods or engineering controls to reduce the occurrence of unacceptable pollution loads.

The selection of visual basic and excel as the programming language have resulted in a model which is relatively easy to operate and easy to view the results. However, the practical application of the model requires an intimate understanding of the processes modelled, the assumptions implicit in the model, and the method of modelling. This would require that potential users of the model aquire the necessary skills and training in this field.

3   RECOMMENDATIONS

The following recommendations are proposed:

- The chemical equilibrium modelling approach adopted requires further development. Numerical instability proved to be a significant problem and it is often very difficult to achieve convergence.

- The focus of future research should be on the verification and application of the *Salmine* model. The application of the model to a set of data for which the important parameters are known, may identify aspects of the model which require further development.

- The proposed kinetic test method for coarse wastes should be applied to a range of problems and further developed and tested.

SECTION THREE

THE PRACTICALITY OF SUBAQUEOUS DISPOSAL
OF SULPHIDE-CONTAINING WASTES
AS A CONTROL TECHNOLOGY
UNDER SOUTH AFRICAN CONDITIONS

OF A
REPORT TO THE WATER RESEARCH COMMISSION ON THE PROJECT

*THE PREDICTION OF POLLUTION LOADS
FROM COARSE SULPHIDE-CONTAINING WASTES*

*PREPARED BY STEFFEN, ROBERTSON AND KIRSTEN CE INC.
IN ASSOCIATION WITH
METAGO ENVIRONMENTAL ENGINEERS*

NOVEMBER 1996

Table of Contents

SUBAQUEOUS DISPOSAL OF SULPHIDE-CONTAINING WASTES

1   INTRODUCTION

Subaqueous disposal refers to the disposal of a sulphide waste in water or under a water cover. The disposal of the waste below the level of the phreatic surface would therefore also be categorised as subaqueous disposal. Inundation of the waste is referred to as the process of placing the waste under water.

Subaqueous disposal is used as a drainage control method to reduce the rate of oxidation of the sulphide minerals.

This Chapter reviews the following aspects relating to subaqueous disposal :

- The   extent to which the sulphide oxidation rate will be reduced by subaqueous disposal.

- The effect of subaqueous disposal on the mobilisation or flushing of stored oxidation products which have accumulated in the waste prior to inundation.

- The practicality of subaqueous disposal under South African conditions.

2   BACKGROUND INFORMATION

The disposal of tailings under or in water is considered one of the most effective methods of preventing acid generation (Robertson, 1991), and is an option which has attracted international attention in recent years.   A major research project into

subaqueous deposition was started in Canada by the National Mine Environment Neutral Drainage (MEND) program in 1988.   According to Fraser et al (1994), it was concluded that:

- The reactivity of the tailings was low in all cases as evidenced by the low dissolved metals content of interstitial water, this verifies the hypothesis of low reactivity due to submerged conditions.

- The metal flux rates from the sediments was low, to the extent that it was predicted that they should not impact on the metal balances within the lake waters.

- Tailings, which with the passage of time became buried with sediments and organic matter, tended to have a negligible impact on the lake water quality.

Work to date has demonstrated that subaqueous disposal has technical and scientific justification.   It is likely that properly controlled and engineered subaqueous disposal will become an important disposal method in future.   The question therefore arises, to what extent, and under what conditions can advantage be taken of the subaqueous disposal option in South Africa, and what are the requirements for effective subaqueous disposal ? These aspects are addressed in this Section of the report.

3   THE EFFECT OF SUBAQUEOUS DISPOSAL ON THE OXYGEN FLUX

The mechanisms by which contaminants are generated in coarse wastes are described in Section 1. The principal effect of subaqueous disposal of wastes is to inhibit the rate of oxygen supply to the reactive particle surfaces. A comparison of the oxygen flux in the case of a waste disposed of under water, and the same waste disposed of in an unsaturated waste pile, will reveal differences of up to

several orders of magnitude in the oxygen flux. The difference is attributable to the fact that the oxygen flux mechanisms responsible for the bulk of the total oxygen flux in the case of unsaturated wastes, are those which take place through the air-filled void spaces. In a saturated waste, since there are no air-filled void spaces, the oxygen flux is limited to diffusion of oxygen through water-filled void spaces and advective transport of oxygen as dissolved oxygen in migrating water. The total oxygen flux may be calculated as the sum of the oxygen flux due to the above two mechanisms.

3.1   Oxygen Flux Due to Diffusion

The oxygen flux due to diffusion through a homogeneous porous media, may be derived from Fick's first Law and is given as:

$$J_p = -D_p \cdot \frac{dC_p}{dz} \qquad (1)$$

Where J_p = flux in the pore space (mole/m² pore area/s)

D_p = pore diffusivity

C_p = concentration of the diffusing component in the total pore fluid (mole/m³ pore volume)

z = depth from the surface of the porous media (m)

Since the pores are filled with air and water, and since the pores occupy only a fraction of the total cross sectional area per square metre of the porous waste, the diffusion flux per unit area is given by (Collin, 1987) :

$$J = -D_p.n(1-S+H.S)\frac{dC_a}{dz} \qquad (2)$$

Where J = oxygen flux per unit surface area of waste

n = porosity of the material

S = degree of saturation

$$C_a = \frac{C_p}{(1-S+H.S)} \quad = \text{ oxygen concentration (mole/m}^3 \text{ waste)}$$

$H \quad = \quad$ *solubility constant* C_{wate}/C_{air} *at a temperature T*

The effective diffusivity D, may be defined as $\quad D = D_p.n(1-S+H.S)$

The effective diffusivity, $\mathbf{\cdot}$, depends on the structure of the air-filled pore space and is a function of the porosity, moisture content or degree of saturation, tortuosity and constrictivity *(Collin, 1987)*. The effect of reducing the air-filled pore space by increasing the degree of saturation is illustrated in Figure 1 which shows the diffusivity D/D_a^o decreasing by a factor of 100 000 as the degree of saturation S, increases over the range $S=0,0$ to $1,0$. D_a^o, the diffusion coefficient of oxygen in air, was assumed to be $9,1 \times 10^{-6}$ m^2.s^{-1} *(Landolt-Börnstein, 1968)*. Equation (3) was used to calculate the pore diffusivity as a function of the degree of saturation and porosity *(Millington and Shearer, 1971)*.

$$\frac{D_a}{D_a^o} = (1-S)^2.[n(1-S)]^{2v} \tag{3}$$

Where x is given by:

$$1 = [n.(1-S)]^{2v} + [1-n(1-S)]^x \tag{4}$$

Degree of Saturation vs. Effective Diffusivity
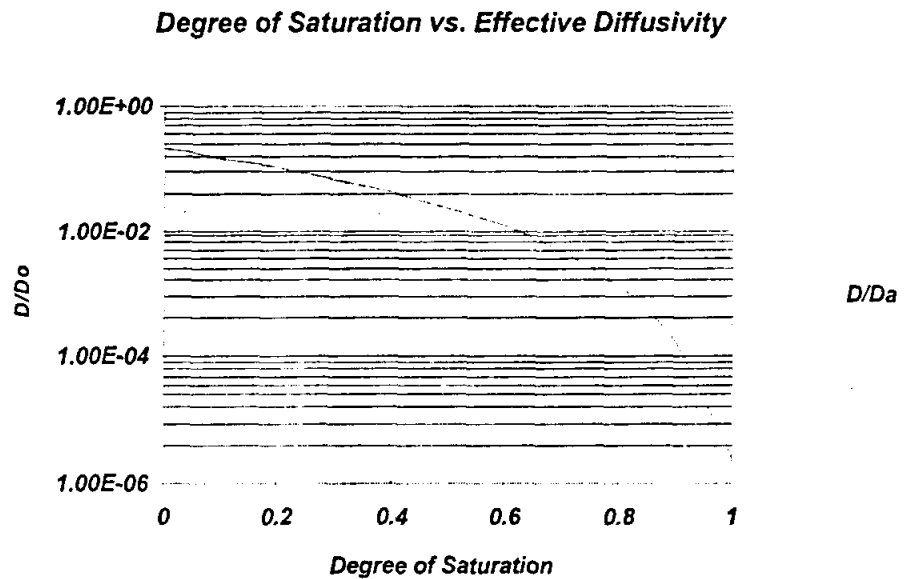
Figure 1: Effective Diffusivity versus Degree of Saturation

Figure 1 shows that the effective diffusivity tends to reduce dramatically as the degree of saturation increases above approximately 0,8.

3.2   Oxygen Flux Due to Advective Transport as Dissolved Oxygen in Water

Equation (5) describes the advective component of the oxygen flux through a

waste.

$$J = K_{sat}.\frac{\Delta h}{\Delta l}.A.H.C_{air}$$ (5)

where J	=	oxygen flux (moles /s)
K_{sat}	=	saturated water permeability (m/s)

A = cross-sectional area

C_{air} = solubility of oxygen in air

Δh = head loss (m)

Δl = flow path length (m)

H = solubility constant

Based on the solubility of oxygen in water and the stoichiometry presented in reaction (6) below, the increase in the sulphate load (attributable to the advective component of oxygen transport only), in the drainage from the downstream end of the saturated waste, may be calculated from equation (7):

$$FeS_2 + \frac{7}{2} O_2 + H_2O \rightarrow Fe^{2+} + 2SO_4^{2-} + 2H^+ \tag{6}$$
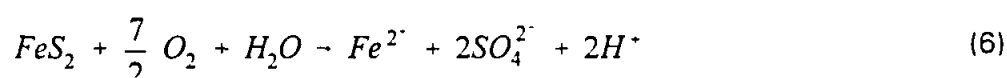
$$\tag{7}$$

where $\dfrac{dS}{dt}$ = sulphate load (g.s^{-1})

γ = stoichiometric ratio of the assumed oxidation reaction, mole SO_4 /mole O_2

The maximum average increase in the concentration of SO_4 in the drainage, calculated by dividing the load by the water flux, is therefore :

$$\Delta[SO_4^{2-}] = 96.H.C_{air}.\gamma = 24 \ mg/litre \tag{8}$$

assuming H = 4,88 x10^{-2} at 0 °C (Perry and Chilton, 1973)

C_{air} = 2,927 mole/m^3

γ = 7/4 base on stoichiometry of reaction (6).

This concentration is relatively low compared to the concentration of sulphates which might be released from an equivalent waste placed in an unsaturated environment.

environment.

3.3   Diffusion of Oxygen through a Water Cover

The effect of inundation on the oxygen diffusion rate through the water and hence the rate of production of sulphate is best illustrated with the aid of an example. Consider a fresh sample of un-oxidised sulphide containing-waste placed under a water cover at depth, d. Assuming that the waste is highly reactive, then the concentration of oxygen in the pore water just below the surface of the tailings will be zero. The oxygen flux due to diffusion only, may be calculated for steady state conditions from equation (9). This assumes that there is no oxygen consumption between the water surface and the waste surface.

$$D_w^o \cdot \frac{\partial^2 C_a}{\partial z^2} = 0 \qquad (9)$$

The equation can be solved by integrating over the depth of the water and solving for the boundary condition $C_a = 0$ at $z = d$ giving :

$$C(x) = c_w (1 - \frac{z}{d}) \qquad (10)$$

The maximum sulphate generation rate (grams.s^{-1}) per unit area of water cover may be estimated from :

$$\frac{dS}{dt} = 96.D_w^o \cdot \frac{c_w}{d} \cdot \gamma \qquad (11)$$

Figure 2 shows the effect of increasing water cover depth on the rate of sulphate generation.

Effect of Water Cover Depth on Sulphide
Oxidation Rate
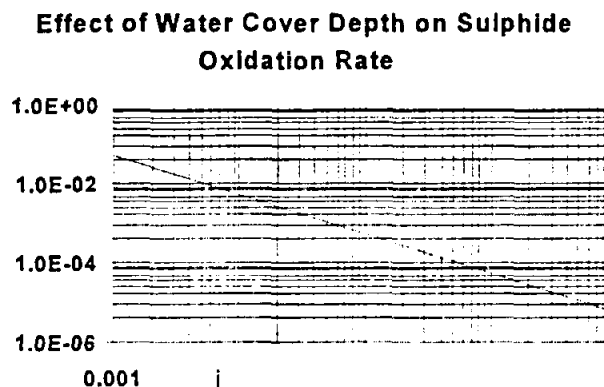
Figure 2 : Effect of Water Cover Depth on the Sulphate
Production Rate Due to Diffusion of Oxygen

---

4   THE EFFECT OF SUBAQUEOUS DISPOSAL ON THE MOBILISATION OF STORED CONTAMINANTS

Initially, inundation of the waste may result in high concentrations of contaminants in the drainage water. This is due to the mobilisation or flushing of previously accumulated oxidation products from the waste. This is potentially a problem in situations where sulphide-containing wastes have been left to oxidise for some time prior to inundation, resulting in the accumulation of oxidation products on particle surfaces. On inundation, the resulting drainage will show elevated concentrations of contaminants until the stored contaminants present on particle surfaces are adequately flushed out of the waste by migrating water.

An indication of the water quality which is likely to arise in the resulting drainage may be obtained from a small scale test in which a sample of the partially oxidised waste is inundated and subject to a through flow rate, Q, The number of times that the pore water must be replaced to flush the readily soluble stored contaminants, provides an indication of the total water flux and time required to flush the waste

pile. The number of pore water replacements, PWR required to flush the waste may be estimated from equation (12):

$$PWR = \frac{Q.t}{n.V}$$ (12)

Where PWR = number of pore water replacements

Q = water flow rate in the test cell $(m^3.s^{-1})$

t = time required for stored products to become flushed from the test cell, indicated by the presence of relatively uncontaminated drainage water, (s)

n = porosity of the waste

V = volume of waste in the test cell (m^3)

Once the PWR value is determined from the test cell, the time it will take to flush the actual waste pile of stored oxidation products, measured from the time of inundation, may be estimated by simply re-arranging equation (12). The values for the parameters V, Q and t would in this case, be applied to the values for the waste pile.

The simple approach described above can be used to estimate the time period or volume of water for which treatment of the mine drainage from the inundated waste will be necessary.

5   THE PRACTICALITY OF SUBAQUEOUS DISPOSAL IN SOUTH AFRICA

In South Africa, the availability of suitable lakes or dams for use as subaqueous disposal sites is severely limited. Potential subaqueous waste disposal sites applicable to South African conditions do however include:

- The portion of the void resulting from opencast mining operations, which is located below the level of the final phreatic surface after backfilling.

• Underground stopes which can be inundated after mining.

• Artificial subaqueous disposal facilities or impoundments designed to maintain the level of the phreatic surface above the upper level of reactive waste.

A key issue relating to these facilities is the maintenance of saturated conditions throughout the life of the waste facility, to ensure that the oxygen diffusivity is minimised. This can present a practical problem since the level of the phreatic surface is often subject to relatively large fluctuations due to annual and seasonal changes. This implies that the waste or a portion of the waste may be unsaturated for extended periods. From Figure 1, it can be seen that the diffusivity of oxygen decreases dramatically as the degree of saturation approaches unity.

As the degree of saturation decreases, the oxygen flux due to diffusion through air-filled void spaces increases. At some point the oxygen flux due to diffusion through air-filled pore spaces exceeds that through water-filled pore spaces. The mass of oxygen per unit volume of waste, contained in the water-filled pore spaces is given by :

$$M_{O_2}(water\text{-}filled) = C_{air}.H.S.n \qquad (13)$$

The maximum mass of oxygen per unit volume of waste contained in the water-filled void space is given by :

$$M_{O_2}(air\text{-}filled) = C_{air}.(1-S).n \qquad (14)$$

The degree of saturation corresponding to the point at which the mass of oxygen in the air-filled void space is equivalent to that in the water-filled pore space, may be determined solving equations (13) and (14) for S. This gives:

$$S = \frac{1}{(1 + H)} \qquad (15)$$

For $H = 4,88 \times 10^{-2}$ at 0 °C *(Perry and Chilton, 1973),* $S = 0,953.$

For most wastes, particularly coarse wastes, the negative pore pressure required to reduce the degree of saturation below 95% is relatively small implying that the air-filled oxygen flux mechanisms would start to predominate very soon, once the level of the phreatic surface drops below the top surface of the waste.

In the case of sulphide-containing wastes located within the zone of fluctuating phreatic surface, the concentration of contaminants in the resulting drainage could be expected to increase significantly each time that the phreatic surface rises, since readily soluble contaminants generated during the period for which the phreatic surface is low, will be mobilised. While the phreatic surface level is low, oxidation of sulphides will take place resulting in significant net accumulation of aqueous products in the waste located above the level of the phreatic surface. A practical requirement for successful subaqueous disposal is therefore that the extent of fluctuations of the phreatic surface should be minimised so as to reduce the effectiveness or frequency of flushing of aqueous species from the waste located in the unsaturated zone, immediately above the phreatic surface.

Finally if the waste is to be disposed of under water, the time taken to inundate the waste should be minimised so as to minimise the build up of stored contaminants, which will be mobilised once the material is inundated.

An evaluation of the practicality of subaqueous disposal in South Africa must be based on the extent to which the conditions listed above can be met. The following options are listed to demonstrate how advantage could be taken of subaqueous disposal :

- *The disposal of wastes in underground mine workings located below the level of the phreatic surface:* The consolidation of the tailings as a result of the load applied to the tailings due to the gradual collapse of the hanging wall, results in a reduction in the air and water permeability. This reduces the susceptibility of the waste to generate acid in the event that the level of

the phreatic surface is reduced below the level of the waste. Disposal of wastes in underground workings is already common in South Africa. Disposal of fine coal slurry from washing operations, in underground workings has been successfully applied at for example, Hlobane Colliery and Arthur Taylor Mine.

- *The disposal of fine portion of waste materials in a conventional tailings dam in which the phreatic surface can be prevented from dissipating*: The maintenance of a high phreatic surface to reduce the long term contaminant load needs to be weighed against any additional risk of dam failure that may result from the elevated phreatic surface. As far as can be ascertained, tailings dams have not been constructed in South Africa which are designed specifically to prevent the dissipation of the level of the phreatic surface within the dam after closure. Given the relatively dry climatic conditions, with net evaporation generally exceeding net rainfall, this approach would require a considerable volume of water to maintain. The contribution to the contaminant load from the zone of tailings immediately above the phreatic surface, is likely to remain high for a long time. This option is unlikely to be of practical significance in most cases.

- *The construction of an artificial impoundment to maintain the waste under water cover*: This differs from the option above in that a wall or embankment is constructed of non-reactive, low permeability material, such that the level of the phreatic surface is effectively maintained above the reactive waste. This method of disposal is not generally suitable for South African conditions given the high net evaporation rate experienced over most of the country. The quantity of make-up water required to maintain such a system, and the reliability of water supplies given the frequency and intensity of droughts, tend to disfavour this control method for most sites. The evaporation loss from the surface of the waste facility may be reduced by placing an inert low permeability cover over the reactive waste. The water level can then be maintained below the surface of the inert cover material but above the level of the waste. This method may be economically viable

in some cases.

- *Early flooding of opencast and underground mine workings:* There are significant potential long term advantages to be realised by planning a mine such that the natural level of the phreatic surface can be re-established as soon after mining as possible. Consideration should be given to actions which enhance the rate at which wastes can be placed below the level of the phreatic surface.

- *The creation of barriers to prevent the loss of water from the mined out areas thus allowing the mine to flood.* Barriers to flow may be formed by leaving critical areas unmined, or by backfilling an area with a low permeability material.

There are several mines which could have used the barrier approach to cause the mine to flood shortly after mining, this might have resulted in significant cost savings. For example, at several coal mines in the Vryheid area, the coal outcrop has been mined by horizontal auguring of the coal. Coal seams in this area, are often accessed by driving horizontal adits into the mountain side. Today, the adits and augur holes provide major conduits for oxygen flux to the underground workings, resulting in poor quality, dispersed drainage. In this particular case, had the implications of the auguring process been realised at the time, it is likely that an economic evaluation of the benefit of mining the last few metres of coal in the vicinity of the outcrop, might have shown that it is not warranted in terms of the additional costs incurred as a result of the requirements for collection and treatment of the contaminated drainage.

- *Selective placement of the most reactive waste at the bottom of an open pit to ensure that this waste is inundated and remains below the phreatic surface.*

In many cases, a relatively small proportion of the waste accounts for a

major proportion of the total contaminant load. Identification, segregation and placement of waste with the highest acid generating potential, at the bottom of a spoil pile, can result in a significant cost saving in terms of the water treatment costs.

- *Mining in a manner that facilitates flooding of the workings soon after extraction of the minerals* : This approach may be applied to both underground and opencast mines. In the case of opencast mines, if the first box cut commences at the lower end of the slope, with the box cut running parallel to the contours, it may be practical to inundate a portion of the spoil soon after mining, thus reducing the extent to which contaminant products accumulate within the spoil prior to inundation. In underground mines it is usually not economically viable to mine the deeper ores first, however, situations may arise where this is justified.

6   CONCLUSIONS

The following conclusions may be drawn:

- Subaqueous disposal of waste offers an effective drainage control method primarily because the component of the oxygen flux, due to oxygen transport through air-filled voids, is eliminated. The oxygen flux due to the transport of oxygen through water-filled voids, is considerably less than that through air-filled voids.

- For wastes placed in a subaqueous environment, the oxygen flux and hence the maximum rate of sulphide oxidation, may be estimated by determining the oxygen flux due to the transport of dissolved oxygen in water, and the diffusion of dissolved oxygen through the water cover and water-filled pore spaces.

- The timing of inundation has a significant effect on the resulting drainage

quality since oxidation or weathering products will accumulate within the waste prior to inundation. These contaminants will be mobilised on inundation of the waste. If a waste is to be inundated, either naturally or through the application of engineered controls, it should be inundated as soon after mining as possible.

• There are several practical options which can be applied in South Africa and which take advantage of the benefits of subaqueous disposal. These include:

- Disposal of waste in underground workings below the level of the final phreatic surface.

- The construction of artificial impoundments to keep highly reactive sulphide containing wastes permanently below the phreatic surface.

- Altering the mine plan to enable early flooding of opencast and underground mine workings.

- The application of barriers to flow to help maintain saturated conditions within the waste.

- The selective placement of highly reactive wastes at the bottom of the open pit.

APPENDIX A

Methods to Assess the Predominant Oxygen Flux Mechanism

The rate of oxygen entry into the waste facility is controlled by site specific factors including:

- The air permeability of the waste or layers of soil cover.

- The cross-sectional area and distribution of fissures, worm holes, root holes etc. in the soil.

- The area and distribution of holes in the case of a synthetic cover material.

The contribution to the oxygen flux due to each oxygen transport mechanism may be estimated by applying the following simple check procedures. The methods described below are intended to provide quick of magnitude type estimates only and may be used to determine the dominant oxygen transport mechanism for a specific case.

Rapid Pressure Equilibration

This mechanism refers to the air flux into or out of a waste dump as a direct result of di-urnal or frontal pressure changes. The upper bound limit for oxygen flux into a waste facility due to rapid pressure equilibration may be estimated by ignoring the resistance to flow due to air permeability, from the following relationship derived from Boyles Law:

$$M_{oxygen} = Y_{O_2}.n.(1-S).V.\frac{\Delta p}{RT} \qquad (1)$$

Where : M_{oxygen} = *moles of oxygen entering the waste dump per time interval*

Y_{O2} = *moles oxygen·m^{-3} air*

V = *volume of dump (m^3)*

Δp = *pressure change (N.m^{-2})*

Advective transport of Oxygen through Water-filled Pore Spaces

The solubility of a gas in water is given by :

$$c_{water} = H.c_{air} \qquad (2)$$

where c_{water} = *concentration in water (mole.m^{-3})*

c_{air} = *concentration in air (mole.m^{-3})*

H = *solubility constant at a particular temperature*

The solubility constant for oxygen in water at 0°C is 4.88 x 10^{-2} (Perry and Chilton,

1973) and decreases marginally at higher temperatures.

Assuming that the atmospheric concentration of oxygen in air to be $9,22$ $mol.m^{-3}$, the concentration of oxygen in water at $0°C$ is $14.4 g.m^{-3}$ $(0.45 mol.m^{-3})$

The water flux through a column of saturated material may be calcuated from Darcy's law as follows:

$$\frac{dS}{dt} = K_{water} \frac{\Delta h}{\Delta l} A.c_{water}.\gamma.96 \tag{3}$$

Where : dS/dt = sulphate production rate $(g\ SO_4 \cdot s^{-1})$
K_{water} = saturated permeability of the material
Δh = head loss (m)
Δl = flow path length (m)
A = cross sectional area perpendicular to the direction of flow(m^2)
γ = stoichiometric ratio of mol.sulphate $\cdot mole^{-1}$ O_2

The maximum concentration of sulphate in the mine drainage water under this condition can be estimated by dividing the sulphate load by the water flow rate giving:

$$[SO_4] = 96 c_{water}.\gamma \approx 24.7 mg \cdot litre^{-1} \tag{4}$$

where : $[SO_4]$ =   maximum increase in sulphate concentration along the flow path due to sulphide oxidation $(mg \cdot litre^{-1})$

From the above calculation it can be seen that irrespective of the water flux, the increase in the concentration of sulphate (and other contaminants) is low irrespective of the flow rate through the material if this mechanism of oxygen supply is dominant. The calculation of the load and concentration does not include the contribution from stored salts within the waste material.

Advective Transport Due to Heating

Advective oxygen transport driven by internal heating caused by the oxidation of sulphides or the spontaneous combustion of coal may predominate over other transport mechanisms in unsaturated waste facilities such as coarse discard dumps and spoil piles. Convective transport can be observed in many parts of South Africa where coal discard dumps ignite due to spontaneous combustion. Air is drawn in through the base of the dump and expelled through the top surface. These dumps have the following features in common:

•   The ratio of the height of the dump to the horizontal extent is high (>0,2 approximately).

•   The materials have a high void ratio or porosity as they have been disposed of in a loose state resulting in a high air permeability. The high air permeability probably gives rise to a high initial oxygen flux due to diffusion. The exothermic reaction of pyrite and coal oxidation gives rise to the production of heat which initiates the convective cycle.

Convective oxygen transport is thus generally associated with extremely rapid oxidation beneath the surface of the waste. The need to model this oxygen transport mechanism for the purpose of predicting water quality falls away since the rate of production of contaminants is so high that the leachate water quality will be governed by the rate and efficiency of contaminant flushing and solubility criteria.

Diffusion through Air-filled Void Spaces

Diffusion of oxygen through air-filled void spaces probably accounts for the bulk of oxygen supply in most waste facilities. The model Salmine, discussed in more detail in Section 2, provides a relatively simple methods of evaluating the contribution of diffusion through air-filled pore spaces.

Diffusion through Water-filled Pore Spaces

This oxygen transport mechasims is not significant in most spoil piles except where the sulphide material is placed below the phreatic surface. The diffusion coefficient for oxygen in water is $2,2 \times 10^{-9} m^2 s^{-1}$ at 22° C, this may be compared with $9,1 \times 10^{-6} m^2 \cdot s^{-1}$ at 22° C *(Landolt-Bornstein, 1968)* which is the diffusion coefficient for oxygen in air. The difference of approximately three orders of magnitude accounts for the relative insignificance of the diffusion of oxygen through water-filled pore spaces in the case of partially saturated spoil piles.

Appendix B
The Effect of the Relative Locations of Sulphide Minerals and Neutralising
Minerals on the Rate of Depletion of Neutralising Minerals and Acidity of the
Resultant Drainage

APPENDIX B

The Effect of the Relative Locations of Sulphide Minerals and Neutralising Minerals
on the Rate of Depletion of the Neutralising Mineral
and the Acidity of the Resultant Drainage Water.

The following two examples are presented to illustrate the influence of mineral location:

Example 1: Dissolution of Calcite where the Calcite is Located upstream of the Acid Generating Zone

Assumptions:
- The system is open to the atmosphere and the partial pressure of $CO_2(g)$ is fixed at $10^{-3.5}$ atmospheres
- There is an infinite amount of calcite available.

Method
MinteqA2 was used to compute the equilibrium concentrations of the species.

Results
In this case approximately 48mg/l calcite will dissolve. The available alkalinity, computed as per equation (1) will be 96mg/l ($CaCO_3$ equivalent) and the pH = 8.3. If this pore water were to come in contact with acid water further down in the spoil pile, the available alkalinity to neutralise the acidity would be 98mg/l.

$$Alkalinity = -[H^+] + [OH^-] + [HCO_3^-] + 2[CO_3^{2-}] \qquad (1)$$

The pH of the leachate at the base of the spoil pile could be very low if the acidity generated in the acidic zone exceeds that of the alkalinity generated in the neutralising zone.

If on the other hand, the water entering the neutralising zone contained acidity, the extent to which the calcite dissolves would increase so as to achieve a state of chemical equilibrium. This may be illustrated with a simple example as follows:

Example 2: Dissolution of Calcite where the Calcite is Located Downstream of the Acid Generating Zone

Assumptions:

In addition to the assumptions of the previous example, the following assumptions were made in this example:

- [Fe] = 50mg/litre, Fe^{2+}/Fe^{3+} redox couple was specified

- [SO_4] = 50mg/litre

- Equilibrium Eh is 0.00millivolts

Results

The results at equilibrium conditions, computed using MinteqA2 are as follows:
- 164mg/l calcite will dissolve compared to the 48mg/litre in Example 1.
- the pH will rise to 8.1

In this case, the pH of the leachate at the base of the spoil pile will not decrease until all the available calcite has dissolved. Thereafter, the pH would decrease rapidly and would be largely determined by the rate of acid generation and the water flux.

In reality, spoil piles would not comprise a single neutralising zone located immediately above a single acid generating zone or visa versa, but rather a series of zones which contain to greater or lesser extent, both acid generating and neutralising potential.

APPENDIX C

Overview of Saturated Permeability Determination Methods

The permeability of a soil is mainly dependent on the following factors:

- the density of the soil
- the grain size distribution
- the particle shape and orientation

The following descriptions outline commonly applied methods to determine the saturated water permeability. The accuracy or reliability of each method varies considerably it is advisable to consult an experienced geotechnical engineer in deciding on the appropriate test method. The methods are presented in general increasing order of reliability and cost.

Values documented in the literature

The Unified Soil Classification System (USCS) provides a useful and practical method of classifying soils with common engineering properties. Table 1 presents the USCS classifications and the typical characteristics of these soils in the natural state. The soil can be classified by obtaining a small sample of the material and submitting the sample to a geotechnical engineering laboratory for a foundation indicator test. This test includes a grading analysis and the determination of the Atterburg Limits.

Table 1 : USCS Classification Sytem and the Associated Typical Properties

USCS	Soil Type	Unit Weight (kg/m^3)	Moisture Content (%)	Porosity (%)	Permeability (m/s)
GW	Well graded gravel (little or no fines)	2000	5 ± 3	30 ± 6	$10^{-1}...10^{-2}$
GP	Poorly graded gravel,(little or no fines)	1900	3 ± 2	32 ± 8	$10^{-1}...10^{-4}$
GM	Silty gravels (small percentage of fines)	2100	8 ± 5	28 ± 8	$10^{-5}...10^{-8}$
GC	Clayey gravels, (small percentage of fines)	2050	11 ± 6	32 ± 8	$10^{-6}..10^{-10}$
GM-ML	Silty gravels, (large percentage of fines)	2150	14 ± 9	30 ± 10	$10^{-5}...10^{-8}$
GM-GC	Silty to clayey gravels	2150	11 ± 4	28 ± 7	$10^{-8}..10^{-10}$
GC-CL	Clayey gravels,(large percentage of fines)	2100	14 ± 6	32 ± 7	$10^{-8}..10^{-10}$

USCS	Soil Type	Unit Weight (kg/m^3)	Moisture Content (%)	Porosity (%)	Permeability (m/s)
GC-CH	Clayey gravels, (fines of high plasticity)	1950	20 ± 10	40 ± 10	$10^{-8}..10^{-10}$
SW	Well graded sands, (little or no fines)	1950	13 ± 10	36 ± 10	$10^{0}...10^{-5}$
SP	Poorly graded sands, (little or no fines)	1850	11 ± 9	38 ± 10	$10^{-2}...10^{-5}$
SM	Silty sands (small percentage of fines)	2000	17 ± 7	37 ± 10	$10^{-5}...10^{-8}$
SC	Clayey sands, (small percentage of fines)	1950	20 ± 10	40 ± 10	$10^{-8}..10^{-10}$
SM-ML	Silty sands, (large percentage of fines)	2000	20 ± 9	38 ± 9	$10^{-5}...10^{-8}$
SM-SC	Silty to clayey sands	2100	15 ± 8	32 ± 10	$10^{-8}..10^{-10}$
SC-CL	Clayey sands (large percentage of fines)	2050	19 ± 10	36 ± 11	$10^{-8}..10^{-10}$
SC-CH	Clayey sands, (fines of high plasticity)	1850	35 ± 15	49 ± 10	$10^{-8}..10^{-11}$
ML	Silt, inorganic slight plasticity	1900	32 ± 21	47 ± 15	$10^{-5}...10^{-8}$
CL-ML	Silt to clayey silt, inorganic, low plasticity	2100	19 ± 7	35 ± 8	$10^{-7}..10^{-10}$
CL	Clayey silt, inorganic, low to medium plasticity	2000	25 ± 10	41 ± 8	$10^{-8}..10^{-10}$
CH	Clay, inorganic, high plasticity	1750	47 ± 24	56 ± 9	$10^{-8}..10^{-10}$
OL	Clayey silt, organic, low plasticity	1700	48 ± 13	57 ± 8	$10^{-6}...10^{-8}$
OH	Clay, organic, medium to high plasticity	1550	68 ± 22	66 ± 8	$10^{-8}..10^{-10}$
MH	Special silts, inorganic, elastic silts, eg. Chalk	1550	73 ± 20	67 ± 7	$10^{-6}...10^{-8}$

Hazen's Empirical Relationship

An empirical relationship for the saturated water permeability proposed by Hazen (*Lambe et al, 1969*) for loose sands is as follows :

$$k=100D_{10}^2 \tag{1}$$

where D_{10} = *the particle size (cm) below which 10% of the material falls.*
   k = *permeability in cm/s*

Equation (1) has been found to be applicable to sands with a coefficient of uniformity of less than 2.

Laboratory Methods

The permeability is primarily controlled by the finer fraction of the material in the case of a granular material such as waste rock or tailings and so the error in sampling the smaller fraction of material from a waste pile which contains a small fraction of large particles or rocks is insignificant. The falling head or constant head permeameter tests provide a good indication of the small-scale permeability of waste materials. These tests involve measuring the permeability of a small column of material by measuring either the rate at which a water in a column falls, or the flow rate through a sample under constant head. This method is most appropriate for fine materials such as tailings but typically under estimates the permeability of more heterogeneous material such as waste rock, where preferential flow paths may control the permeability.

Field Tests

Field tests present a means of obtaining permeability values over a large scale and generally represent the most accurate measure of average permeability of the material. There are several field tests which can be used to determine the in-situ permeability of a waste pile including:

- Pump tests (with or without packers) in which the permeability is measured either from the draw down of the phreatic surface caused by pumping, or by the rate of dissipation of excess head in a borehole which has been partially filled by pumping water into the well.

- Double ring infiltrometer tests which can be used to measure the permeability of near surface soil layers.

Determination of the Unsaturated Permeability

The unsaturated permeability of fine materials such as tailings can be determined in the laboratory as a function of the negative pore pressure. Examples of these functions are shown in Figure 3 of Section 1. Laboratory tests are generally time consuming and expensive and not warranted for the purpose of acid mine drainage prediction modeling. In general, for poorly graded coarse sandy or gravelly materials, the unsaturated permeability versus negative pore pressure gradient is steep and tends towards infinity with increasing uniformity of particles. For example, for marbles the curve is essentially vertical for all values of pore pressure

below zero. Well graded finer materials tend to exhibit a flatter pore pressure versus permeability gradient.

APPENDIX D

The Role of Acid Base Accounting Tests

1   **The Objective of Static Testing**

Static testing is used to test representative samples of each geological unit to determine their potential for acid generation. A static test defines the balance between potentially acid generating compounds (sulphide minerals) and acid consuming minerals (carbonate minerals). If the neutralising potential is well in excess of the acid generating potential, the sample is unlikely to generate acidity at any stage during the life of the waste facility. On the other hand, should the acid generating potential exceed the neutralising potential, the material will generate acidity if not immediately, then at some later stage. If the acid generating potential is similar to the neutralising potential, then it is not possible to conclude with any degree of certainty, the likelyhood of acid drainage.

2   **Acid Base Accounting Test Procedures and Interpretation**

The acid generating potential, (AP) of a sample is calculated by measuring the total sulphur content of the sample. Since the measurement of total sulphur includes the measurement of both sulphur in the form of oxidisible sulphides and sulphur in the form of leachable sulphur and sulphates, the result of this test is referred to as maximum potential acidity, since the total sulphur content is assumed to be in the form of oxidisable sulphur. Further tests may be performed on the sample to determine the quantity of non-acid generating sulphur and reactive sulphur in the sample.

The neutralising potential, (NP) of a sample is determined from the total amount of neutralising minerals present in the sample including carbonates and hydroxides. This test is performed by treating the sample with a known excess of hydrochloric acid. The sample and acid mixture is heated to ensure complete reaction and the amount of unconsumed hydrochloric acid is determined by titrating with standard

sodium hydroxide solution. The neutralising potential is calculated by converting the amount of base to calcium carbonate equivalent. The test has important limitations in so far as the method does not indicate the pH to which the sample can neutralise acidity and cannot predict the rate and extent of neutralisation which will take place.

Additional tests may be performed to establish the amount of strongly neutralising carbonate minerals present in a sample.

The net neutralising potential (NNP) is calculated by subtracting the maximum potential acidity (based on total sulphur) from the gross neutralising potential. The theory is based on the assumption that neutralising minerals are consumed completely to release carbon dioxide. In practise, at least in the early stages of acid generation, approximately neutral pH conditions exist within the pore water and carbonates neutralise the acidity incompletely, forming the bicarbonate ion (HCO_3^-). Experience has shown that values of NNP in the range -20 to +20 tonnes of $CaCO_3$ /1000t of sample may be considered uncertain in terms of their ability to generate acidity. Results which indicate a NNP of less than 20 tonnes of Ca CO_3 per 1000t of sample should be regarded as acid generating or potentially acid generating. Kinetic testing should be carried out on geological units which show a NNP of less than 20t $CaCO_3$ per 1000t of rock.

Static tests are relatively inexpensive and quick to perform and are therefore particulary useful in assisting in the classification of geological units in terms of their acid generating/neutralising capacity. Considerable care should be exercised in ensuring that the samples are representative of each geological/ geochemical unit with respect to both chemical and physical features.

APPENDIX E
SALMINE OPERATING MANUAL

1 INTRODUCTION

This appendix describes how to operate the programme *Salmine*. It is assumed that users are familar with Excel version 5 and Windows 95. *Salmine* has a few specific built-in macros which have been programmed in visual basic. These macros can be executed using the buttons provided on the spreadsheets.

2 LOADING *SALMINE*

Copy the file *Salmine.xlw* onto the harddisk of the computer.

Start excel in the usual manner and open the file *Salmine.xlw* using the open file button -

Salmine will open and display the worksheet labelled *Data*.

3 *SALMINE* WORKSHEETS

3.1 *Data Sheet*

All data required to run Salmine is entered on the Salmine Data sheet. The layout of the data sheet is shown as Figure 1. The data sheet has been divided into categories to simplify data entry and provide a logically set out page which summarises the data used in each analysis.

Several buttons are built into the data sheet which start the operation of Salmine and provide help information on the programme's data requirements. Pressing the **START SALMINE** button brings up the Salmine operations Dialog box.

Pressing the [HELP] buttons located adjacent to the data entry groups will bring up a dialog box which provides limited information regarding the model's data requirements.

3.2 *Salmine Calculation Sheet*

All modules, except for the chemical equilibrium submodules are written in the Salmine sheet. The calculations for each module are presented one after the other moving downwards through the spreadsheet. Headings are provided to mark the start of a particular module. The sheet is protected to prevent inadvertent alteration of the code.

3.3 *The Infiltrate Sheet*

The *infiltrate* sheet comprises a table which specifies the sequence of infiltration events to be used in the programme. The infiltrate sheet need not be used as the programme allows the user to specify a uniform infiltration rate as an alternative. The units for the infiltration sheet must be the same as the time step selected. If the user has selected a time step of one week, then weekly infiltration depths must be specified.

Space is provided to store up to five different infiltration sequences. The infiltration sequence to be used is selected using the *simulation settings* dialog box described further on.

3.4 *The Graphs Sheet*

The *graphs* sheet provides several standard graphs to assist the user to understand the acid generation processes active in the spoil pile. The standard graphs included in the model are :

- Sulphide balance in each layer versus time
- Oxygen concentration versus depth
- Porosity and degree of saturation versus depth
- Sulphate concentration in the pore water in each layer versus time

• The Outflow Water Quality parameters and leachate volume/m² of spoil.

3.5 *The Results Sheets*

The results of each time step are written to the results sheets at the end of each time step as follows:
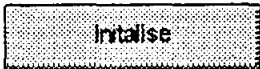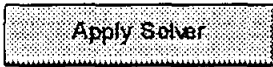
Deg Sat   Stores the degree of saturation at the end of each time step

FeS2   The sulphides balance in each layer and sulphide oxidation reaction rate for each layer at the end of each time step is stored.

IRON   The total mass of Fe^{2+} and Fe^{3+} solid and aqueous phase species generated as a result of the oxidation of pyrite are stored.

CO3 2-   The total mass of CO_3^{2-} solid and aqueous phase species in each layer at the end of each time step are stored.

CA 2 +   The total mass of Ca^{2+} solid and aqueous phase species in each layer at the end of each time step are stored.

SO4 2-   The total mass of SO_4^{2-} solid and aqueous phase species in each layer at the end of each time step are stored.

OUTFLOW   The leachate water volume and water quality (in terms of component concentrations) is stored for each time step.

3.6 *The Thermodynamic Solution Modules*

The chemical equilibrium modules for each layer numbered 1 to 10 are contained in the next ten sheets entitled L1_CHEM to L10_CHEM.respectively.

Buttons are attached to each sheet to assist the user to apply the visual basic programmes which apply numerical solution techniques to find the solution to the

chemical equilibrium problem. The operation of the buttons is as follows:

Initalise	Sets the saturation indices for each solid to a negative value.
Apply Solver	Applies Excel's solver add in to minimise the objective function for the current specified combination of precipitates
Update SI's	Sets the assumed saturation indices values to the current calculated values.
Species Conc.	Applies the calculated species concentrations to calculate the ionic strength.
Auto-Solve Routine	Automatically applies a solution sequence in an attempt to converge to a solution. This procedure does at times result in errors or convergence to the incorrect solution, in which case the manual solution procedure described below should be attempted.

The manual solution sequence typically follows the following steps:

Step 1   Press the Initialise button

Step 2   Press the Apply Solver button. The solver will set up the problem and apply a numerical solution technique to minimise the objective function. The activities of the components and solids quantities will change during the solution procedure.

Step 3   Press the species Conc. Button. The ionic strength will be recalculated based on the current estimated species concentrations.

Step 4   Press the Apply Solver button again. The activities and solids quantities will be re-calculated.

Step 5   Repeat steps 3 and 4 until there is no change in the value of the objective function from one trial solution to the next.

Step 6   Compare the assumed saturation indices with the calculated saturation indices.

3.7 *The Visual Basic Routines*

The dialog boxes and visual basic programmes are contained in the final sheets in the workbook. These sheets are protected to avoid inadvertent changes to the programmes.

If the sign of the assumed and calculated saturation indices differ, press the Update SI's button and then repeat steps 2 to 6 until the final solution is found in which the sign of the assumed saturation indices is the same as that of the calculated saturation indices.

4   SALMINE DIALOG BOXES

4.1 *The Salmine Operations Dialog Box*

The Salmine operations dialog box is displayed every time that the Start Salmine button on the Data sheet is pressed. The Salmine operations dialog box is shown below:
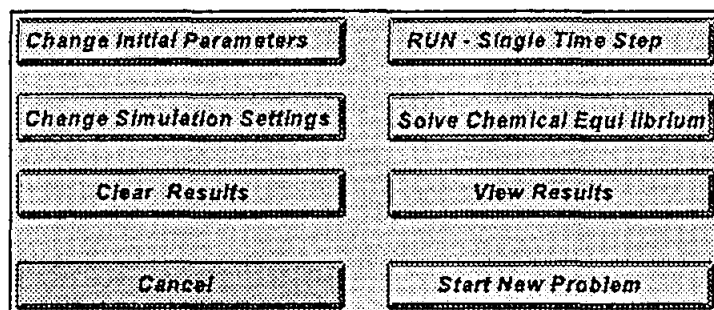
4.2 *The Simulation Settings Dialog Box*

The *simulation settings* buttons display the simulation settings dialog box shown below.

The three option buttons provided for each layer allow the user to specify one of three options to determine the chemical component aqueous phase concentrations as follows :

Option 1 :   The built in thermodynamic chemical equilibrium programme will be used for each time step to calculate component concentrations. It is recommended that this option only be selected when single time steps are carried out.

Option 2 :   The chemical component concentrations will be determined by applying the results trending routine based on previous results of the built in chemical equilibrium routine.

Option 3 :   The concentrations of aqueous phase components will be limited by the concentrations specified on the data sheet. These concentrations may be based on the results of field tests, laboratory tests or other thermodynamic or kinetic models.

Once the *Ok* button is pressed Salmine will carry out calculations for the number of time steps specified on the dialog box and apply either a uniform infiltration rate or a non-uniform infiltration rate depending on the selection.

Arthur Taylor Kinetic Test Results

Arthur Taylor (Kinetic Test) — pH vs Weeks

Arthur Taylor (Kinetic Test) — TDS vs Weeks

Arthur Taylor (Kinetic Test) — Sulphate (mg/litre) vs Weeks

Arthur Taylor (Kinetic Test) — Iron (mg/litre) vs Weeks

Arthur Taylor (Kinetic Test) — Alkalinity (CaCO3 Equiv) vs Weeks

Arthur Taylor (Kinetic Test) — Acidity(as H+) vs Weeks
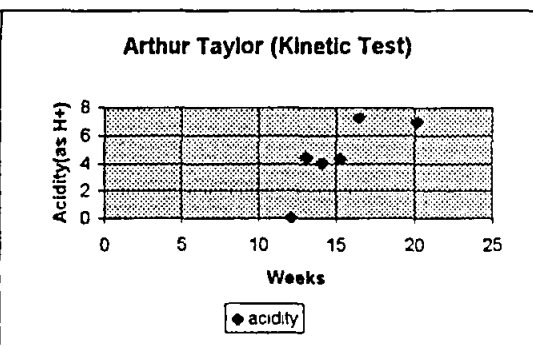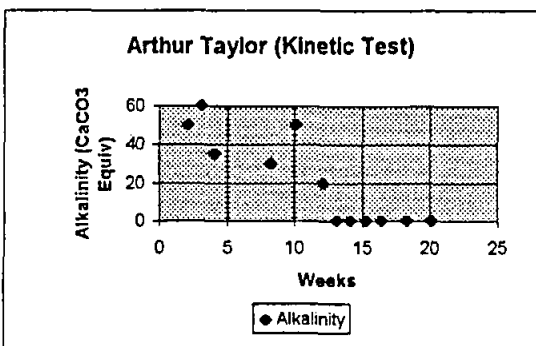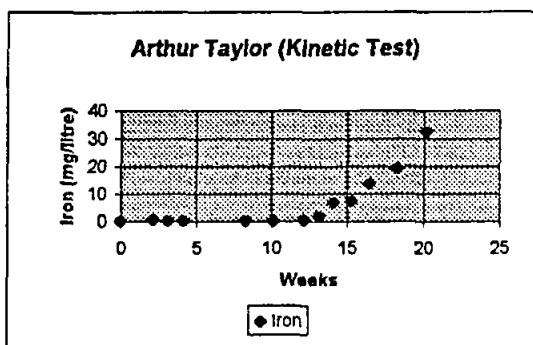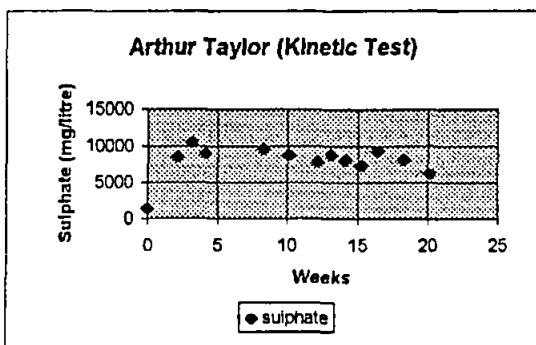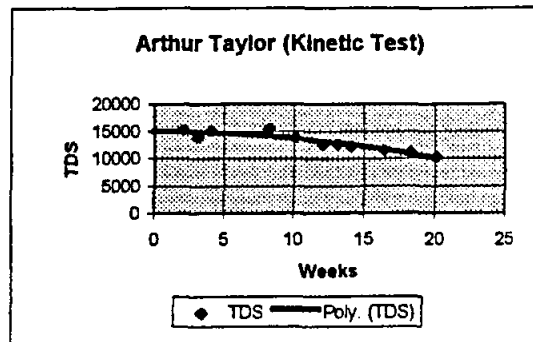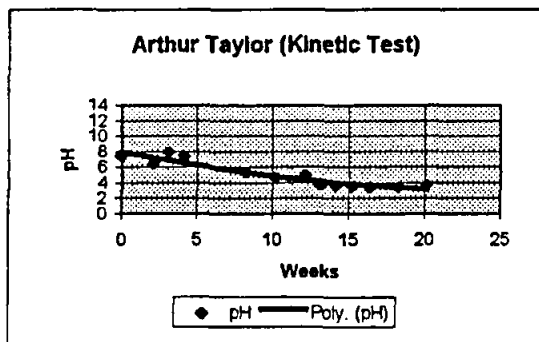
ArthurTaylor
Kinetic

date	weeks	pH	TDS	Alkalinity	acidity	sulphate	Iron
1-Jan-95	0	0	7.35			1317	<0.01
16-Jan-95	15	2	6.35	15200	50	8530	0.37
23-Jan-95	22	3	7.85	13850	60	10453	<0.01
30-Jan-95	29	4	7.35	14960	35	8959	<0.01
28-Feb-95	58	8	5.3	15340	30	9527	<0.01
13-Mar-95	71	10	4.6	13740	50	8665	<0.01
27-Mar-95	85	12	4.9	12393	20	0	7840	0.19
3-Apr-95	92	13	3.7	12600	0	4.4	8800	1.66
10-Apr-95	99	14	3.55	12135	0	4	8040	6.8
18-Apr-95	107	15	3.5		0	4.3	7270	7.3
26-Apr-95	115	16	3.35	11380	0	7.2	9248	13.5
9-May-95	128	18	3.35	11060	0		8096	19.3
22-May-95	141	20	3.65	10080	0	6.9	6130	32

Arthur Taylor Drum Test

Arthur Taylor (Drum Test) — pH vs Weeks

Arthur Taylor (Drum Test) — TDS (mg/litre) vs Weeks

Arthur Taylor (Drum Test) — sulphate (mg/litre) vs Weeks

Arthur Taylor (Drum Test) — Iron (mg/litre) vs Weeks

Arthur Taylor (Drum Test) — Alkalinity (CaCO3 Equiv.) vs Weeks
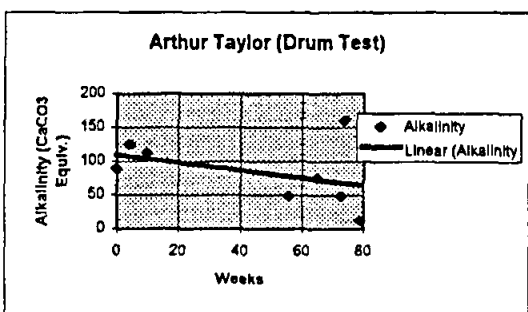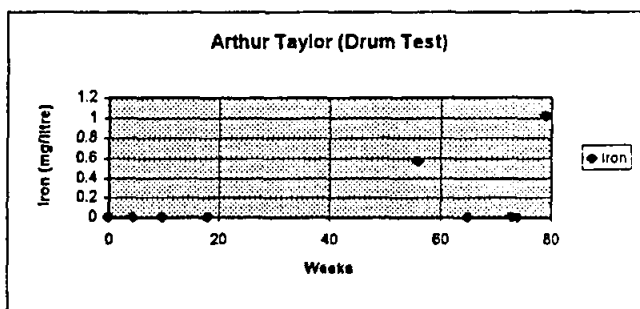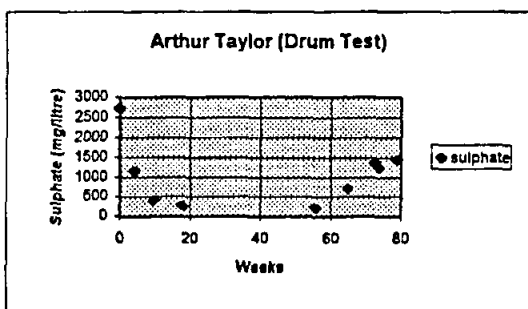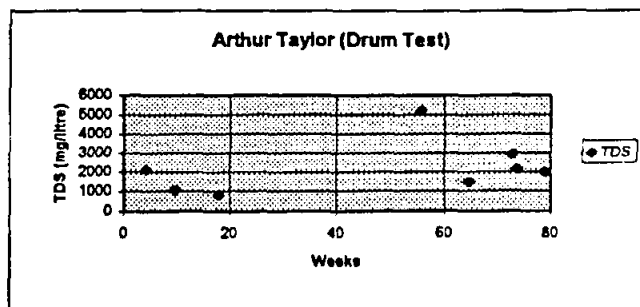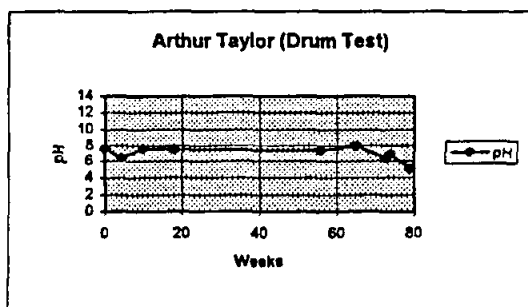
ArthurTaylor
Outside

date	days	weeks	pH	TDS	Alkali	acidity	sulphate	Iron
2-Nov-93	0	0	7.5		88		2710	<0.01
3-Dec-93	31	4	6.4	2100	124		1137	<0.01
10-Jan-94	69	10	7.5	1053	112		395	<.01
8-Mar-94	126	18	7.45	793			253	<0.01
28-Nov-94	391	56	7.28	5176	48		205	0.57
30-Jan-95	454	65	7.95	1440	75		700	<.01
27-Mar-95	510	73	6.3	2908	48		1361	<0.01
3-Apr-95	517	74	6.95	2100	160		1224	<0.01
9-May-95	553	79	5	1960	12		1432	1.02

Middelburg Mine Kinetic Test Results

Middelburg Mine (Kinetic Test)

Middelburg Mine (Kinetic Test)

Middelburg Mine (Kinetic Test)

Middelburg Mine (Kinetic Test)
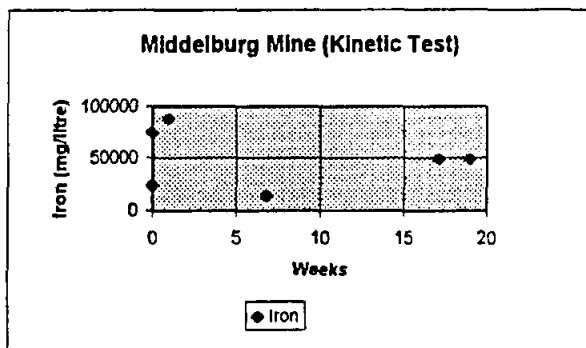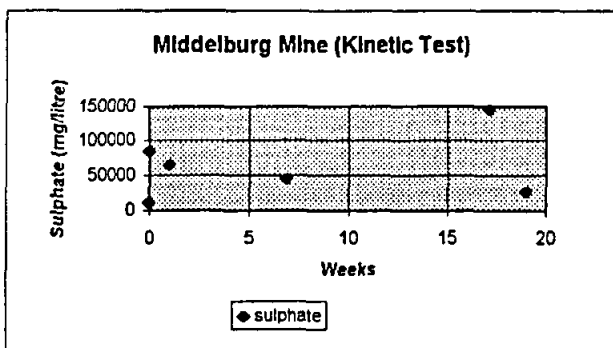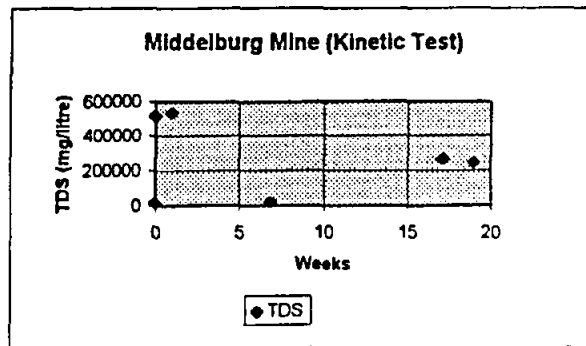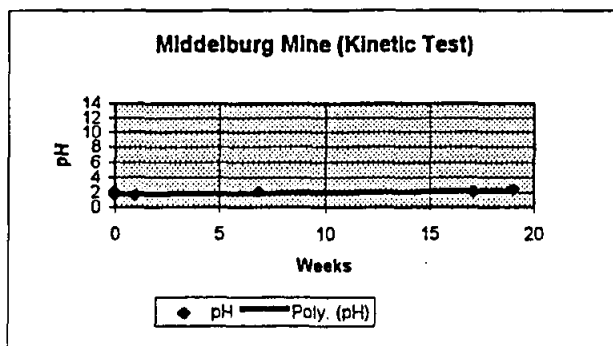
Middelburg
Kinetic

date	days	weeks	pH	TDS	Alkalinity	Acidicty	sulphate	Iron
19-Jan-94	0	0	2	15240			83110	23000
8-Mar-94	48	7	1.95	19500			44367	13400
9-Jan-95	0	0	1.65	509740	1.65		10317	73800
16-Jan-95	7	1	1.52	532160	0		64130	87400
9-May-95	120	17	1.95	263980	0		144447	48200
22-May-95	133	19	2.3	240150	0		25056	48000

Middelburg Drum Test

Middelburg Drum Test (Sulphate vs Weeks)

Middelburg Drum Test (pH vs Weeks)

Middelburg Drum Test (Iron vs Weeks)

Middelburg Drum Test (Acidity vs Weeks)
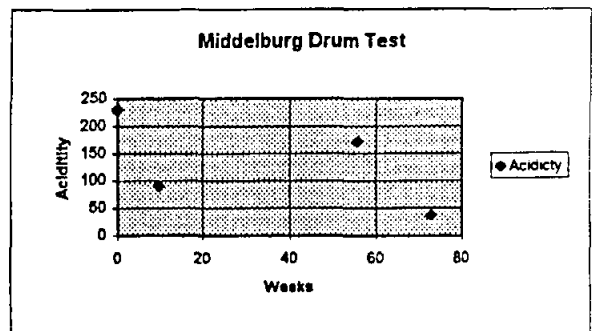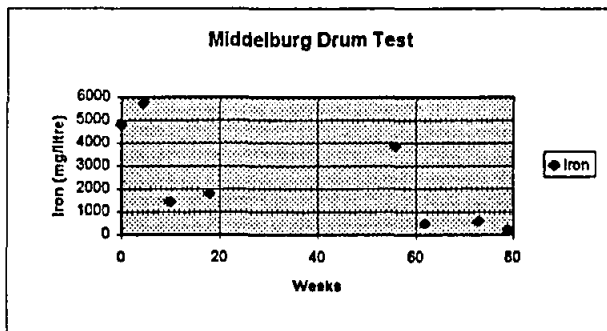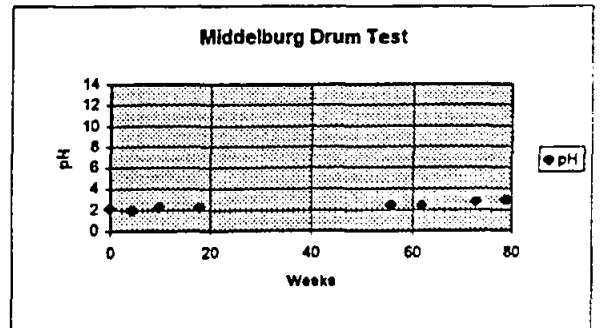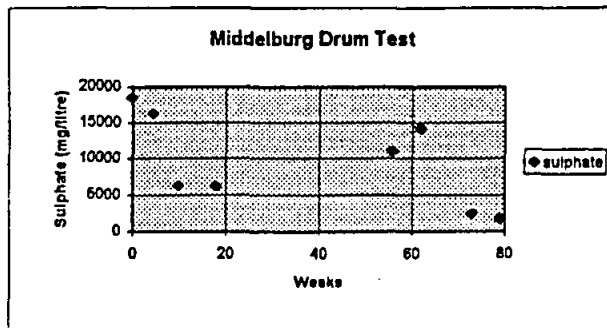
Middelburg
Drum

date	days	weeks	pH	TDS	Alkalinity	Acidicty	sulphate	Iron
2-Nov-93	0	0	2.1			228	18427	4790
3-Dec-93	31	4	1.95		0		16150	5720
10-Jan-94	69	10	2.25	6880	0	90	6233	1440
8-Mar-94	126	18	2.25	5750			6145	1780
28-Nov-94	391	56	2.4	19930		170	10874	3830
9-Jan-95	433	62	2.35	3692	0		14134	460
27-Mar-95	510	73	2.7	4307	0	36	2448	567
9-May-95	553	79	2.85	3300	0		1688	185

SITE CELL TESTING

The purpose of the site column testing is to simulate the site conditions as closely as possible but without limiting the amount of oxygen that can reach the sample. The test cell at the mine represents field conditions with respect to rainfall frequency, duration, and rain water quality. In addition the material has been selected based on what we believe to be potentially the most prolific acid generating lithology.

The results of these tests should therefore represent an upper bound result for the pollutant loads.
The test cell is not intended to be representative with regard to :

• infiltration characterisitics

• oxygen flux characteristics

• permeability characterisitics

The proposed procedure for carrying out sampling is as follows:

• On a weekly basis, collect samples from the base of the cell into a clean sample bottle. Mark the bottle clearly with the date of the sample. The pH and conductivity should be read immediately. Each time that a sample is taken, the base of the cell must be emptied so that the sample taken represents the sample quality for the week. (Note, it is expected that very often there will be no sample since there will be no rain.

• The cell should be emptied each time into a container (eg. measuring cylinder) and the total volume of leachate produced recorded.

• One sample should be submitted to a suitable laboratory every four weeks for the following tests:
    - pH
    - Conductivity
    - Ca
    - Mg
    - Fe
    - SO_4
    - total alkalinity

• The rainfall should be recorded on a daily basis and the pH and conductivity tested.

• All samples should be stored in case further testing is required at a later date.

• Where the test cell yields insufficient leachate to carry out the test, combine the sample of that week with the sample from the next week(s) until there is sufficient sample.

• The test cell should be checked on a weekly basis to ensure that no deleterious materials have been placed in the cell. Care should also be taken to ensure that the tap is not damaged and remains sealed.

SALMINE INITIAL DATA SHEET

PROJECT DESCRIPTION
PROJECT NAME :   Test Case 1 : Middelburg Mine
DATE OF ANALYSIS :
ANALYSIS BY :   A R James
DESCRIPTION OF PROBLEM :   Kinetic test prediction
DESCRIPTION OF ANALYSIS :   1

INFILTRATION RATE

TO LAYER 1

Uniform infiltration rate   mm/time step   9

ATMOSPHERIC PROPERTIES

Atmospheric pressure =	Patm	N/m2	101325	101325
Atmospheric Oxygen Concentration =	CaO	mole/m3 gas	8.15	8.15
Ambient Temperature =	Temp	Kelvin	288	288
Diffusion Coefficient of Oxygen in Air =	Doxyair	m2/s	1.90E-05	1.90E-05

PHYSICAL PROPERTIES

			LAYER 1	LAYER 2	LAYER 3	LAYER 4	LAYER 5	LAYER 6	LAYER 7	LAYER 8	LAYER 9	LAYER 10
Layer Description		text										
layer thickness =	thk	m	0.01	0.05	0.05	0.05	0.05	0.05	0.05	0.05	0.05	0.09

GEOTECHNICAL PROPERTIES

		soil LAYER 1	SPOIL LAYER 2	SPOIL LAYER 3	SPOIL LAYER 4	SPOIL LAYER 5	SPOIL LAYER 6	SPOIL LAYER 7	SPOIL LAYER 8	SPOIL LAYER 9	SPOIL LAYER 10
porosity =	dimensionless	0.4	0.4	0.4	0.4	0.4	0.4	0.4	0.4	0.4	0.4
specific gravity =	dimensionless	2.7	2.7	2.7	2.7	2.7	2.7	2.7	2.7	2.7	2.7
Saturated Water Permeability	m/s	1.00E-02	1.00E-02	1.00E-02	1.00E-02	1.00E-02	1.00E-02	1.00E-02	1.00E-02	1.00E-02	1.00E-02
Proportion of flow to RFP's	dimensionless	0.20	0.20	0.20	0.20	0.20	0.20	0.20	0.20	0.20	0.20
Initial Degree of saturation	dimensionless	0.2	0.2	0.2	0.2	0.2	0.2	0.2	0.2	0.2	0.2
Residual Degree of saturation	dimensionless	0.05	0.05	0.05	0.05	0.05	0.05	0.05	0.05	0.05	0.05
Calibration constant for flow velocity	dimensionless	1	1	1	1	1	1	1	1	1	1
pore size distribution factor	dimensionless	2	2	2	2	2	2	2	2	2	2

SULPHIDE OXIDATION PROPERTIES

		LAYER 2	LAYER 3	LAYER 4	LAYER 5	LAYER 6	LAYER 7	LAYER 8	LAYER 9	LAYER 10
Initial Sulfide concentration =	g pyrite/ kg bed	20	20	20	20	20	20	20	20	20
Initial oxidation rate =	g pyrite/kg bed. week	3.76E-01	3.76E-01	3.76E-01	3.76E-01	3.76E-01	3.76E-01	3.76E-01	3.76E-01	3.76E-01

MICROBAL AND PLANT ROOT CONSUMPTION OF OXYGEN

		LAYER 1
Oxygen Consumption Rate	moles/m3/s	0.00E+00

NEUTRALISATION PROPERTIES

		LAYER 1	LAYER 2	LAYER 3	LAYER 4	LAYER 5	LAYER 6	LAYER 7	LAYER 8	LAYER 9	LAYER 10
Initial Available Calcite Equivalent Concentration	g/kg bed	5.00	5.00	5.00	5.00	5.00	5.00	5.00	5.00	5.00	5.00

CHEMICAL SATURATION CONCENTRATIONS (EXTERNAL TREND ANALYSIS ONLY)

		LAYER 1	LAYER 2	LAYER 3	LAYER 4	LAYER 5	LAYER 6	LAYER 7	LAYER 8	LAYER 9	LAYER 10
pH		7	7	7	7	7	7	7	7	7	7
[SO4] aq species	moles/litre	2.00E-02	2.00E-02	2.00E-02	2.00E-02	2.00E-02	2.00E-02	2.00E-02	2.00E-02	2.00E-02	2.00E-02
[CO3-] aq species	moles/litre	1.00E-03	1.00E-03	1.00E-03	1.00E-03	1.00E-03	1.00E-03	1.00E-03	1.00E-03	1.00E-03	1.00E-03
[Ca2+] species	moles/litre	1.00E-03	1.00E-03	1.00E-03	1.00E-03	1.00E-03	1.00E-03	1.00E-03	1.00E-03	1.00E-03	1.00E-03
[Fe] aq species	moles/litre	1.00E-06	1.00E-06	1.00E-06	1.00E-06	1.00E-06	1.00E-06	1.00E-06	1.00E-06	1.00E-06	1.00E-06

QUALITY OF WATER INFILTRATING LAYER 1

		LAYER 1	mg/litre
pH		7	
[SO4] aqueous species	moles/litre	0.00E+00	0
[CO3-] aq ueous species	moles/litre	1.00E-22	6E-18
[Ca2+] aqueous species	moles/litre	1.00E-22	4E-18
[Fe] aqueous species	moles/litre	0.00E+00	0

FeS2

Record of Kr Values									
Current	1.74E-07	1.75E-07	1.75E-07	1.75E-07	1.76E-07	1.76E-07	1.76E-07	1.76E-07	1.76E-07
TIME	LAYER 2	LAYER 3	LAYER 4	LAYER 5	LAYER 6	LAYER 7	LAYER 8	LAYER 9	LAYER 10
layer	Kr1	Kr1	Kr1	Kr1	Kr1	Kr1	Kr1	Kr1	Kr1
0	6.8E-07	6.8E-07	6.8E-07	6.8E-07	6.8E-07	6.8E-07	6.8E-07	6.8E-07	6.8E-07
1	6.56E-07	6.56E-07	6.56E-07	6.56E-07	6.56E-07	6.56E-07	6.56E-07	6.56E-07	6.56E-07
2	6.32E-07	6.32E-07	6.32E-07	6.33E-07	6.33E-07	6.33E-07	6.33E-07	6.33E-07	6.33E-07
3	6.09E-07	6.09E-07	6.1E-07	6.1E-07	6.1E-07	6.1E-07	6.1E-07	6.1E-07	6.11E-07
4	5.87E-07	5.88E-07	5.88E-07	5.88E-07	5.88E-07	5.88E-07	5.89E-07	5.89E-07	5.89E-07
5	5.66E-07	5.66E-07	5.67E-07	5.67E-07	5.67E-07	5.67E-07	5.68E-07	5.68E-07	5.68E-07
6	5.46E-07	5.46E-07	5.46E-07	5.47E-07	5.47E-07	5.47E-07	5.47E-07	5.47E-07	5.48E-07
7	5.26E-07	5.26E-07	5.27E-07	5.27E-07	5.27E-07	5.28E-07	5.28E-07	5.28E-07	5.28E-07
8	5.07E-07	5.07E-07	5.08E-07	5.08E-07	5.08E-07	5.09E-07	5.09E-07	5.09E-07	5.09E-07
9	4.88E-07	4.89E-07	4.89E-07	4.9E-07	4.9E-07	4.9E-07	4.91E-07	4.91E-07	4.91E-07
10	4.71E-07	4.71E-07	4.72E-07	4.72E-07	4.73E-07	4.73E-07	4.73E-07	4.73E-07	4.73E-07
11	4.54E-07	4.54E-07	4.55E-07	4.55E-07	4.56E-07	4.56E-07	4.56E-07	4.56E-07	4.56E-07
12	4.37E-07	4.38E-07	4.38E-07	4.39E-07	4.39E-07	4.4E-07	4.4E-07	4.4E-07	4.4E-07
13	4.22E-07	4.22E-07	4.23E-07	4.23E-07	4.23E-07	4.24E-07	4.24E-07	4.24E-07	4.24E-07
14	4.06E-07	4.07E-07	4.07E-07	4.08E-07	4.08E-07	4.09E-07	4.09E-07	4.09E-07	4.09E-07
15	3.92E-07	3.92E-07	3.93E-07	3.93E-07	3.94E-07	3.94E-07	3.94E-07	3.94E-07	3.95E-07
16	3.77E-07	3.78E-07	3.79E-07	3.79E-07	3.79E-07	3.8E-07	3.8E-07	3.8E-07	3.8E-07
17	3.64E-07	3.64E-07	3.65E-07	3.65E-07	3.66E-07	3.66E-07	3.66E-07	3.67E-07	3.67E-07
18	3.51E-07	3.51E-07	3.52E-07	3.52E-07	3.53E-07	3.53E-07	3.53E-07	3.53E-07	3.54E-07
19	3.38E-07	3.39E-07	3.39E-07	3.4E-07	3.4E-07	3.4E-07	3.41E-07	3.41E-07	3.41E-07
20	3.26E-07	3.26E-07	3.27E-07	3.27E-07	3.28E-07	3.28E-07	3.28E-07	3.29E-07	3.29E-07
21	3.14E-07	3.15E-07	3.15E-07	3.16E-07	3.16E-07	3.16E-07	3.17E-07	3.17E-07	3.17E-07
22	3.03E-07	3.03E-07	3.04E-07	3.04E-07	3.05E-07	3.05E-07	3.05E-07	3.05E-07	3.05E-07
23	2.92E-07	2.92E-07	2.93E-07	2.93E-07	2.94E-07	2.94E-07	2.94E-07	2.94E-07	2.95E-07
24	2.81E-07	2.82E-07	2.82E-07	2.83E-07	2.83E-07	2.83E-07	2.84E-07	2.84E-07	2.84E-07
25	2.71E-07	2.72E-07	2.72E-07	2.72E-07	2.73E-07	2.73E-07	2.73E-07	2.74E-07	2.74E-07
26	2.61E-07	2.62E-07	2.62E-07	2.63E-07	2.63E-07	2.63E-07	2.64E-07	2.64E-07	2.64E-07
27	2.52E-07	2.52E-07	2.53E-07	2.53E-07	2.54E-07	2.54E-07	2.54E-07	2.54E-07	2.54E-07
28	2.43E-07	2.43E-07	2.44E-07	2.44E-07	2.44E-07	2.45E-07	2.45E-07	2.45E-07	2.45E-07
29	2.34E-07	2.34E-07	2.35E-07	2.35E-07	2.36E-07	2.36E-07	2.36E-07	2.36E-07	2.36E-07
30	2.25E-07	2.26E-07	2.26E-07	2.27E-07	2.27E-07	2.27E-07	2.28E-07	2.28E-07	2.28E-07
31	2.17E-07	2.18E-07	2.18E-07	2.19E-07	2.19E-07	2.19E-07	2.19E-07	2.2E-07	2.2E-07
32	2.09E-07	2.1E-07	2.1E-07	2.11E-07	2.11E-07	2.11E-07	2.12E-07	2.12E-07	2.12E-07
33	2.02E-07	2.02E-07	2.03E-07	2.03E-07	2.03E-07	2.04E-07	2.04E-07	2.04E-07	2.04E-07
34	1.94E-07	1.95E-07	1.95E-07	1.96E-07	1.96E-07	1.96E-07	1.97E-07	1.97E-07	1.97E-07
35	1.87E-07	1.88E-07	1.88E-07	1.89E-07	1.89E-07	1.89E-07	1.89E-07	1.9E-07	1.9E-07
36	1.81E-07	1.81E-07	1.82E-07	1.82E-07	1.82E-07	1.82E-07	1.83E-07	1.83E-07	1.83E-07

SULPHIDE BALANCE								
Current	5.118912	5.133192	5.14466	5.154729	5.16332	5.170431	5.176056	5.18019	5.183367
TIME	Sulphide	Sulphide	Sulphide	Sulphide	Sulphide	Sulphide	Sulphide	Sulphide	Sulphide
Time	LAYER 2	LAYER 3	LAYER 4	LAYER 5	LAYER 6	LAYER 7	LAYER 8	LAYER 9	LAYER 10
0	20	20	20	20	20	20	20	20	20
1	19.27858	19.28249	19.28596	19.28898	19.29156	19.29369	19.29538	19.29663	19.29759
2	18.58204	18.58798	18.59323	18.5978	18.6017	18.60494	18.6075	18.6094	18.61085
3	17.9106	17.91833	17.92515	17.93109	17.93617	17.94037	17.9437	17.94617	17.94805
4	17.26337	17.2727	17.28091	17.28807	17.29418	17.29923	17.30325	17.30622	17.30849
5	16.63949	16.65024	16.65967	16.66789	16.67491	16.68073	16.68534	16.68875	16.69136
6	16.03811	16.05011	16.06061	16.06977	16.07759	16.08407	16.08921	16.09301	16.09591
7	15.45843	15.47152	15.48296	15.49294	15.50145	15.50851	15.51411	15.51824	15.52141
8	14.89967	14.91372	14.92596	14.93664	14.94576	14.95332	14.95931	14.96374	14.96712
9	14.36107	14.37594	14.38888	14.40017	14.4098	14.41778	14.42411	14.42879	14.43237
10	13.84191	13.85749	13.87101	13.88281	13.89289	13.90123	13.90785	13.91274	13.91648
11	13.34149	13.35767	13.37169	13.38391	13.39435	13.403	13.40986	13.41493	13.41881
12	12.85913	12.87582	12.89024	12.90282	12.91356	12.92246	12.92951	12.93473	12.93872
13	12.39419	12.41129	12.42603	12.4389	12.44988	12.45898	12.4662	12.47153	12.47561
14	11.94603	11.96347	11.97846	11.99155	12.00272	12.01198	12.01932	12.02474	12.02889
15	11.51406	11.53176	11.54694	11.56019	11.5715	11.58088	11.58831	11.59379	11.598
16	11.09769	11.11559	11.13089	11.14425	11.15566	11.16512	11.17261	11.17814	11.18238
17	10.69636	10.71439	10.72976	10.74319	10.75466	10.76416	10.77169	10.77725	10.78151
18	10.30952	10.32763	10.34303	10.35649	10.36798	10.3775	10.38504	10.39061	10.39487
19	9.936656	9.954795	9.970182	9.983626	9.995105	10.00461	10.01215	10.01771	10.02197
20	9.577264	9.595387	9.610719	9.624118	9.635558	9.645035	9.652546	9.658087	9.662332
21	9.230855	9.248923	9.264166	9.27749	9.288866	9.29829	9.305757	9.311265	9.315486
22	8.896964	8.91494	8.930064	8.943287	8.954575	8.963927	8.971336	8.9768	8.980988
23	8.575138	8.592991	8.607968	8.621065	8.632247	8.641509	8.648847	8.654258	8.658405
24	8.264941	8.282642	8.29745	8.310401	8.321458	8.330616	8.337871	8.34322	8.34732
25	7.965956	7.983479	7.998096	8.010883	8.021799	8.030841	8.038003	8.043282	8.047329
26	7.677777	7.6951	7.709507	7.722114	7.732877	7.74179	7.74885	7.754053	7.758043
27	7.400013	7.417117	7.4313	7.443713	7.45431	7.463085	7.470036	7.475156	7.479084
28	7.132291	7.149158	7.163102	7.175309	7.18573	7.19436	7.201194	7.206227	7.210089
29	6.874246	6.890861	6.904555	6.916547	6.926783	6.93526	6.941972	6.946914	6.950707
30	6.62553	6.641881	6.655315	6.667083	6.677127	6.685445	6.69203	6.696878	6.700598
31	6.385807	6.401882	6.415048	6.426584	6.436432	6.444585	6.451039	6.45579	6.459436
32	6.15475	6.170541	6.183433	6.194732	6.204377	6.212362	6.218682	6.223333	6.226904
33	5.932048	5.947546	5.960159	5.971217	5.980655	5.988469	5.994653	5.999203	6.002696
34	5.717399	5.732599	5.744929	5.755742	5.764971	5.77261	5.778656	5.783103	5.786518
35	5.510512	5.525408	5.537452	5.548019	5.557036	5.5645	5.570406	5.57475	5.578085
36	5.311106	5.325695	5.337452	5.34777	5.356575	5.363862	5.369628	5.373867	5.377124

IRON

WEEK		IRON					grams				
Current	-1.6E-65	7.059178	435.0605	521.4337	611.8709	528.7315	535.4709	445.5421	457.6988	2172.932	
Time	1	2	3	4	5	6	7	8	9	10	total
0	0	0	0	0	0	0	0	0	0	0	
1	-2.1E-07	26.68613	26.54129	26.41304	26.3013	26.20601	26.12708	26.06449	26.01819	46.76906	257.1266
2	-2.6E-07	52.45196	52.23219	52.03802	51.8688	51.72443	51.60485	51.51	51.43983	92.49518	507.3652
3	-5.6E-09	77.28916	77.00303	76.75078	76.53089	76.34327	76.18784	76.06456	75.97337	136.6266	748.7695
4	-1.2E-10	101.2307	100.8855	100.5819	100.3171	100.0912	99.90404	99.75559	99.6458	179.2113	981.6231
5	-2.7E-12	124.3087	123.9112	123.5622	123.258	122.9983	122.7832	122.6126	122.4864	220.3019	1206.222
6	-5.8E-14	146.5542	146.1105	145.7219	145.383	145.0938	144.8542	144.6641	144.5236	259.9489	1422.854
7	-1.3E-15	167.9971	167.5129	167.0898	166.7207	166.4057	166.1448	165.9378	165.7847	298.2018	1631.795
8	-2.7E-17	188.6663	188.1468	187.6939	187.2987	186.9614	186.682	186.4603	186.2965	335.1081	1833.314
9	-5.9E-19	208.5897	208.0396	207.561	207.1435	206.7871	206.4918	206.2577	206.0846	370.7139	2027.669
10	-1.3E-20	227.794	227.2176	226.7174	226.2809	225.9083	225.5996	225.3548	225.1739	405.0638	2215.11
11	-2.8E-22	246.3051	245.7064	245.1881	244.7357	244.3496	244.0296	243.7759	243.5884	438.201	2395.88
12	-6.1E-24	264.148	263.5306	262.9974	262.532	262.1347	261.8055	261.5445	261.3516	470.1672	2570.211
13	-1.3E-25	281.3467	280.7139	280.1687	279.6928	279.2866	278.9499	278.683	278.4859	501.0029	2738.33
14	-2.9E-27	297.9244	297.2792	296.7248	296.2407	295.8274	295.485	295.2135	295.013	530.7471	2900.455
15	-6.3E-29	313.9034	313.2486	312.6873	312.1972	311.7786	311.4319	311.157	310.9541	559.4376	3056.796
16	-1.4E-30	329.3054	328.6434	328.0774	327.5831	327.161	326.8113	326.5341	326.3294	587.1109	3207.556
17	-3E-32	344.1512	343.4842	342.9154	342.4187	341.9944	341.643	341.3644	341.1588	613.8024	3352.932
18	-6.4E-34	358.4607	357.7908	357.221	356.7234	356.2983	355.9462	355.6671	355.4611	639.5461	3493.115
19	-1.4E-35	319.3356	368.6219	372.0815	374.508	367.7299	369.3704	369.7433	368.7477	742.0928	3652.231
20	-3E-37	279.7123	378.9563	386.4469	391.7987	378.6685	382.3026	383.328	381.5434	843.7567	3806.513
21	-6.6E-39	239.6086	388.8119	400.3346	408.613	389.1317	394.76	396.4387	393.8654	944.5687	3956.133
22	-1.4E-40	199.042	398.2058	413.7618	424.9677	399.1361	406.7594	409.0919	405.7304	1044.558	4101.254
23	-3.1E-42	158.029	407.1546	426.7449	440.8791	408.698	418.3169	410.8964	418.1841	1136.813	4225.716
24	-6.8E-44	116.5859	415.6743	439.2998	456.363	417.8331	429.4481	412.275	430.2122	1228.302	4345.993
25	-1.5E-45	74.72803	423.7802	451.4416	471.4347	426.5564	440.1681	413.2427	441.8297	1309.296	4452.478
26	-3.2E-47	32.47044	431.4872	463.1852	486.1086	434.8826	450.4913	413.8141	453.0511	1389.577	4555.068
27	-7E-49	0	438.8096	474.5448	500.3991	442.8257	460.4319	414.003	455.1349	1475.21	4661.359
28	-1.5E-50	0	445.7613	485.5342	514.3198	450.3994	470.0033	413.823	456.8499	1560.18	4796.87
29	-3.3E-52	0	452.3555	496.1665	527.8838	457.6167	479.2186	413.2872	458.2093	1644.509	4929.247
30	-7.2E-54	0	458.6051	506.4546	541.1039	464.4904	488.0905	412.4081	459.2254	1728.221	5058.599
31	-1.6E-55	0	464.5225	516.4108	553.9923	471.0327	496.6311	411.1979	459.9106	1793.376	5167.074
32	-3.4E-57	0	470.1196	526.0469	566.5609	477.2553	504.8522	409.6683	460.2765	1857.958	5272.737
33	-7.4E-59	0	475.4079	535.3744	578.821	483.1696	512.7652	407.8307	460.3344	1921.985	5375.688
34	-1.6E-60	0	480.3986	544.4045	590.7838	488.7867	520.381	405.6959	460.0952	1985.477	5476.022
35	-3.5E-62	0	485.1024	553.1477	602.4599	494.117	527.7102	403.2746	459.5695	2048.453	5573.835
36	-7.6E-64	0	489.5295	561.6143	613.8594	499.171	534.7629	400.5769	458.7674	2110.932	5669.214

WEEK		Ca (T)			grams						
Current	9E-22	122.1368	152.7529	113.5936	122.9915	121.1618	119.9948	159.5854	151.9259	267.1177	1064.143
Ca_T	1	2	3	4	5	6	7	8	9	10	
1	31.752	158.76	158.76	158.76	158.76	158.76	158.76	158.76	158.76	285.768	1301.832
2	31.57733	158.0243	158.0834	158.1131	158.2472	158.0937	158.0349	158.0436	158.0431	284.4766	1296.261
3	31.5054	157.845	157.9169	157.952	158.1211	157.9214	157.8465	157.8539	157.8433	284.1128	1294.805
4	11.88894	168.1672	157.7349	157.7931	157.9974	157.7532	157.6647	157.6742	157.6609	281.7269	1284.335
5	0	178.4893	157.5529	157.6341	157.8737	157.5851	157.4829	157.4946	157.4787	279.3436	1281.591
6	0	169.7176	157.3709	157.4751	157.75	157.417	157.3011	157.315	157.2965	277.3883	1271.643
7	0	179.0991	157.1889	157.3162	157.6263	157.2489	157.1193	157.1354	157.1143	275.433	1279.848
8	0	166.7171	157.4523	157.1376	157.5026	157.0808	156.9375	156.9558	156.9848	275.1338	1266.768
9	0	175.2443	157.7157	156.959	157.3789	156.9126	156.7558	156.7762	156.8552	274.8346	1274.598
10	0	162.8837	157.9441	156.8419	157.2935	156.8088	156.666	156.6791	156.7595	274.6483	1261.877
11	0	171.411	158.1725	156.7248	157.2081	156.705	156.5762	156.582	156.6639	274.4619	1270.043
12	0	160.8362	158.085	156.603	157.1227	156.6011	156.4864	156.4849	156.5862	274.2723	1258.806
13	0	171.1729	157.9975	156.4811	157.0373	156.4973	156.3966	156.3878	156.5085	274.0826	1268.479
14	0	160.6241	157.91	156.3593	156.9519	156.3935	156.3069	156.2907	156.4308	273.893	1257.267
15	0	170.965	157.8416	156.3059	156.8532	156.2896	156.2171	156.1936	156.3532	273.7033	1267.019
16	0	160.392	157.7733	156.2526	156.7546	156.1858	156.1273	156.0965	156.2755	273.5137	1255.857
17	0	170.733	157.7049	156.1992	156.6559	156.082	156.0375	155.9994	156.1978	273.324	1265.61
18	0	160.1914	157.6365	156.1458	156.5573	155.9781	155.9477	155.9023	156.1196	273.173	1254.479
19	0	170.5324	157.5682	156.0924	156.4587	155.8743	155.858	155.8052	156.0414	273.022	1264.23
20	0	157.391	157.5698	155.826	156.3916	155.6834	155.5928	155.6566	155.5627	272.9166	1249.674
21	0	165.1668	157.5714	155.5595	156.3245	155.4925	155.3276	155.5081	155.0841	272.8113	1256.034
22	0	152.0634	157.5731	155.2931	156.2574	155.3016	155.0624	155.3595	154.6054	272.706	1241.516
23	0	159.8391	157.5747	155.0266	156.1903	155.1107	154.7972	155.211	154.1267	272.6007	1247.876
24	0	146.694	157.5763	154.7602	156.1232	154.9198	154.532	155.0418	153.9499	272.366	1233.597
25	0	154.4697	157.578	154.4937	156.0561	154.7289	154.2668	154.8725	153.773	272.1314	1240.239
26	0	141.3705	157.5796	154.2273	155.989	154.5381	154.0016	154.7032	153.5961	271.7928	1226.005
27	0	149.1462	157.5812	153.9609	155.9219	154.3472	153.7364	154.534	153.4192	271.4542	1232.647
28	0	135.9965	157.5829	153.6944	155.8548	154.1563	153.4712	154.3647	153.2835	271.0979	1218.404
29	0	143.7722	157.5845	153.428	155.7877	153.9654	153.206	154.1955	153.1477	270.7415	1225.087
30	0	130.6781	157.5861	153.1615	155.7206	153.7745	152.9408	154.0262	153.012	270.3852	1210.9
31	0	138.4538	157.5878	152.8951	155.6535	153.5836	152.6756	153.857	152.8762	270.0288	1217.583
32	0	125.2985	157.5894	152.6286	155.5865	153.3927	152.4104	153.6877	152.7405	269.6129	1203.334
33	0	133.0742	157.5911	152.3622	155.5194	153.2018	152.1452	153.5184	152.6047	269.1971	1210.017
34	0	119.9862	157.5927	152.0957	155.4523	153.0109	151.88	153.3492	152.469	268.7812	1195.836
35	0	127.762	157.5943	151.8293	155.3852	152.82	151.6148	153.1799	152.3332	268.3653	1202.519
36	0	114.5999	157.596	151.5628	155.3181	152.6292	151.3497	153.0107	152.1974	267.9494	1188.264
37	0	122.3757	157.5976	151.2964	155.251	152.4383	151.0845	152.8414	152.0617	267.5335	1194.946

RESULTS OF TIME SIMULATION				CO3_T			grams				
Current	-0.00021	0.040618	0.122405	0.195419	0.236898	0.258375	0.259613	0.190588	2.299723	32.21733	
CO3_T	1	2	3	4	5	6	7	8	9	10	
1	47.628	238.14	238.14	238.14	238.14	238.14	238.14	238.14	238.14	428.652	2381.4
2	43.62754	238.7938	220.4266	224.3492	212.0402	225.1699	212.3207	213.4154	213.421	384.1602	2187.725
3	42.16258	239.419	215.5842	220.9324	205.218	222.0073	205.4935	206.8296	206.4953	371.5627	2135.705
4	26.6927	245.24	210.8894	217.5608	198.512	218.9319	198.8962	200.5901	200.1697	356.0466	2073.529
5	11.22282	251.061	206.1945	214.1894	191.8063	215.8569	192.3	194.3528	193.849	340.5496	2011.382
6	-4.24705	256.882	201.4997	210.8179	185.1007	212.7818	185.7039	188.1155	187.5283	316.8113	1940.994
7	3.114505	252.8797	196.8048	207.4464	178.395	209.7068	179.1077	181.8781	181.2076	294.7076	1885.248
8	-2.28397	201.6601	156.0361	209.6767	171.6893	206.6317	172.5115	175.6408	138.1249	278.9545	1708.642
9	1.674912	150.1655	124.692	210.6171	164.9837	203.5567	165.9154	169.4035	105.5044	262.997	1559.51
10	-1.22827	114.3377	99.28237	163.7451	132.0121	160.0486	132.5627	133.8658	85.1215	247.1778	1266.925
11	0.90073	85.19091	78.87851	127.3783	105.4805	125.9107	105.8349	105.828	68.5896	231.8704	1035.863
12	-0.66054	64.82841	62.48186	99.14047	84.17332	99.10471	84.43867	83.69445	55.2054	217.1581	849.5648
13	0.484393	48.32922	49.4062	77.19699	67.0919	78.04115	67.32643	66.21279	44.38707	203.0963	701.5725
14	-0.35522	36.75764	38.97031	60.13426	53.41987	61.47943	53.652	52.39875	35.65534	189.7181	581.8305
15	0.260496	27.41701	30.69386	46.85821	42.49237	48.44991	42.73306	41.47819	28.61691	177.0392	486.0392
16	-0.19103	20.84182	24.12461	36.52351	33.76974	38.19396	34.02036	32.84169	22.95004	165.0618	408.1365
17	0.140089	15.55337	18.93805	28.47449	26.8153	30.11742	27.07243	26.00915	18.39229	153.7777	345.2903
18	-0.10273	11.81761	14.83995	22.20342	21.27657	23.75453	21.53497	20.60208	14.73008	143.1715	293.8279
19	0.075337	8.823142	11.61647	17.31576	16.86971	18.73984	17.12393	16.32188	11.79002	133.2217	251.8978
20	-0.05525	6.700832	9.079095	13.50539	13.36659	14.78639	13.61182	12.93285	9.431599	123.9034	217.2627
21	0.040514	5.005148	7.089534	10.5341	10.58422	11.66871	10.81666	10.24885	7.541099	115.1888	188.7176
22	-0.02971	3.799556	5.528472	8.216763	8.376024	9.209497	8.592974	8.122782	6.026701	107.0487	164.8917
23	0.021788	2.839262	4.307735	6.409159	6.624794	7.269264	6.824578	6.438376	4.814325	99.45306	145.0023
24	-0.01598	2.154477	3.352552	4.999066	5.236906	5.73821	5.418726	5.103677	3.844281	92.37179	128.2037
25	0.011717	1.610606	2.607349	3.898976	4.137675	4.529856	4.301444	4.045941	3.068536	85.77507	113.9872
26	-0.00859	1.221674	2.025649	3.040735	3.267589	3.576068	3.413758	3.207596	2.448468	79.63375	101.8267
27	0.006301	0.913626	1.572751	2.371164	2.57927	2.823141	2.70868	2.543073	1.953057	73.91959	91.39066
28	-0.00462	0.692745	1.219964	1.848816	2.035039	2.228728	2.148787	2.016287	2.031379	68.54429	82.76141
29	0.003389	0.518255	0.945785	1.441337	1.604954	1.759434	1.704292	1.598658	2.093413	63.55987	75.22938
30	-0.00248	0.392821	0.732607	1.123498	1.265241	1.388908	1.351491	1.26755	2.142534	58.93791	68.60007
31	0.001822	0.293978	0.567195	0.875603	0.997034	1.096359	1.071528	1.005026	2.181416	54.65205	62.74201
32	-0.00134	0.222752	0.438797	0.682285	0.785379	0.865378	0.84941	0.796871	2.212182	50.67786	57.52957
33	0.00098	0.166756	0.33931	0.531548	0.618422	0.68301	0.673222	0.631823	2.236511	46.99266	52.87424
34	-0.00072	0.126314	0.262199	0.414033	0.486779	0.53903	0.533491	0.500951	2.255737	43.57545	48.69326
35	0.000527	0.09459	0.202528	0.322432	0.383023	0.425361	0.422693	0.397179	2.270917	40.40673	44.92598
36	-0.00039	0.071628	0.156339	0.251044	0.301278	0.335628	0.334854	0.314894	2.282887	37.46844	41.51661
37	0.000283	0.053654	0.120638	0.195419	0.236898	0.264796	0.265227	0.249648	2.292314	34.74382	38.4227

OUTFLOW & WATER QUALITY OF LEACHATE						
current	9.030088	0.50	227179.99	1274.22	219.48	75121.59
WEEK	litres		mg/l	mg/l	mg/l	mg/l
0	outflow	pH	SO4 aq	CO3 aq	Ca 2+ aq	Fe(aq)
1	38.66891	6.535238	12868.56	6209.0209	180.6391	0.000497
2	9.48315	6.535234	12868.42	6209.0209	180.6391	0.000497
3	9.03387	6.218814	10859.42	8286.9469	1186.738	0.000436
4	9.030107	6.219011	10861.18	8286.9469	1186.738	0.000436
5	9.030088	6.150704	10811.74	12443.31	977.2551	0.000428
6	9.030088	6.150704	10811.74	11618.947	977.2551	0.000428
7	9.030088	6.276148	29456.06	10808.301	161.6874	0.000709
8	9.030088	6.276148	29456.06	10230.56	161.6874	0.000709
9	9.030088	6.699945	48994.43	9645.3089	101.7516	0.001641
10	9.030088	6.699945	48994.43	9065.1633	101.7516	0.001641
11	9.030088	7.009678	73798.54	8503.7679	101.7516	0.003545
12	9.030088	7.009678	73798.54	7964.1998	101.7516	0.003545
13	9.030088	7.009678	73798.54	7448.4887	101.7516	0.003545
14	9.030088	7.009678	73798.54	6957.8483	101.7516	0.003545
15	9.030088	7.009678	73798.54	6492.853	101.7516	0.003545
16	9.030088	7.009678	73798.54	6053.5838	101.7516	0.003545
17	9.030088	7.70118	119880.8	5639.7458	82.88731	0.007755
18	9.030088	7.70118	119880.8	5250.7648	82.88731	0.007755
19	9.030088	0.368596	118033.3	4885.8615	97.85769	52259.16
20	9.030088	0.368596	118033.3	4544.1152	97.85769	52259.16
21	9.030088	0.368596	118033.3	4224.5102	97.85769	52259.16
22	9.030088	0.368596	118033.3	3925.9742	97.85769	52259.16
23	9.030088	0.518897	192588.7	3647.4071	134.426	63280.82
24	9.030088	0.518897	192588.7	3387.704	134.426	63280.82
25	9.030088	0.5151	195424.2	3145.7716	185.3361	64361.23
26	9.030088	0.5151	195424.2	2920.5408	185.3361	64361.23
27	9.030088	0.505329	221893.4	2710.9759	190.3349	73132.65
28	9.030088	0.505329	221893.4	2513.8384	190.3349	73132.65
29	9.030088	0.505329	221893.4	2331.0364	190.3349	73132.65
30	9.030088	0.505329	221893.4	2161.5276	190.3349	73132.65
31	9.030088	0.49918	227180	2004.3453	219.479	75121.59
32	9.030088	0.49918	227180	1858.5931	219.479	75121.59
33	9.030088	0.49918	227180	1723.4399	219.479	75121.59
34	9.030088	0.49918	227180	1598.1148	219.479	75121.59
35	9.030088	0.49918	227180	1481.9032	219.479	75121.59
36	9.030088	0.49918	227180	1374.1424	219.479	75121.59

RESULTS OF TIME SIMULATION			Sulphate Component				grams			
Current	-0.04785	329.4557	495.4314	992.7175	613.7578	2529.818	2425.231	1512.127	1475.691	6332.552	
SO4_T	1	2	3	4	5	6	7	8	9	10	
0	0	0	0	0	0	0	0	0	0	0	Total
1	0	57.54767	85.60973	33.73391	54.98612	40.60297	54.23642	51.97397	52.6268	94.91493	526.2325
2	0	120.6458	200.0042	110.5697	145.4444	125.2377	144.0042	138.8329	138.8671	249.7589	1373.365
3	0	165.9128	323.3463	184.4587	233.0242	207.1736	231.1726	223.343	223.2871	419.7365	2211.455
4	0	208.0986	443.6325	255.3152	317.5917	286.1152	315.3617	304.8871	304.755	584.3993	3020.156
5	0	247.3141	560.9714	323.2454	399.2513	362.1644	396.6714	383.5622	383.3615	744.3687	3800.91
6	0	283.6658	675.4678	388.3524	478.1045	435.4216	475.2009	459.4665	459.2042	899.3728	4554.257
7	0	357.0821	677.5643	519.7407	554.2494	505.9835	551.0461	532.6951	514.0314	1059.844	5272.237
8	0	427.8369	677.0172	648.5014	627.7807	573.944	624.2996	603.34	566.2808	1215.684	5964.684
9	0	496.0259	674.8069	722.6936	700.7483	652.4693	683.0096	675.5095	641.5647	1382.633	6629.46
10	0	561.7414	670.138	794.4406	771.2823	728.5712	739.3043	745.2704	714.4448	1545.261	7270.454
11	0	583.4866	708.1805	861.302	839.4684	802.3342	793.2676	812.7059	757.2519	1749.937	7907.934
12	0	602.9331	743.9368	925.8882	905.3891	873.84	844.9806	877.8965	797.8181	1950.585	8523.267
13	0	620.1637	777.4885	988.2799	969.124	943.1675	894.5216	940.9201	836.2209	2147.344	9117.23
14	0	620.0465	804.9119	1005.046	1093.933	1010.393	941.9663	1001.852	872.5353	2340.348	9691.032
15	0	617.8701	830.2854	1019.771	1216.707	1075.591	987.388	1060.765	906.8337	2529.728	10244.94
16	0	613.7087	853.6823	1032.527	1337.519	1138.831	1030.857	1117.729	939.1861	2715.608	10779.65
17	0	607.6336	875.1734	1043.383	1456.437	1200.183	1072.443	1172.812	928.4306	2883.41	11239.91
18	0	599.714	894.8269	1052.408	1573.529	1259.714	1112.21	1226.081	915.8622	3047.951	11682.3
19	0	595.9504	884.8796	1070.338	1523.326	1367.605	1188.057	1252.125	1022.799	3183.513	12088.59
20	0	590.4727	873.2239	1086.565	1471.424	1473.8	1262.211	1276.48	1128.047	3316.038	12478.26
21	0	583.3428	859.9211	1101.149	1417.882	1578.359	1334.732	1299.203	1231.666	3445.633	12851.89
22	0	574.6202	845.0302	1114.148	1362.76	1681.34	1405.678	1320.353	1333.713	3572.399	13210.04
23	0	564.3623	828.6081	1125.62	1306.112	1782.8	1475.103	1322.919	1371.731	3800.075	13577.33
24	0	552.6245	810.7097	1135.618	1247.995	1882.79	1543.062	1324.02	1408.286	4025.117	13930.22
25	0	539.4603	791.3881	1144.196	1188.459	1981.365	1609.607	1323.708	1443.429	4222.014	14243.62
26	0	524.9209	770.6943	1151.404	1127.555	2078.573	1674.787	1322.032	1477.208	4416.458	14543.63
27	0	509.0562	748.6775	1157.291	1065.332	2174.464	1738.65	1319.041	1482.785	4631.311	14826.61
28	0	491.9138	725.3854	1161.904	1001.837	2269.084	1801.243	1314.78	1487.093	4843.881	15097.12
29	0	473.54	700.8636	1165.29	937.1145	2362.478	1862.612	1309.296	1490.178	5054.25	15355.62
30	0	453.979	675.1564	1167.491	871.2092	2454.69	1922.799	1302.63	1492.082	5262.495	15602.53
31	0	433.2739	648.3064	1168.55	804.1631	2545.761	1981.847	1294.826	1492.847	5420.953	15790.53
32	0	411.4659	620.3547	1168.508	736.0169	2635.733	2039.795	1285.923	1492.515	5577.433	15967.75
33	0	388.5948	591.3408	1167.405	666.8097	2724.645	2096.684	1275.961	1491.122	5732.007	16134.57
34	0	364.699	561.3031	1165.278	596.5795	2812.534	2152.55	1264.976	1488.708	5884.742	16291.37
35	0	339.8155	530.2783	1162.165	525.3629	2899.437	2207.431	1253.005	1485.309	6035.703	16438.51
36	0	313.9801	498.302	1158.101	453.1952	2985.389	2261.36	1240.084	1480.958	6184.953	16576.32

GLOSSARY OF SYMBOLS

γ = *stoichiometric ratio of mol sulphate $\cdot$ mole^{-1} O_2*

γ_i = *activity coefficient of species i*

δ = *an empirical constant dependent on the pore size distribution.*

Δh = *head loss (m)*

ΔH_i = *enthalpy of evaporation(J/mol)*

Δl = *flow path length (m)*

Δp = *pressure change (Pa)*

ΔT = *temperature rise in the material (K)*

Δt = *length of time step (seconds)*

Δx = *the thickness of the layer surrounding the particle (m)*

Θ = *volume water/ total volume = volumetric water content*

θ_{infilt} = *thickness of wetting front associated with the infiltrated water (m)*

θ_{start} = *thickness of the wetting front prior to infiltration*

θ_{start} = *Thickness of wetting front in layer at the end of the previous time step (m)*

λ = *the pore size distribution index, defined as the negative slope of the effective degree of saturation, S_e, versus matric suction, $(u_a - u_w)$, curve.*

μ_a = *fluid viscosity (Ns $\cdot$ m^{-2})*

M_{oxygen} = *moles of oxygen entering the waste dump/ time interval*

ρ = *bulk density of the material(kg m^{-3})*

ρ_{dry} = *dry density of the waste*

ρ_{oxygen} = maximum concentration of oxygen in the atmosphere $(g\,m^{-3})$

Υ = stoichiometric constant relating oxygen uptake to mineral oxidation

υ = proportion of water which moves along SFP's

φ_j = total molar concentration of component (aqueous phase plus solid phase) j (moles · litre^{-1})

χ = factor to account for evaporation and absorption losses from the kinetic test cell (approx 1,05)

Υ_{oxygen} = maximum dissolved oxygen content in the water $(g\,m^{-3})$

ω = number of times that the leachate collected is re-circulated through the kinetic test cell prior to laboratory analysis

ξ_j = proportion of aqueous phase components available for movement from layer j

A = cross sectional area perpendicular to the direction of flow(m^2)

a = the specific surface area of sulphide minerals $(m^2\,m^{-3})$

$a^\bullet$ = surface area of the reacting front (m^2)

A_o = microbial oxygen consumption rate $(mole\,m^{-3}\cdot s^{-1})$

a_{ij} = stoichiometric coefficient of component j in species i

A_r = Arrhenius pre-exponential factor

$a_{sulphide}$ = the sulphide surface area available for reaction (m^2)

B = a biological scaling factor used to fit site specific data

$B_1\;B_2$ = constants which depend on the boundary conditions

C = concentration of oxygen in the pore space $(moles\,m^{-3})$

$C^\bullet$ = concentration of oxygen within the particle $(mol\,m^{-3})$

C_a $=$ oxygen concentration (mol m^{-3} gas)

$C_a(z)$ $=$ concentration of oxygen at depth z (mole m^{-3} gas)

C_{air} $=$ concentration of a gas in air (mole m^{-3})

C_{i-1} $=$ equilibrated aqueous phase concentration of component j in layer i-1

C_{oxygen} $=$ maximum dissolved oxygen content in water (g m^{-3})

C_P $=$ heat capacity of the solids(J kg^{-1} K^{-1})

c_p $=$ concentration of diffusing component in the total pore fluid (mole m^{-3} pore volume)

C_{pyrite} $=$ concentration of pyrite (grams $\cdot kg^{-1}$ waste)

C_w $=$ molar heat capacity of water (J mol^{-1} K^{-1})

C_{water} $=$ concentration of a gas in water (mole $\cdot m^{-3}$)

$d_{i,j}$ $=$ distance from the top of layer i to the top of layer j

D $=$ effective diffusion coefficeint based on the concentration in the gas phase (m^2 s^{-1})

D_{10} $=$ the particle size (cm) below which 10% of the material falls.

D_a^o $=$ binary diffusion coefficient in air ($m^2 \cdot s^{-1}$)

D_e $=$ effective diffusivity of oxygen in the pore spaces ($m^2 \cdot s^{-1}$)

D_e^* $=$ effective diffusion coefficient of oxygen within the particle ($m^2 \cdot s^{-1}$)

D_P $=$ pore diffusivity (m^2 s^{-1})

dS/dt $=$ sulphide oxidation rate rate

d_{test} $=$ minimum required diameter of kinetic test cylinder (mm)

D_w^o $=$ binary diffusion coefficient in water ($m^2 \cdot s^{-1}$)

e = void ratio

E_a = Arrhenius activation energy $(J\ mol^{-1})$

E_w = evaporation water loss $(mol \cdot m^{-3} \cdot s^{-1})$

$f(T)$ = bi-modal distribution for the residence time in the waste material

G_s = particle specific gravity

H = total head

or H = solubility constant at a particular temperature

I = solution ionic strength

J = flux calculated per unit cross sectional area area of the porous material $(mol\ m^{-2} \cdot s^{-1})$

J_p = flux in the pore space $(mole \cdot m^{-2}$ pore area,s)

k = thermal conductivity $(J \cdot m^{-1} \cdot K^{-1}\ s^{-1})$

K_0 = initial oxidation rate $(grams\ sulphide \cdot kg^{-1}\ bed \cdot week^{-1})$

k_1 = decay constant (per week)

k_a = air permeability of the porous material $(m \cdot s^{-1})$

k_B = biological surficial reaction rate constant $(mol \cdot m^{-2} \cdot s^{-1})$

k_c = chemical surficial reaction rate constant $(mol\ m^{-2}\ s^{-1})$

k_i = equilibrium constant for the formation of species I

k_r = reaction rate constant $(m^3\ O_2\ per\ m^3\ waste \cdot sec^{-1})$

k_r = overall specific reaction rate of the rock surfaces $(mol\ sulphide \cdot m^{-2} \cdot s^{-1})$

K_{sat} = saturated water permeability $(m \cdot s^{-1})$

k_x, k_y
or k_z =   *hydraulic conductivity in the x, y or z directions*

k' =   *first order reaction rate constant (m^3 gas $\cdot m^{-2}$ sulphide surface.s)*

L =   *depth (m)*

i =   *thickness of the layer (m)*

m_w =   *slope of the soil water characteristic curve*

MAI =   *mean annual infiltration rate (mm $\cdot$ annum^{-1})*

$M(aq)_j$ =   *mass of component j in the aqueous phase (grams)*

$M(s)_j$ =   *mass of component j in the solid phase (grams)*

n =   *porosity of the material*

n_a =   *air filled porosity ($m^3 \cdot m^{-3}$)*

n_{sample} =   *average sampling rate in the kinetic test (samples $\cdot$ annum^{-1})*

P_{atm} =   *Atmospheric pressure (Pa)*

$PDF(T_1), PDF(T_2)$ =   *probability distributions for the residence time for the slow and fast flow paths respectively*

PVR =   *pore volume replacements required to supply sufficient oxygen to oxidise the pyrite*

Q =   *flow rate ($m^3 \cdot s^{-1}$)*

q =   *water flux or flow rate ($m^3 \cdot m^{-2} \cdot s^{-1}$)*

q_{SFP} & q_{RFP} =   *the mean water fluxes in the relatively slow flow paths,(SFF), and the preferential or rapid flow paths, (RFP), respectively.*

q_{air} =   *air flux ($m^3 \cdot m^{-2} \cdot s^{-1}$)*

q_{new} =   *depth to the combined wetting front (m)*

Q_{RV} = sulphide reaction enthalpy generation $(J \cdot m^{-3} \cdot s^{-1})$

$q_t^\bullet$ = distance moved by a wetting front in time T, $(m \cdot m^{-2})$

R = Universal molar gas constant $(J \, mol^{-1} \, K^{-1})$

r_{oxygen} = oxygen consumption rate

r = radial distance within the particle (m)

R_{sp} = overall specific reaction rate $(mol \, kg^{-1} \cdot S^{-1})$ for fine particles

S = degree of saturation

S_r = residual degree of saturation

S_t = Pyrite balance at time step t $(g \, pyrite \cdot kg^{-1} \, bed)$

St_{start} = degree of saturation at the start of the time step

T = Temperature (Kelvin)

t = time (s)

$t^\bullet$ = kinetic test equivalent reaction point (weeks)

T_j = total analytical aqueous phase concentration of component j $(moles \cdot litre^{-1})$

V = volume of dump (m^3)

V_i = volume of water in layer i before flow

$V_{infiltration}$ = total volume of water infiltrated to layer I from layer I-1

V_{sample} = minimum sample volume of leachate required for the laboratory analysis (ml)

V_v = volume of voids

V_w = volume of water in the layer (litres)

w =   *moisture content*

X_j =   *activity of component j*

Y_j =   *error in the mass balance equation*

Y_{O_2} =   *moles oxygen/cubic metre air*

Y_{oxygen} =   *mole fraction of oxygen in air (moles O_2 m^{-3} air)*

z =   *depth from the surface (m)*

Z_i =   *charge on species I*

$[O_2]$ =   *oxygen concentration (mol m^{-3})*

$[S_i]$ =   *Ci, the concentration of species I*

BIBLIOGRAPHY

Barton-Bridges JP and Robertson A. 1989. Design and Reclamation of Mine Drainage. Canadian Land Reclamation Association and the American Society for Surface Mining and Reclamation, Calgary.

Bennett JW and Ritchie AIM.1991. Measurements of the Transport of Oxygen into Two Rehabilitated Waste Rock Dumps. In: MEND, pp 289-298.

Bennet JW, Gibson DK, Ritchie A I M. Tan Y, Broman PG, Jonsson H. 1994. Oxidation Rates and Pollution Loads in drainage; Correlation and measurement in a Pyritic Waste Rock Dump. In Proceddings of the 3rd International Conference on Acidic Mine Drainage, Pittsburgh PA, April 24-29, Vol 2.

Bhattacharya D .1981. Precipitation of Heavy Metals with Sodium Sulphide: Bench Scale and Full Scale Experimental Results. AIChE Symp. Series, 77, 31-38.

Bowers TS and Cathles LM.1987. A Simplified Approach to Fluid/Rock Modelling: Two Requirements for Low Water/Rock Ratios. Abstract with Programs Geological Society of America 19/7:596, (Abstract).

Bradham WS and Caruccio FT. 1991. A Comparative Study of Tailings Analysis using Acid/Base Accounting, Cells, Columns and Soxhlets. Second International Conference on the Abatement of Acid Drainage. Montreal. Canada. 16-18 September 1991.

Brady K. 1994. Evaluation of acid-base accounting to predict the quality of drainage at surface coal mines in Pennsylvania, U.S.A. In Proceedings of the Third International Conference on the Abatement of Acidic Drainage, Vol 1.

Britton RR and Gozon JS, 1991. Acid Mine Drainage Control by Re-Mining. Second International Conference on the Abatement of Acid Drainage. Montreal. Canada. 16-18 September 1991.

Brodie MJ, Broughton LM and Robertson AM. 1991. A Conceptual Rock Classification System for Waste Management and a Laboratory Method for ARD Prediction from Rock Piles. Second International Conference on the Abatement of Acid Drainage. Montreal. Canada. 16-18 September 1991.

Broughton LM and Robertson AM. Modelling of Leachate Quality from Acid Generation Waste Rock Dumps.. Second International Conference on the Abatement of Acid Drainage. Montreal. Canada. 16-18 September 1991.

Broughton LM, and Robertson AM. 1991. Modelling of Leachate Quality from Acid Generating Waste Dumps. Proceedings of the Second International Conference on the Abatement of Acidic Drainage. Montreal, Quebec, September.

Broughton LM, Chambers RW and Robertson AM. 1992. Mine Rock Guidelines - Design and Control of Damage Water Quality. Steffen Robertson and Kirsten (BC) Inc.

Butters GL, Jury WA and Ernst FF. 1989. Field scale transport of bromide in unsaturated soil,1. Experimental methodology and results. Water Resour. Res.,28:1377-1388.

Canmet-MEND. 1989. Subaqueous Disposal of Reactive Mine Wastes: An Overview. MEND Project 2.11.1a, Ottowa.

Cathles GB and Schlitt WJ. 1980. A Model of the Dump Leaching Process that Incorporates Oxygen Balance, Heat Balance, and Two Dimensional Air Convection in WJ Schlitt (ed.) Proceedings of the Symposium on Leaching and Recovery Copper from As-Mined Materials.

Cathles LM and Bowers TS. 1987. A Simplified Approach to Fluid/Rock Modelling: 1 Kinetic and Computation Advantages. Abstracts with Programs Geological Society of America 19/7:615, (Abstract).

Cathles LM.1979. Predictive Capabilities of a Finite Difference Model of Copper Leaching in Low Grade Industrial Sulphide Waste Dumps. Math Geol. Vol. 11. pp 175-191.

Cathles LM, and Apps JA. 1975. A Model of the Dump Leaching Process that incorporates Oxygen Balance, Heat Balance, and Air Convection. Metallurgical Transactions B, Vol. 6B, pp 617-624.

Cathles LM.1979. Predictive Capabilities of a Finite Difference Model of Copper Leaching in Low Grade Industrial Sulphide Waste Dumps. Mathematical Geology 11 (2):175-191.

Collin M. 1987. Mathematical Modelling of Water and Oxygen Transport in Layered Soil Covers for Deposits of Pyritic Mine Tailings. Licentiate Treatise, Royal Institute of Technology, Stockholm, Sweden.

Collin M. 1987. Mathematical Modelling of Water and Oxygen Transport in Layered Soil Covers for Deposits of Pyritic Mine Tailings, Royal Institute of Technology Department of Chemical Engineering S-100 44, Stockholm, Sweden, pp 1-189.

Corey AT. 1954. Producer's Monthly vol. 19 p.38.

Cravotta, C. K. Brady, M, Smith and R. Beam. 1990. Effectiveness of the Addition of Alkaline Materials at Surface Coal Mines in Preventing and Abating Acid Mine Drainage: Part 1. Geochemical Considerations. In Proceedings of the 1990 Mining and Reclamation Conference. (Morgantown, WV, April 23 -26,1990)

Davis GB and Ritchie AIM. 1986. A Model of Oxidation in Pyritic Mine Wastes: Part 1 Equations and Approximate Solution. Appli. Math. Modelling 10:315-329.

Davis GB and Ritchie AIM. 1986. A Model of Oxidation in Pyritic Mine Wastes: Part 1, Equations and Approximate Solutions. Appli. Math. Modelling, Vol 10, pp 314-322.

Davis GB and Ritchie AIM. 1986. A Mathematical Model of Pyritic Oxidation in Waste Dumps in Proceedings of 5th Conference of Simulation Society of Australia, pp 137-141.

Davis GB and Ritchie AIM. 1986. A Model of Oxidation in Pyritic Mine Waste I: Equations and Approximate Solutions. Appl. Math. Modelling. Vol 10. pp 314-329.

Davis, GB, Doherty G and Ritchie AIM. 1986. A Model of Oxidation in Pyritic Mine Waste II: Comparison of Numerical and Approximate Solutions. Appl. Math. Modelling. Vol 10. pp 323-329.

Day SJ. 1994. Evaluation of acid generating rock and acid consuming rock mixing to prevent acid rock drainage: In Proceedings of Third International Conference on the Abatement of Acidic Drainage, Vol. 2.

Destouni G. ,1993. Field scale solute flux through macroporous soils, in Water flows and solute transport in soils (eds. Russo, D. and Dagan,G.), Springer- Verlag, Heidelberg,33-44.

Doepker DD and Drake PL. 1991. Laboratory Study of Submerged Metal-Mine Tailings 3" Factors influencing the Dissolution of Metals. Second International Conference on the Abatement of Acid Drainage. Montreal. Canada. 16-18 September 1991.

Doepker, DD, 1991. Column Leach Study IV: Factors affecting the Dissolution of Metals from Sulphidic Metal - Mine Tailings. Second International Conference on the Abatement of Acid Drainage. Montreal. Canada. 16-18 September 1991.

Environment Canada. 1990. Compendium of Waste Leaching Tests. Reports EPS 3/HA/7 Environmental Protection Series.

Eriksson N and Destouni G. 1994. Modelling Field-Scale Transport of Weathering Products in Mining Waste Rocks Dumps. Third International Conference on the Abatement of Acidic Drainage. Pittsburgh, USA.

Evangelou VP and Sainju UM. 1991. Evaluation and Qualification of Armouring Mechanisms of Calcite, Dolomite and Rock Phosphate by Manganese. In: Proceedings Second International Conference on the Abatement Of Acidic Drainage, September 16-18, 1991, Montreal, MEND, 1991, pp 363-382.

Evangelou VP, Phillips RE and Shepard JS. 1982. Salt Generation in Pyritric Coal Spoils and its Effect on Saturated Hydraulic Conductivity. Soil Science Society of America Journal. Madison, Wisconsin. Vol 46, No 3, pp 457-460.

Feasby DG, Blanchette M and Tremblay G. 1991. The Mine Environment Neutral Drainage (MEND) Program. Second International Conference on the Abatement of Acid Drainage. Montreal. Canada. 16-18 September 1991.

Ferguson KD and Morin KA. 1991. The Prediction of Acid Rock Drainage - Lessons from the Database. Second International Conference on the Abatement of Acid Drainage. Montreal. Canada. 16-18 September 1991.

Ferguson KD. 1985. Static and Kinetic Methods to Predict Acid Mine Drainage. In: The International Symposium on Biohydrometallurgy, Vancouver, BC, August 22-24, 1985.

Filipek LH, Gormley JT, Ewing R and Ellsworth D. 1991. Kinetic Acid-Prediction Studies as Aids to Waste-Rock and Water Management during Advanced Exploration of a Massive Sulphide Deposit.. Second International Conference on the Abatement of Acid Drainage. Montreal. Canada. 16-18 September 1991.

Fredlund DG and Rahardjo H.1993. Soil Mechanics for Unsaturated Soils. John Wiley and Sons.

Geidel G. 1979. Alkaline and Acid Production Potentials of Overburden material: the Rate of Release. Reclamation Review, 1979, Vol 2, No 3-4, pp 101-107.

Geosoft, SEEP/W Version 3 User manual.

Hart WM, Batarseh KI, Swaney GP and Stiller AH. 1991. A Rigorous Model to Predict the AMD Production Rate of Mine Rock. Second International Conference on the Abatement of Acid Drainage. Montreal. Canada. 16-18 September 1991.

Harvard University Cambridge, Massachusetts. 1970. Oxygenation of Ferrous Iron. Prepared for the Federal Water Quality Adminstration, Department of the Interior, pp 2-1 to 2-5.

Hawkins, JW and Aljoe, WW, 1991. Hydrologic Characteristics of a Surface Mine Spoil Aquifer. Second International Conference on the Abatement of Acid Drainage. Montreal. Canada. 16-18 September 1991.

James AR. 1995. A Model to Predict Acid and Salt Generation in Coarse Rock Materials. In Proceedings of the Water Institute of Southern Africa Conference, 1996, Port Elizabeth.

James DB, Rogowski AS, and Pionke HB. 1984. Acid Mine Drainage from Reclaimed Coal Strip Mines 1. Model Description Water Resources Research, Vol 20, pp 233-242.

Jaynes DB, Pionke HB and Rogowski AS.1992. Acid Mine Drainage from Reclaimed Coal Strip Mines 2. Simulation Results of Model. Water Resources Research 20 (2):243-250.

Jaynes DB, Rogowski AS and Pionke HB.1984. Acid Mine Drainage from Reclaimed Coal Strip Mines 1. Model Description. Water Resources Research 20 (2):233-242.

Jaynes DB.1991. Modelling Acid Mine Drainage from Reclaimed Coal Strip Mines. In: Proceedings, Second International Conference on the Abatement of Acidic Drainage, September 16-18, Montreal: NEDEM 1991 MEND, 1991, pp 191-210.

Kondos PD, MacDonald RJC and Zinck JM. 1991. Studies on the Removal of Heavy Metals from Acidic Mineral Effluents. Second International Conference on the Abatement of Acid Drainage. Montreal. Canada. 16-18 September.

Kwong YTJ. 1991. Acid Generation in Waste Rock as Exemplified by the Mount Washington Minesite, British Columbia, Canada. Second International Conference on the Abatement of Acid Drainage. Montreal. Canada. 16-18 September 1991.

Lapakko K and Antonson D. 1991. Mixing of Limestone with Acid Producing Rock. Second International Conference on the Abatement of Acid Drainage. Montreal. Canada. 16-18 September.

Levenspiel O. 1972. Chemical Reaction Engineering. (John Wiley, New York),p578.

Liljedahl T. 1984. Pyritvittring I sulfidhaltiga sandupplag, laboratorieforsok, uppsala universitet. (in Swedish)

Mangold DC and Tsang Chin-Fu. 1991. A Summary of Subsurface Hydrological and Hyydrochemical Models. Reviews of Geophysics, 19, 1, Feb, 1991 pp 51-79. Paper No 90RG01715.

McKibben MA and Barnes HL. 1986. Oxidation of pyrite in low temperature acidic, solutions. Geochim. et Cosmochim. Acta 50:1509 -1520

Miller SD, Jeffery JJ and Wong JWC. 1991. Use and Misuse of the Acid-Base Account for 'AMD' Prediction. In" Proceedings Second International Conference on the Abatement of Acidic Drainage, September 16-18, 1991, Montreal, MEND, pp 489-506.

Morel F and Morgan JA. 1972. Numerical Method for Computing Equilibria in Aqueous Chemical Systems. Environ, Sci. Technol 6(1):58-67.

Morin KA and Hutt NM. 1994. An empirical technique for predicting the chemistry of water seeping from mine rock piles in Proceedings of the Third International Conference on the Abatement of Acidic Drainage, vol. 1, 1994.

Rasmuson A and Eriksson J. 1987. Capillary Barriers in Covers for Mine Tailings Dumps. Nat. Swedish Env. Protection Bd. Rep. 3307, Stockholm.

Moses CO and Herman JS. 1991. Pyrite oxidation at circumneutral pH. Geochim. et Cosmochim. Acta 55:471-482.

Ohio State University Research Foundation. 1970. Sulphide to sulfate Reaction Mechanism For: Water pollution Control research Services 14010 FPS 02/70. Federal Water Pollution Control Adminsitration, Washington D.C. p115.

Reisenauer AE, Key KT, Narashimhan TN, Nelson RW. 1982. "TRUST: A Computer Program for Variably Saturated Flow in Multidimensional, Deformable Media", US Nuclear Regulatory Commission, NUREG/CR-2360.PNL-3975, Pacific Northwest Laboratory, Richland, Washington.

Ritcey GM, 1991. Deep Water Disposal of Pyritic Tailings - A Simulation for Acid Prediction. Second International Conference on the Abatement of Acid Drainage. Montreal. Canada. 16-18 September 1991.

Ritchie, AIM, 1977. "Mathematical Model for Pyrite Oxidation:AAEC/E365.

Robertson AM. 1987. Alternative Acid Mine Drainage Abatement Measure. Province of British Columbia, Mine Reclamation Symposium Focus on AMD. Campbell River, BC April.

Roth K, Jury A, Fluhler H and Attinger W. 1991. Transport of chloride through unsaturated field soil. Water Resour. Res.,27:2533-2541.

Rymer TE, Skousen JG, Renton JJ, Zondlo AM and Ziemkiewicz PF. 1991. Undetected Sources of Detectable Acid Mine Drainage: some Statistical Considerations in Rock Sampling. Second International Conference on the Abatement of Acid Drainage. Montreal. Canada. 16-18 September 1991.

Sassner M K, Jensen H, and Destouni G. 1994. Chloride migration in heterogeneous soil,1. Experimental methodology and results. Water Resour. Res.

Scharer JM.1994. Mathematical Simulation of a Waste Rock Heap. Third International Conference on the Abatement of Acidic Drainage. Pittsburgh.

Scharer JM, Garga V, Smith R and Halbert BE. 1991. Use of State for Assessing Acid Generation in Pyritic Mine Tailings. Second International Conference on the Abatement of Acid Drainage. Montreal. Canada. 16-18 September.

Schroeder PR, Gibson AC and Smolen MD. 1984. The Hydrologic Evaluation of Landfill Performance (HELP) Model, Volume II. US. EPA Report Number PB85-100832, Washington, DC.

SENES Consultants Limited and Beak Consultants LTD. 1988. Adaptation of the reactive acid tailings assessment programme to base metal mines. CANMET DSS#15SW-2344-7-9208

Singer PC and Stumm W. 1970. Acidic Mine Drainage: The Rate Determining Step. Science. Vol 167. Feb 1970.

Smith A and Barton-Bridges J. 1991. Considerations in the Prediction and Control of Acid Drainage Impact from mining Waster on Water Resource Utilisation. EPPIC 1991. Environmental Conference" Water. Randburg, South Africa. 16-17 May.

Sobek AA, Schuller WA, Freeman JR, and Smith RM. 1978. Field and Laboratory Methods Applicable to Overburden and Minesoils, EPA 600/2-78-054, 203 pp.

Steffen Robertson and Kirsten (BC) Inc, in association with Norecol Environmental Consultants and Gormely Process Engineering. 1989. Draft Acid Rock Drainage Technical Guide. Prepared for British Columbia Acid Mine Drainage Task Force, Volumes I and II.

Steffen, Robertson and Kirsten, 1992. Mine Rock Guidelines. Design and Control of Drainage Water Quality. Report No 93301. Saskatchewan Environment and Public Safety. Mines Pollutions Control Branch. April 1992.

Steffen, Robertson and Kirsten (BC) Inc, 1992. Rock Pile Water Quality Modelling Phase 1 Draft Report. Prepared for BC AMD Task Force.

Stumm W and Morgan J. 1981. Aquatic Chemistry: An Introduction Emphasising Chemical Equilibria in Natural Waters. 2nd Edition. John Wiley and Sons.

United States Environment Protection Agency (EPA). 1978. Field and Laboratory Methods Applicable to Minesoils. EPC-600/2-78-054.

United States Environment Protection Agency (EPA). 1991. MinteqA2/ProdefA2, A Geochemical Assessment Model for Environmental Systems: Version 3.0 User's Manual.

Westall JC, Zachary JL and Morel FMM. 1976. MINEQL, a Computer Program for the Calculation of Chemical Equilibrium Composition of Aqueous Systems. Technical Note 18, Cambridge, MA: Massachussetts Institute of Technology.

White III WW. 1992. Chemical Predictive Modelling of Acid Mine Drainage from Metallic Sulphide-Bearing Waste Rock. In: Salt Lake City: US Department of the Interior, Bureau of Mines, pp 1-31.

Yanful EK. 1991. Engineered Soil Covers for Reactive Tailings Management: Theoretical Concepts and Laboratory Development. Second International Conference on the Abatement of Acid Drainage. Montreal. Canada. 16-18 September.